

~~SECRET~~
JAN 19 1972

T. & A. M. REPORT NO. 337

FATIGUE FAILURE PREDICTIONS FOR
COMPLICATED STRESS-STRAIN HISTORIES

BY

N. E. DOWLING

Sponsored by

Naval Air Development Center
Warminster, Pennsylvania 18974
Contract No. N00156-70-C-1256

Department of Theoretical and Applied Mechanics
University of Illinois
Urbana, Illinois
January 1971

FOREWORD

This investigation was conducted in the H. F. Moore Fracture Research Laboratory of the Department of Theoretical and Applied Mechanics, University of Illinois, Urbana. Sponsorship was provided by the Naval Air Development Center under Contract No. N00156-70-C-1256. The research performed under this contract is a continuation of the work of Contracts N-156-46083 and N00156-67-C-1875, the aim of these three contracts being to develop basic mechanics and materials principles to improve methods of designing aircraft structures to resist fatigue loading.

F. F. Borriello and R. E. Vining of the Naval Air Development Center acted as technical liaison. The author is indebted to Professor JoDean Morrow, the Principal Investigator, for suggestions, constructive criticisms, and encouragement. The technical aid and advice provided by J. F. Martin is appreciated by the author, as are the contributions of undergraduate lab assistant M. E. Baker, draftsman A. D. Zanolgia, and typist Mrs. R. A. Mathine.

The results of this investigation will at a later date become part of the author's Ph.D. thesis.

ABSTRACT

A cumulative fatigue damage procedure that considers sequence and mean stress is proposed for engineering metals. Fatigue life data for prestrained specimens are used to account for sequence effects due to crack initiation. Histories with fluctuating mean stress are analyzed by determining the mean stress of each cycle. The rain flow cycle counting method, which counts all closed stress-strain hysteresis loops as cycles, is employed in the damage procedure.

Axially loaded unnotched specimens of 2024-T4 aluminum were tested to failure using various complicated stress or strain control conditions. Life predictions using the proposed cumulative damage procedure were made prior to testing for 83 specimens. The predicted lives were within a factor of three of the actual lives for all of the tests and within a factor of two for more than 90% of the tests. In some of the tests there were large plastic strains, and in others the strains were predominantly elastic. Some of the stress control histories were similar to the load histories for actual machines, vehicles, and aircraft in that there were irregular loadings superimposed on changes in the static level.

It is shown that the use of the average mean stress to make life predictions can result in large nonconservative errors. The rain flow cycle counting method allows satisfactory predictions of the effects of different block sizes, different sequences of applying the same strain peaks, and superimposed loadings. The range pair counting method is nearly identical to the rain flow method, but the use of any of the other well known cycle counting methods, such as peak counting, level crossing counting, or range counting, can result in large differences between predicted and actual fatigue lives.

TABLE OF CONTENTS

	<u>Page</u>
FOREWORD	ii
ABSTRACT	iii
LIST OF TABLES	v
LIST OF FIGURES	vi
LIST OF SYMBOLS	viii
INTRODUCTION	1
LITERATURE SURVEY	2
Sequence Effects	
Cycle Counting	
Mean Stress	
Mean Stress and Cycle Counting	
Predicting Cyclic Stress-Strain Response	
PROPOSED CUMULATIVE DAMAGE PROCEDURE	7
GENERAL DESCRIPTION OF TESTS	8
TEST RESULTS AND DISCUSSION	9
Effect of Prestrain	
Cause of Mean Stress Effect	
Block Size Effect	
Low Cycle Fatigue with Complicated Strain Histories	
Complicated Histories with Periodic Variation of the Mean Stress	
CONCLUSIONS	15
RECOMMENDATIONS FOR FUTURE RESEARCH	17
REFERENCES	18
TABLES	23
FIGURES	37
APPENDIX: RANGE PAIR AND RAIN FLOW CYCLE COUNTING METHODS . .	74

LIST OF TABLES

<u>No.</u>	<u>Title</u>	<u>Page</u>
1	CYCLE COUNTING METHODS	23
2	EFFECT OF NUMBER OF CYCLES AND AMPLITUDE OF PRESTRAIN .	25
3	FATIGUE LIVES AT \pm 40 ksi AFTER CYCLING IN COMPRESSION . . .	26
4	EFFECT OF OVERLOAD CYCLES ON THE FATIGUE LIVES AT DIFFERENT MEAN STRESSES	27
5	STRAIN CONTROL BLOCK SIZE EFFECT TESTS	28
6	STRESS CONTROL BLOCK SIZE EFFECT TESTS	29
7	STRAIN CONTROL MEMORY EFFECT TESTS	30
8	TESTS WITH SINUSOIDAL VARIATION OF THE MEAN STRAIN.	31
9	STRAIN CONTROL RANDOM SEQUENCE TESTS	32
10	CONSTANT AVERAGE MEAN STRESS TESTS	33
11	TESTS WITH SINUSOIDAL VARIATION OF THE MEAN STRESS.	34
12	STRESS CONTROL RANDOM SEQUENCES AT TWO STATIC LEVELS . .	35
13	STRESS CONTROL RANDOM SEQUENCES AT FIVE STATIC LEVELS. .	36

LIST OF FIGURES

<u>No.</u>	<u>Title</u>	<u>Page</u>
1	Fatigue failure predictions by linear summation of cycle ratios based on strain amplitude	37
2	Sequence effects due to crack initiation	38
3	Comparison of crack initiation and effect of prestraining	38
4	Sequences which cause problems for several cycle counting methods	39
5	The effect of ignoring all excursions smaller than a specified value	39
6	Two sequences for which several counting methods give the same result . .	40
7	A change in sequence that can affect the fatigue life	40
8	Two sequences which have the same average mean stress.	40
9	Test specimen	41
10	The random sequence	42
11	Fatigue data from Refs. 12 and 45 for 2024-T4 Al	43
12	Stress-strain record for incremental step test.	44
13	Effect of number of cycles and amplitude of prestrain	45
14	Examples of stress-strain response during prestraining	46
15	Simulated removal of residual stress by prestraining 10 cycles at ± 0.0048	48
16	Fatigue lives at ± 40 ksi after cycling in compression 0 to -50 ksi.	49
17	Plastic strain range during cycling at ± 40 ksi after cycling in compression .	49
18	Effect of overload cycles on the fatigue lives at different mean stresses . .	50
19	Plastic strain range during overload cycles	51
20	Effect of mean stress on hysteresis loops	51

LIST OF FIGURES (Continued)

<u>No.</u>	<u>Title</u>	<u>Page</u>
21	Strain control block size effect tests	52
22	Variations of total stress range, mean stress, and plastic strain range during strain control block size effect tests	54
23	Stress control block size effect tests	55
24	Strain control memory effect tests	56
25	Typical variations of total stress range and plastic strain range during memory tests	58
26	Tests with sinusoidal variation of the mean strain	59
27	Stress-strain behavior during sinusoidal variation of the mean strain . . .	61
28	Strain control random sequence tests	63
29	Stress range vs. strain range for closed hysteresis loops during strain control random sequence tests	65
30	Constant average mean stress tests	66
31	Tests with sinusoidal variation of the mean stress	67
32	Stress control random sequences at two static levels	69
33	Strain response during two level random tests	71
34	Stress control random sequences at five static levels.	72
35	Distribution of failure predictions	73
A1	Examples of range pair counting method	76
A2	Example of rain flow cycle counting method	77
A3	Additional example of rain flow cycle counting method	78

LIST OF SYMBOLS

Block	A sequence of straining or stressing that is repeatedly applied to a specimen until failure occurs
ϵ	Strain measured on the gage length of a smooth specimen
$\Delta\epsilon$	Strain range
$\Delta\epsilon_1$	Total strain range during one complete block
$\Delta\epsilon_2$	Minor strain range
$\Delta\epsilon_{rs}$	The maximum strain range during one repetition of the random sequence in strain control
$\Delta\epsilon_p$	The total plastic strain during one block of straining or stressing, i. e., the width along the strain axis at zero stress of the stress-strain record for one block
j	The number of repetitions of the random sequence between changes in the static stress level
k	Minor cycles per block; where the control consists of two superimposed signals of different frequencies, k is also the ratio of the higher frequency to the lower
n	Number of cycles applied during the fatigue life at a given strain amplitude and mean stress
N_f	Cycles to failure
N_o	Cycles reduction in life due to prestraining
N_p	Cycles to failure for a prestrained specimen
$\frac{n}{N_f}$	Ratio of cycles applied at a certain strain amplitude and mean stress to the expected life for a test at that level run to failure
σ	Load per unit area for a smooth specimen
$\Delta\sigma, \Delta\sigma_1, \Delta\sigma_2$	Stress ranges similarly defined as for strain
$\Delta\sigma_{rs}$	The maximum stress range during one repetition of the random sequence in stress control
σ_o	Mean stress
$\Delta\sigma_o$	Range of variation of the mean stress
σ_{ave}	Average mean stress

INTRODUCTION

A cumulative damage procedure is developed to predict the fatigue failure of engineering metals subjected to complicated stress-strain histories. Histories with plastic strainings and cycles not completely reversed in stress are considered.

Most previous workers in the area of cumulative damage have employed notched or bending members as test specimens. In such members the stresses and strains at the location of the fatigue failure are related to the applied loads in a complicated nonlinear manner (1, 2) and are usually unknown. The two variables most significant in determining fatigue life can therefore not be isolated for study. In this investigation the relationship between stress-strain behavior and fatigue life is investigated for unnotched axially loaded specimens for which the stresses and strains can be measured for the duration of all tests. Since either the stress history or the strain history was known before each test was conducted, the other could be estimated and a life prediction made.

Simple linear summation of cycle ratios based on strain amplitude is illustrated in Fig. 1. Failure predictions on this basis are often in error because sequence effects and mean stresses are not accounted for. For some stress-strain histories it is difficult to define a cycle, and some method of cycle counting must be employed. The simple procedure of Fig. 1 is modified and extended to make it consistent with existing fatigue data and to make it applicable to complicated stress-strain histories. The resulting more general cumulative damage procedure is used to make life predictions for a wide variety of complicated history tests on 2024-T4 aluminum.

LITERATURE SURVEY

In this section the literature that relates to predicting fatigue lives from stress-strain histories is surveyed. Sequence effects, especially the high-low effect due to crack initiation, are discussed. The various methods of counting cycles and of handling mean stresses are reviewed. Cyclic stress-strain response is treated briefly. At several points during the literature survey, conclusions are stated which contribute to the proposed cumulative damage procedure.

The reader may omit this section without serious loss of continuity if he is familiar with the topics covered.

Sequence Effects

Crack initiation is defined as the portion of fatigue life prior to the existence of a tensile mode crack across several grains. For strengthened aluminum alloys and steels the initiation period is observed (3-8) to be short in the low cycle region, most of the life being spent in crack propagation. At longer lives an increasingly smaller fraction of the life is spent in propagation, until at long lives most of the fatigue life is required for crack initiation.

These observations on crack initiation explain the sequence effects (9, 10) shown schematically in Fig. 2. The deviations from linear summation of cycle ratios indicated in Fig. 2 are more pronounced when the difference between the two levels is larger (11). For the high-low sequence, a crack can be initiated by the high level that would ordinarily take many cycles to initiate at the low level. Failure then occurs after fewer cycles at the low level than predicted. The high-low effect can be quite drastic (12) if the high level is in the low cycle region and the low level is in the long life region. For the low-high sequence, the cycles at the low level are spent in initiating a crack that would have been initiated very soon after the beginning of the high level even if they had not been applied. A large number of cycles at the low level can therefore be applied without significantly affecting the number of cycles required for failure at the high level. Damage summations greater than two are not possible for this low-high effect, because failure is expected if the constant amplitude fatigue life at either level is exceeded. Multiple changes in level are similar to the high-low sequence in that a crack initiated at the high level can propagate at the low level. The sequence effects of Fig. 2 do not occur if all of the levels cause significant plastic straining (13-17), which is consistent with the observation that the initiation period is short in the low cycle region.

Grover (18) proposed that the sequence effects due to crack initiation be accounted for by using linear summation of cycle ratios separately over the initiation and propagation periods. It was shown (18) that this is the simplest damage rule that is mathematically possible for multilevel tests where the fraction of the fatigue life required for crack initiation is not constant for the different levels.

Topper and Sandor (12) used constant amplitude data on specimens prestrained 10 cycles at ± 0.02 to calculate the damage for all cycles after significant plastic straining occurred. Summations of cycle ratios close to unity were obtained for a wide variety of low-high, high-low, and two level repeated block tests on both 2024-T4 aluminum and SAE 4340 steel.

In view of the crack initiation studies cited above (3-8), it is likely that the prestraining done by Topper and Sandor (12) was sufficient to cause crack initiation. If this assumption is made, the damage procedure used by Topper and Sandor is essentially equivalent to the damage rule proposed by Grover (18). Linear summation of cycle ratios should give summations of cycle ratios close to unity for prestrained specimens only if prestraining causes crack initiation.

Some additional evidence supporting the assumption that prestraining causes crack initiation is given in Fig. 3. This assumption for the data of Topper and Sandor (12) on 2024-T4 is in reasonable agreement with microscopic observations of crack initiation made by Hunter and Fricke (3) on the same alloy with T3 heat treatment.

Grover's damage rule and the assumption that prestraining causes crack initiation will be used in the proposed cumulative damage procedure.

There are other important sequence effects. Different sequences of straining can affect the fatigue life because different mean stresses are induced or because different amounts of plastic strain occur. These effects will be treated in detail later in this paper. Due to the coaxing effect (19), which occurs in strain aging metals, damage summations much greater than unity can be obtained by gradually increasing the stress amplitude from below the endurance limit. Coaxing will not be considered here because 2024-T4 aluminum does not strain age, and because the effect of coaxing is probably small, even for strain aging metals, if the load history is irregular (10). Initial plastic straining usually causes rapid cyclic softening or hardening, depending on the material, which may alter the stable stress-strain hysteresis behavior at subsequent lower levels. This effect is not thought to be important for 2024-T4, because no significant dependence of the stable behavior on the previous history has been observed.

Cycle Counting

Six well known cycle counting methods (20, 21) are described in Table 1. The range pair (21, 22) and the rain flow (23) counting methods are described and compared in the Appendix.

If the various cycle counting methods are compared on the basis of their applicability to complicated strain histories, it is easily seen that for most of them there are situations where unreasonable results are obtained. In the sequence shown in Fig. 4 (a), the small reversals do some fatigue damage that

may or may not be significant compared to the damage done by the large cycle on which they are superimposed. Peak counting gives the same result for (a) and (b) of Fig. 4, but (b) is very likely more damaging than (a). Mean crossing peak counting gives the result that (a) is equivalent to (c), which is nonconservative in cases where the small reversals do significant damage.

The range and range mean counting methods have the characteristic that if small reversals are counted, the large ranges are broken up and counted as several smaller ones. This gives the unrealistic result that small excursions do negative damage, as the calculated damage can be decreased by including them (see Fig. 5). For example, in Fig. 4 (a) the large cycle on which the smaller ones are superimposed is not recognized by range counting; therefore the calculated damage could easily be less than for Fig. 4 (c). The range pair and rain flow counting results are much more reasonable, the small reversals being treated as interruptions of the larger strain ranges, and the damages for the large and small strain ranges are simply added.

No information whatever is given on sequence by the peak, mean crossing peak, level crossing, or fatiguemeter counting methods. These methods all give the same counting result for (a) and (b) of Fig. 6. Some calculations using the damage procedure of Topper and Sandor (12), which was fairly successful in predicting the fatigue failure of specimens repeatedly subjected to blocks of straining similar to those shown in Fig. 6, will show that (b) is usually much more damaging than (a). In Fig. 7, (a) and (b) are identical except that the signs of the smaller peaks are opposite. The peaks and level crossings are the same for these two sequences, but the range pair and rain flow counting methods predict that (a) will be more damaging than (b). It will be experimentally shown that (a) will cause more plastic straining than (b) and that the fatigue lives can be significantly different.

All of the counting methods, with the exception of the range pair and rain flow methods, have been shown to have serious flaws. The comparison of these two counting methods in the Appendix shows that they are nearly identical. No test could be devised which showed either of them to be superior, nor could any test be devised for which either gave an unreasonable prediction. The rain flow method applied to a strain history gives information on the stress response in that all closed stress-strain hysteresis loops are counted as cycles.

Mean Stress

In stress-strain histories where relatively large mean stresses are present for a significant number of cycles, the fatigue life cannot be adequately predicted without considering the effect of mean stress. Tensile mean stresses shorten the fatigue life, and compressive mean stresses prolong it.

Most studies of the effect of mean stress have employed parameter methods rather than seeking the basic cause of this phenomenon. Some of the possibilities are that mean stress affects the stable stress-strain behavior, the rate of crack initiation, the size of shear crack necessary to start a normal mode crack, the

crack propagation rate, or the crack size necessary to cause final failure. Several of these possibilities are explored in the test results to be presented, but it is probably not possible to thoroughly investigate the effect of mean stress without making extensive microscopic studies.

Several methods for predicting the effect of mean stress on fatigue life have been proposed. Each can be expressed as a parameter that can be plotted versus cycles to failure and should bring data for various mean stresses all onto one line. Five of the parameters are as follows:

- (a) $\frac{\Delta\sigma/2}{1 - \sigma_o/S_u}$ Smith (24)
- (b) $\Delta\sigma/2 + c\sigma_o$ Stulen (25)
- (c) $\frac{\Delta\sigma/2}{1 - \sigma_o/\sigma'_f}$ Morrow (26)
- (d) $(\Delta\epsilon/2) E + \sigma_o^a$ Topper and Sandor (12)
- (e) $[(\sigma_o + \Delta\sigma/2) (\Delta\epsilon/2) E]^{\frac{1}{2}}$ Smith, Watson and Topper (27)

In these parameters, the ultimate tensile strength, S_u , and the modulus of elasticity, E , are defined in the usual manner. The quantity σ'_f , which is approximately equal to the true fracture strength, is defined in Ref. 26. In (b) and (d), c and a are material constants found by trial and error, making these parameters inconvenient to apply to a new material. Note that all of the above parameters reduce to stress amplitude when the mean stress is zero and the strains are elastic.

A literature search for mean stress data on axially loaded unnotched specimens was made. The results of comparing the test results of Refs. 12 and 27-34 for the five parameters was inconclusive because the scatter in the data was greater than the differences between the various parameters. Parameters (c) and (e) gave fair agreement with the data in most cases, but (a) was often excessively conservative for ductile metals. There was little data at large tensile or compressive mean stresses.

In this investigation it was not necessary to use a mean stress parameter because fatigue data at different mean stresses (12) were available. Such data can be used to estimate the fatigue life for desired combinations of strain amplitude and mean stress.

Mean Stress and Cycle Counting

To predict the fatigue life for complicated stress-strain histories, it is necessary to use some method of accounting for mean stress in combination with a cycle counting method. An average mean stress is sometimes defined (e.g. Ref. 35). If the average mean stress was the significant variable, (a) and (b) of Fig. 8 would be equally damaging, but this is not likely because (a) has more cycles at a high tensile mean stress. The use of the average mean stress would necessitate the assumption that equal numbers of cycles equally above and below the average mean have a cancelling effect. It will be shown experimentally that this is not so.

It has been suggested (20, 36) that the average mean stress be defined for sections of the stress-strain history. Such a procedure could be applied to the sequences of Fig. 8, but for more irregular histories arbitrary divisions of the history into sections would have to be made. The life predictions could vary considerably depending on how the mean levels were chosen.

None of these difficulties are encountered if the mean stress of each cycle is determined. This is conveniently done when cycles are defined by the rain flow counting method.

Predicting Cyclic Stress-Strain Response

If the strain history at the location critical for fatigue failure is known, the stress history can be estimated. If the rain flow cycle counting method is applied to the strain history, the strain ranges which form closed stress-strain hysteresis loops, and those few strain ranges which do not, are identified. Stable stress-strain hysteresis loops from low cycle fatigue tests or the results of an incremental step test (37) can then be used to estimate the stress history. A computer simulation of the response of the material during cyclic loading could also be used to estimate the stress history. Martin et. al. (38) have successfully employed such a computer program for 2024-T4 aluminum, and work is in progress for other metals.

In situations where a known load or nominal strain history causes plastic straining at a stress concentration, the fatigue life can be predicted if the local stresses and strains at the stress concentration can be estimated (1, 38-43). Tucker (44) has developed a procedure for predicting the fatigue failure of notched parts subject to service loadings by using the simulated cyclic response of the material and Neuber's rule to estimate the local stresses and strains at the notch.

PROPOSED CUMULATIVE DAMAGE PROCEDURE

If both the strain history and the stress history at the location critical for fatigue failure are known or can be estimated, and if axial strain versus cycles to failure data for prestrained and non-prestrained specimens are available, the following cumulative damage procedure is recommended:

1. Apply the rain flow counting method to the strain history.
2. Use the stress history to determine the mean stress for each cycle defined by the rain flow counting method. Convert each cycle that has a significant mean stress to an equivalent completely reversed cycle by means of one of the mean stress parameters. If mean stress data are available for the material being used, these data may be used instead of a mean stress parameter.
3. Sum cycle ratios separately over the initiation and propagation periods based on the assumption that a few cycles of plastic prestraining causes crack initiation. Specifically, assume that the initiation period ends when $\Sigma (n/N_0) = 1$, the N_0 value for a given strain range being equal to $N_f - N_p$. Next sum damage using the strain-life curve for prestrained specimens. At strain ranges too large for there to be a significant effect of prestrain, $N_p = N_f$. Failure is predicted when $\Sigma (n/N_p) = 1$. Note that if significant plastic straining occurs near the beginning of the test, the initiation period is short and can be ignored.

GENERAL DESCRIPTION OF TESTS

Axially loaded unnotched specimens of 2024-T4 aluminum with cylindrical cross sections and having the dimensions shown in Fig. 9 were tested in either strain control or stress control. The specimens were machined from 3/4 in. rods of 2024-T4 which were purchased at the same time as those used in Refs. 12, 13, 38 and 45. The tensile properties, cyclic properties, composition, and source of this metal are given in Ref. 45.

All tests were conducted on an MTS closed loop axial hydraulic materials testing system. Strains were measured over a gage length of 0.55 in. using an Instron clip gage. Both the stresses and the strains were recorded for the duration of all tests.

In addition to the function generator that normally controls the testing system, a second function generator was employed so that two superimposed signals of different frequencies could be used as the control signal. A Hewlett-Packard Model 3722A Noise Generator at a setting of $n = 11$ was used to control some of the tests. This output, which consists of a sequence of approximately 200 peaks that is repeated continuously, is shown in Fig. 10 and will be referred to as the random sequence. An electronic switching and delay circuit was used so that the static stress level could be changed at intervals of one or more repetitions of the random sequence.

Ninety-eight specimens were tested to failure using a variety of strain or stress control conditions. These tests were conducted in twelve groups. In each group one or two test parameters were varied while the others were held constant. Within each group the tests were conducted in arbitrary order so as to avoid the possibility of systematic errors appearing as trends in the data.

In all but the first group, the test results are compared to the fatigue lives predicted* using the proposed cumulative damage procedure. The predictions were based on the data from Refs. 12 and 45 that is shown in Fig. 11. To predict the fatigue lives for some of the strain control tests, it was necessary to estimate the stable mean stresses. This was done using the rain flow counting method and the cyclically stabilized incremental step test result shown in Fig. 12.

For the stress control tests, the rain flow counting method was applied to the stress history instead of to the strain history. This was permissible because in all of these tests the plastic strains after cyclic stabilization were small.

*For each group of tests, the predictions were made before any tests in that group were conducted. Note that this is contrary to the common practice in cumulative damage studies, which is to conduct the tests and then to make fatigue life calculations, adjusting parameters until there is agreement with the actual fatigue lives.

TEST RESULTS AND DISCUSSION

Under this heading each group of tests is described and the results are presented and discussed. The effect of prestrain is investigated and the possible causes of this effect are explored. Next there are two groups of tests relating to the cause of the mean stress effect. Block size effects are shown to exist for histories with significant plastic strains and for histories with predominantly elastic strains. The next subheading is concerned with complicated strain control histories during which large plastic strains occur. Finally, there are four groups of stress control tests which have programmed variations of the static stress.

Effect of Prestrain

The effect of prestrain could be due to causes other than crack initiation. A number of specimens were prestrained 1, 3, 10 or 20 cycles at various amplitudes of prestrain and were then cycled to failure under stress control at ± 30 ksi. These data are shown in Fig. 13 and Table 2 and some examples of the stress-strain responses during prestraining are shown in Fig. 14 (a), (b), and (c). The specimens prestrained at ± 0.005 generally required a greater number of cycles for failure than did those prestrained at larger amplitudes. Other than this, there are no significant trends with either number of cycles or amplitude of prestrain, the bulk of the data lying in a scatter band roughly symmetrical about 3.5×10^5 cycles.

Slight buckling of the specimen during the compressive portion of the prestrain cycles could reduce the subsequent fatigue life due to superimposed bending stresses. The fatigue life would be expected to be shorter both for greater prestrain amplitude and number of cycles, but the data do not show this.

Cyclic hardening during prestraining could reduce the amount of plastic strain that occurs during the subsequent cycling, but this should cause prestraining to have a beneficial effect rather than the observed detrimental effect.

If the effect of prestrain were due to the removal of compressive surface residual stresses induced during fabrication (12), the specimens prestrained at ± 0.005 should have had fatigue lives similar to the others. It was verified that ± 0.005 is a sufficient amplitude to remove residual stresses by preloading a specimen to a compressive stress of 35 ksi (see Fig. 15) so as to simulate a residual stress of that value. The specimen was then cycled under strain control for 10 cycles at ± 0.0048 about the new strain zero and the resulting mean stress was observed to be 3.6 ksi in compression, which is insignificant compared with the original value.

Unloading from near the tip of a hysteresis loop after cycling at a large strain amplitude can cause a surface residual stress (46) which is compressive for unloading from tension. On one of the specimens the strain amplitude was gradually reduced to zero after prestraining (See Fig. 14 (c)) so as to avoid

any compressive residual stress. The subsequent fatigue life was not less than for the other prestrained specimens as would be expected if residual stresses induced by unloading after prestraining were significantly affecting the fatigue lives.

The test data are consistent with the assumption that prestraining causes damage to the material that could be attributed to the initiation of a crack. There was no evidence that buckling, cyclic hardening, or residual stresses cause the prestrain effect for 2024-T4 aluminum.

Cause of Mean Stress Effect

It was proposed by Takao and Endo (47) that crack initiation depends only on the amplitude of shear stress, mean stress having no effect. Since a tensile stress is thought to be necessary for crack propagation, compressive cycling should initiate a crack without causing any additional damage. Specimens that have been cycled in compression a sufficient number of cycles could then be tested to failure at different mean stresses. The results could be used to determine the effect of mean stress on the lengths of the initiation and propagation periods.

Seven specimens of 2024-T4 were cycled from zero to 50 ksi in compression for various numbers of cycles and were then cycled to failure at ± 40 ksi. These data are shown in Fig. 16 and Table 3. Note that the numbers of cycles to failure at ± 40 ksi are in close agreement with the lives of two specimens which had no compressive cycles applied and also with the fatigue life from Fig. 11 for non-prestrained specimens, which is 8.0×10^4 cycles. There was no tendency for the fatigue lives to be reduced to that for prestrained specimens, 3.5×10^4 cycles, even though as many as 3×10^6 compressive cycles were applied.

The compressive cycles therefore cause no significant fatigue damage. A greater number of compressive cycles or a larger compressive stress might have caused significant damage. Greater numbers of compressive cycles were not applied because of the excessive testing time necessary. A larger compressive stress would have resulted in large plastic strains at the beginning of the compressive cycling. Using the method proposed in Ref. 47, it is not practical and is probably not possible to determine if mean stress has an effect during crack initiation for 2024-T4 aluminum.

The variations in plastic strain range during the cycling at ± 40 ksi are plotted in Fig. 17 for some of the specimens. The hardening behavior was not significantly affected by the compressive cycling.

Fracture mechanics studies (e.g. Ref. 48) indicate that the size of fatigue crack necessary to cause final failure of a specimen should be smaller for tests in which higher maximum stresses frequently occur. One possible cause of the effect of mean stress is that, for a given constant amplitude, fewer cycles at a tensile mean stress are necessary to cause a crack of critical size than for zero or compressive mean stress simply because the critical crack size is smaller if the maximum stress is more tensile.

A number of prestrained specimens were tested at the same stress amplitude, but at different mean stresses. At intervals of 5% of the predicted lives, one cycle at ± 60 ksi was applied to exclude any effect of critical crack size. The results of these tests are given in Fig. 18 and Table 4. All of the specimens overloaded at ± 60 ksi would have had similar fatigue lives if the effect of mean stress was due solely to the critical crack size. But the overload cycles, and therefore the critical crack size, had no significant effect on the fatigue lives.

Tensile overload cycles could increase the fatigue life by causing crack blunting (49) or local compressive residual stresses (50), and compressive overloads could have the opposite effect. Tensile overloads alone could therefore obscure the effect of critical crack size. It was for this reason that the tensile overloads were followed by compressive overloads. For comparison, three specimens were tested with -60 ksi overloads. (See Table 4 and Fig. 18). As neither the ± 60 ksi nor the -60 ksi overloads had a significant effect on the fatigue lives, no evidence was found that either crack sharpening/blunting or local residual stresses are important for the specimens used here. The plastic strain ranges occurring on the overload cycles are plotted versus number of overload cycles in Fig. 19.

Mean stress could affect the fatigue life by changing the stable stress-strain hysteresis behavior. It is difficult to investigate this effect during simple stress control tests because plastic strains large enough to conveniently measure cause cycle-dependent creep if there is a significant mean stress. This problem was overcome by using a symmetrical strain control program where there were two loops having the same strain limits but different mean stresses. The result of such a program after the stress-strain response had stabilized is shown in Fig. 20. Note that for the two small loops in the center, the stress ranges are equal and the plastic strain ranges are equal. As no effect of the mean stress was found, this idea was not pursued further.

Block Size Effect

One group of tests was conducted in strain control with the mean strain changed alternately between equal positive and negative values. Between each change of the mean strain a number of cycles were applied, this number being varied for different specimens. Typical strain-time and stress-time histories, typical stress-strain behavior, and plotted test results are given in Fig. 21. The tabular results are in Table 5. The test results are seen to be in excellent agreement with the curve predicted by the proposed cumulative damage procedure. When k , the number of cycles per block at $\Delta\epsilon_2 = 0.0072$, is large, the cycles at $\Delta\epsilon_1 = 0.0150$ that occur one per block are too infrequent to have a significant effect. At small values of k the number of cycles to failure at $\Delta\epsilon_2 = 0.0072$ is reduced because the cycles at $\Delta\epsilon_1 = 0.0150$ contribute a major portion of the damage. The block size in a two level test can thus affect the fatigue life.

The variations in the total stress range, mean stress during the minor cycles, and plastic strain range are plotted in Fig. 22. Life predictions were made using the estimated stable value of the mean stress shown in Fig. 22. This value is a few ksi smaller than the measured values for most of the tests because slightly more cyclic hardening occurred than was predicted.

A similar block size effect can also occur where the strains are essentially elastic as is illustrated by the next group of tests. Stress control with an input signal consisting of a sine wave superimposed on a triangular wave of lower frequency was employed. Typical stress-time recordings are shown in Fig. 23 (a), and the results of these tests are given in Fig. 23 (b) and Table 6. The data show a trend similar to the predicted line, but there was a tendency for failures to occur at about half the predicted lives.

For the first specimens tested, excessive overstraining was avoided by gradually increasing the amplitude of the triangular wave as cyclic hardening progressed during the first few blocks. This procedure resulted in a tensile mean strain of approximately 0.02 which was considered to be a prestrain. Two specimens were prestrained 10 cycles at ± 0.012 before testing. There was no significant trend in the data due to the two different test procedures.

Low Cycle Fatigue with Complicated Strain Histories

Three groups of strain control tests were conducted in which strain ranges on the order of 0.02 or 0.03 were imposed. The first of these is illustrated in Figures 7 and 24 (a) and (b). By changing the sequence of the strain peaks, the stress-strain behavior was altered. Note that more plastic straining occurs for (a) than for (b). This difference is caused by the fact that the metal behaves differently depending on the sign of the previous large strain peak, i. e. there is a memory effect.

Tests were conducted using different values of $\Delta\epsilon_2$ (defined in Fig. 7) while $\Delta\epsilon_1$ was kept constant at 0.020. The results are given in Fig. 24 (c) and Table 7. There is a significant difference in the fatigue lives for the two different sequences of straining and the agreement of the data points with the predicted lines is reasonable. Typical variations in the total stress range and plastic strain range during these tests are shown in Fig. 25. In each of the memory effect tests there were small closed hysteresis loops at equal strain ranges but with different mean stresses. There was never any measurable dependance of the shape of these loops on the mean stress.

Typical stress-strain, strain-time, and stress-time recordings for the second group of low cycle tests are shown in Figs. 26 (a) and (b). Two sine waves having frequencies with a ratio of 50 were superimposed to obtain the control signal. The amplitude of the lower frequency wave was varied while that of the higher frequency wave was kept constant.

Results for this group of tests are given in Fig. 26 (c) and Table 8. The data show the same trend as the predicted line, but the failures usually occurred at 60 or 70% of the predicted lives. According to the proposed damage procedure, most of the damage was done by the minor cycles for the smaller values of $\Delta\epsilon_1$, but at the larger values of $\Delta\epsilon_1$ the minor cycles were less important. The variations in the total stress range and the plastic strain range during these tests are shown in Fig. 27 (a). In Fig. 27 (b) the stable

(half life) values of $\Delta\sigma_1$ are plotted against $\Delta\epsilon_1$. Note that most of the points lie above the cyclic stress-strain curve, indicating that more cyclic hardening occurred than for simple constant amplitude tests.

To predict the fatigue lives for these tests, it was necessary to estimate the mean stress of each small cycle in one block of straining after cyclic stabilization. This was done using the incremental step test of Fig. 12. Stress range versus strain range for this incremental step test is also shown in Fig. 27 (b). The largest mean stresses for each test were underestimated by half the distance between the plotted points and this curve. The line in Fig. 27 (b) for the incremental step test lies slightly below the cyclic stress-strain curve. It is likely that the specimen used for this test was of slightly less than average hardness, because other incremental step test results for 2024-T4 aluminum (37, 51) are in closer agreement with the cyclic stress-strain curve.

The third group of low cycle tests employed the random sequence (Fig. 10) as the strain control signal. The random sequence was repeatedly applied and was attenuated, but not distorted, by various amounts to give different values of $\Delta\epsilon_{rs}$. Typical stress-strain, strain-time, and stress-time recordings are shown in Fig. 28 (a) and (b), and the test results in Fig. 28 (c) and Table 9. The test results are in excellent agreement with the predicted line.

For one of the strain control random tests, the strain ranges counted as cycles by the rain flow counting method, which are the strain ranges for all closed hysteresis loops, are plotted against the corresponding stable stress ranges in Fig. 29. The plotted points lie slightly but not significantly below the cyclic stress-strain curve. Similar plots for several of the other strain control random block tests showed similar or better agreement with the cyclic stress-strain curve. It is interesting that the cyclic stress-strain curve is valid for this type of history.

Complicated Histories with Periodic Variation of the Mean Stress

Four groups of tests were conducted in stress control with programmed periodic changes in the static stress level. All specimens were prestrained 10 cycles at ± 0.012 similar to Fig. 14 (c). If the specimens had not been intentionally prestrained, large plastic strains would have occurred during cyclic hardening for most of the tests. Emphasis on predicting the fatigue lives of prestrained specimens is proper because most locations critical for fatigue in real machines or structures will probably be plastically strained, if not during fabrication or manufacture, at some time during the service life. If significant plastic straining does not occur, the assumption that it has occurred will lead to conservative predictions.

In the first group of tests an average mean stress of 10 ksi was used with the mean stress varied in a square wave about 10 ksi, different amplitudes of variation being used for different specimens. Forty cycles at a stress range of 50 ksi were applied during each cycle of the mean stress.

Typical stress histories are shown in Fig. 30 (a). After the cyclically stable state was reached, no measurable plastic strains were recorded in any of these tests. The test results are shown in Fig. 30 (b) and Table 10. The predicted and actual fatigue lives did not differ by more than 30%.

If equal numbers of cycles equally above and below the average mean stress have cancelling effects, the fatigue lives of all of the specimens would be similar to the fatigue life of the specimen that was tested at a constant mean of 10 ksi. The dominant effect was that the cycles at the high tensile mean stress shortened the fatigue lives. Note that the use of the average mean stress to make the life predictions would have resulted in significant nonconservative errors for any variation of the mean greater than ± 5 ksi.

Stress histories for the next group of tests are shown in Fig. 31 (a). Two sine waves having frequencies with a ratio of 50 were superimposed so that the peak tensile and compressive stresses in each block were +50 ksi and -50 ksi respectively. The results of these tests are given in Fig. 31 (b) and Table 11. Where $\Delta\sigma_2$ was small, the minor cycles were predicted to have little effect and the fatigue damage for each block was calculated to be the same as for one cycle at ± 50 ksi. For $\Delta\sigma_2$ near 50 ksi, the calculated damage per block approaches the value for 50 cycles at ± 50 ksi. At small and large values of $\Delta\sigma_2$ the test results and predictions are in excellent agreement, but for intermediate values there is a tendency for the failures to occur at about half of the predicted lives.

In another group of stress control tests the static level was changed between equal tensile and compressive values with one random sequence (See Fig. 10) applied for each change in level. Typical stress histories are shown in Fig. 32 (a), and the test results are given in Fig. 32 (b) and Table 12. The quantity $\Delta\sigma_1$ was kept constant at 120 ksi and $\Delta\sigma_{rs}$ was varied over a wide range. Agreement between the actual and predicted fatigue lives was good except for $\Delta\sigma_{rs}$ between 80 and 110 ksi where there was a tendency for failure at summations of cycle ratios around 0.4 or 0.5. Typical stress-strain response and typical variations of the plastic strain range are shown in Fig. 33.

The final group of tests employed the random sequence at five different static levels as shown in Fig. 34 (a). At each level the random sequence was repeated a number of times. The number of repetitions was the same for all levels of each test, but was varied for different tests. Values of $\Delta\sigma_1 = 120$ ksi and $\Delta\sigma_{rs} = 50$ ksi were used in all of the tests. As it has been noticed from the other test groups that the largest differences between the actual and predicted lives occurred where there were superimposed loadings and predominantly elastic behavior, this group of tests was designed as an extreme case of that situation. The test results in Fig. 34 (b) and Table 13 show that the data have a trend similar to the predictions and that summations of cycle ratios near 0.4 were obtained.

CONCLUSIONS

The proposed cumulative damage procedure gives reasonable predictions of the fatigue failure of 2024-T4 aluminum for a wide variety of complicated stress-strain histories. Tests were conducted to investigate all histories the author could devise which might deceive the proposed procedure. For the 83 specimens tested to failure for which failure predictions were made, the summations of cycle ratios were all between 0.36 and 1.50. The values are distributed as shown in Fig. 35. Most of the values below 0.60 occurred in situations where there were large changes in the mean stress with superimposed minor cycles for which the calculated damage was significant. It is likely that the damages due to large transition cycles and the minor cycles superimposed on them simply do not add linearly. In situations where there are significant minor cycles superimposed on large changes in the mean stress, an adjustment of a factor of two in life predictions could be made, but a more complicated damage procedure is not justified.

To apply the proposed cumulative damage procedure to a new material, it is necessary to have completely reversed strain-life data for prestrained and non-prestrained specimens. Strain-life data at mean stresses other than zero are desirable but not essential. A set of stable hysteresis loops from the low cycle strain-life tests or the result of an incremental step test is needed. A computer simulation of the stable cyclic response of the material would greatly increase the efficiency of the calculations in those situations where the stress history or both the stress history and the strain history must be estimated.

The following specific conclusions are supported by the test data on 2024-T4 aluminum:

1. For prestrains larger than ± 0.005 , the effect on the subsequent fatigue life is not dependent on the number of cycles or amplitude of prestrain. The effect of prestrain is consistent with the assumption that prestraining causes crack initiation. The effect is not caused by cycle-dependent buckling, cyclic hardening, or residual stresses.
2. No significant fatigue damage was caused by as many as 3×10^6 cycles from 0 to -50 ksi, which is approximately the largest compressive stress that can be applied without causing significant plastic straining near the beginning of the test.
3. There was no evidence that the effect of mean stress on the fatigue life is due to the inverse relationship between critical crack size and maximum tensile stress.
4. Significant block size effects exist and are accounted for if damage is calculated for the major cycle that occurs once per block.

5. In tests with complicated histories that cause large plastic strains, the counting of all closed hysteresis loops as cycles by means of the rain flow counting method allows accurate life predictions.
6. In complicated history tests where there are closed hysteresis loops at different mean stresses, there is no measurable effect of the mean stress on the stable stress-strain hysteresis behavior.
7. The stable stress-strain relationship for closed hysteresis loops during complicated histories is in general agreement with the cyclic stress-strain curve. The largest deviations occurred for the tests with superimposed sine waves in strain control where some of the stress ranges were about 5% larger than the values from the cyclic stress-strain curve.
8. The use of the average mean stress is an approximation that should be used with extreme caution. It is valid only if the variations in the mean stress are small.
9. Using the rain flow counting method, the strain-life curve for prestrained specimens, and the mean stress of each cycle gives reasonable predictions of the fatigue lives of prestrained specimens subjected to complicated histories where there is a changing mean stress. Some of the tests of this type were similar to service loadings for actual machines, vehicles, and aircraft (20) in that there were irregular loadings superimposed on changes in the static level.
10. The use of any method of cycle counting other than the range pair or rain flow methods can result in inconsistencies and gross differences between predicted and actual fatigue lives.

RECOMMENDATIONS FOR FUTURE RESEARCH

Complicated history tests on smooth axially loaded specimens of other engineering metals, particularly steels, are needed. The proposed cumulative damage procedure should be extended to include the effect of unstable cyclic softening in steels (52). History or strain rate dependence of the stable stress-strain behavior might also be important for certain metals.

Additional studies (See Refs. 38, 43, and 44) are needed in which the fatigue lives of notched members subjected to complicated load histories are predicted by first estimating the stresses and strains at the critical location. Strain measurements in notch roots during irregular load histories are needed so that methods of calculating local stresses and strains (1, 41) can be evaluated.

REFERENCES

1. J. H. Crews, Jr. and H. F. Hardrath, "A Study of Cyclic Plastic Stresses at a Notch Root," *Experimental Mechanics*, SESA, Vol. 6, No. 6, June 1966, pp. 313-320.
2. A. A. Blatherwick and B. K. Olson, "Stress Redistribution in Notched Specimens Under Cyclic Stress," *Experimental Mechanics*, SESA, Vol. 8, No. 8, Aug. 1968, pp. 356-361.
3. M. S. Hunter and W. G. Fricke, Jr., "Metallographic Aspects of Fatigue Behavior of Aluminum," *Proc. ASTM*, Vol. 54, 1954, p. 717-732.
4. M. S. Hunter and W. G. Fricke, Jr., "Fatigue Crack Propagation in Aluminum Alloys," *Proc. ASTM*, Vol. 56, 1956, p. 1038-1046.
5. M. S. Hunter and W. G. Fricke, Jr., "Effect of Alloy Content on the Metallographic Changes Accompanying Fatigue," *Proc. ASTM*, Vol. 55, 1955, pp. 942-953.
6. P. J. E. Forsyth, "A Two Stage Process of Fatigue Crack Growth," *Proc. of the Crack Propagation Symposium*, Cranfield, England, 1961, Vol. I, pp. 76-94.
7. M. Hempel, "Metallographic Observations on the Fatigue of Steels," *International Conference on Fatigue of Metals*, IME and ASME, London and New York, 1956, pp. 543-544.
8. R. C. Boettner, C. Laird, and A. J. McEvily, "Crack Nucleation and Growth in High Strain-Low Cycle Fatigue," *Trans. AIME*, Vol. 233, No. 1, 1965, pp. 379-387.
9. H. F. Hardrath, "A Review of Cumulative Damage for Fatigue Committee of the Structures and Materials Panel Advisory Group for Aeronautical Research and Development," *NASA Langley Research Center*, Hampton, Virginia, June 1965.
10. H. T. Corten, "Overstressing and Understressing in Fatigue," *Metals Engineering Design*, ASME Handbook ed. by O. J. Horger, McGraw-Hill, 1965, pp. 231-241.
11. S. S. Manson, J. C. Freche, and C. R. Ensign, "Application of a Double Linear Damage Rule to Cumulative Fatigue," *ASTM STP No. 415*, 1966, pp. 384-412.
12. T. H. Topper and B. I. Sandor, "Effects of Mean Stress and Prestrain on Fatigue Damage Summation," *ASTM STP No. 462*, 1970, pp. 93-104.

13. T. H. Topper, B. I. Sandor, and J. Morrow, "Cumulative Fatigue Damage Under Cyclic Strain Control," *Journal of Materials*, ASTM, Vol. 4, No. 1, March 1969, pp. 189-199.
14. K. Ohji, W. R. Miller and J. Marin, "Cumulative Damage and Effect of Mean Strain in Low-Cycle Fatigue of a 2024-T351 Aluminum Alloy," *Trans. ASME, Journal of Basic Engineering*, Dec. 1966, pp. 801-810.
15. R. D'Amato, "A Study of the Strain-Hardening and Cumulative Damage Behavior of 2024-T4 Aluminum Alloy in the Low-Cycle Fatigue Range," WADD TR60-175, Wright Air Development Center, Ohio, April 1960.
16. D. E. Gucer, "Cumulative Fatigue at High Plastic Strains," *Trans. Quarterly, ASM*, Vol. 54, No. 2, June 1961, pp. 176-184.
17. T. Nakagawa and S. Nitta, "Plastic Fatigue Life of Steel Under Periodical Multi-Stage Stress Amplitudes," *Proc. of the Symposium on Fatigue of Metals Under Service Loads*, The Society of Materials Science, Kyoto, Japan, 22 Sept. 1967, pp. 73-83.
18. H. J. Grover, "An Observation Concerning the Cycle Ratio in Cumulative Damage," *ASTM STP 274*, 1959, pp. 120-124.
19. G. M. Sinclair, "An Investigation of the Coaxing Effect in Fatigue of Metals," *Proc. of ASTM*, Vol. 52, 1952, pp. 743-751.
20. G. H. Jacoby, "Fatigue Life Estimation Processes Under Conditions of Irregularly Varying Loads," AFML TR 67-215, Air Force Materials Lab., Wright-Patterson AFB, Ohio, Aug. 1967.
21. J. Schijve, "Analysis of Random Load-Time Histories with Relation to Fatigue Tests and Life Calculations," *Fatigue of Aircraft Structures*, ed. by W. Barrios & E. L. Ripley, Pergamon Press, 1963, pp. 115-148.
22. A. Burns, "Fatigue Loadings in Flight: Loads in the Tailplane and Fin of a Varsity," *Aeronautical Research Council Technical Report C. P. 256*, London, 1956.
23. M. Matsuishi and T. Endo, "Fatigue of Metals Subjected to Varying Stress," Paper presented at Japan Society of Mechanical Engineers, Fukuoka, Japan, March 1968.
24. J. O. Smith, "The Effect of Range of Stress on the Fatigue Strength of Metals, Bulletin No. 334, University of Illinois, Engineering Experiment Station, Urbana, Feb. 1942.
25. F. L. Stulen, "Fatigue Life Data Displayed by a Single Quantity Relating Alternating and Mean Stress," AFML TR 65-121, Air Force Materials Lab., Wright-Patterson AFB, Ohio, July 1965.

26. J. Morrow, "Fatigue Properties of Metals," Section 3.2 of Fatigue Design Handbook, Society of Automotive Engineers, 1968. Section 3.2 is a summary of a paper presented at a meeting of Division 4 of the SAE Iron and Steel Technical Committee, Nov. 4, 1964.
27. K. N. Smith, P. Watson, and T. H. Topper, "A Stress-Strain Function for the Fatigue of Metals," Report No. 21, Solid Mechanics Division, University of Waterloo, Ontario, Canada, Oct. 1969.
28. R. W. Landgraf, "Effect of Mean Stress on the Fatigue Behavior of a Hard Steel," M. S. Thesis, Dept. of Theoretical and Applied Mechanics, University of Illinois, Urbana, 1966. See also T. & A. M. Report No. 662.
29. H. J. Grover et al, "Axial-Load Fatigue Properties of 24S-T and 75S-T Aluminum Alloy as Determined in Several Laboratories," NACA TN 2928, National Advisory Committee for Aeronautics, Wash., D. C., May 1953.
30. A. A. Blatherwick and B. J. Lazan, "Fatigue Properties of Extruded Magnesium Alloy ZK 60 Under Various Combinations of Alternating and Mean Axial Stresses," WADC TR 53-181, Wright Air Development Center, Ohio, Aug. 1953.
31. B. J. Lazan and A. A. Blatherwick, "Fatigue Properties of Aluminum Alloys at Various Direct Stress Ratios," WADC TR 52-307, Wright Air Development Center, Ohio, 1952.
32. F. M. Howell and J. L. Miller, "Axial-Stress Fatigue Strengths of Several Structural Aluminum Alloys," Proc. ASTM, Vol. 55, 1955, pp. 955-967.
33. H. C. O'Connor and J. L. M. Morrison, "The Effect of Mean Stress on the Push-Pull Fatigue Properties of an Alloy Steel," International Conference on Fatigue of Metals, IME and ASME, London and New York, 1956, pp. 102-109.
34. H. J. Grover, S. M. Bishop, and L. R. Jackson, "Fatigue Strength of Aircraft Metals: Axial Load Fatigue Tests on Unnotched Sheet Specimens of 24S-T3 and 75S-T6 Aluminum Alloys and of SAE 4130 Steel," NACA TN 2324, National Advisory Committee for Aeronautics, Wash., D. C., March 1951.
35. W. H. Raser, Jr., "Fatigue Analysis and Measurement of Random Loading," Metal Fatigue: Theory and Design, ed. by A. F. Madaayag, John Wiley & Sons, 1969, pp. 247-288.
36. H. L. Leve, "Cumulative Damage Theories," Metal Fatigue: Theory and Design, ed. by A. F. Madaayag, John Wiley & Sons, 1969, pp. 170-203.
37. R. W. Landgraf, J. Morrow, and T. Endo, "Determination of the Cyclic Stress-Strain Curve," Journal of Materials, ASTM, Vol. 4, No. 1, March 1969, pp. 176-188.

38. J. F. Martin, T. H. Topper, and G. M. Sinclair, "Computer Based Simulation of Cyclic Stress Strain Behavior," T. & A. M. Report No. 326, Dept. of Theoretical and Applied Mechanics, University of Illinois, Urbana, July 1969. To be published in Materials Research and Standards, ASTM.
39. S. S. Manson and M. H. Hirschberg, "Crack Initiation and Propagation in Notched Fatigue Specimens," Proc. of the First International Conference on Fracture, The Japanese Society for Strength and Fracture of Materials, Sendai, Japan, Sept. 1965, Vol. 1, pp. 479-498.
40. T. J. Dolan, "Non-Linear Response Under Cyclic Loading Conditions," Proc. of the 9th Midwestern Mechanics Conference, Madison, Wis., Aug. 1965, pp. 3-21.
41. R. M. Wetzel, "Smooth Specimen Simulation of Fatigue Behavior of Notches," Journal of Materials, ASTM, Vol. 3, No. 3, Sept. 1968, pp. 646-657.
42. T. H. Topper, R. M. Wetzel, and J. Morrow, "Neuber's Rule Applied to Fatigue of Notched Specimens," Journal of Materials, ASTM, Vol. 4, No. 1, March 1969, pp. 200-209.
43. S. J. Stadnick, "Simulation of Overload Effect in Fatigue Based on Neuber's Analysis," M. S. Thesis, Dept. of Theoretical and Applied Mechanics, University of Illinois, Urbana, 1969. See also T. & A. M. Report No. 325.
44. L. E. Tucker, "A Procedure for Designing Against Fatigue Failure of Notched Parts," M. S. Thesis, Dept. of Theoretical and Applied Mechanics, University of Illinois, Urbana, 1970.
45. T. Endo and J. Morrow, "Cyclic Stress-Strain and Fatigue Behavior of Representative Aircraft Metals," Journal of Materials, ASTM, Vol. 4, No. 1, March 1969, pp. 159-175.
46. S. Taira and M. Kitagawa, "X-Ray Study of Low Cycle Fatigue: Effect of Residual Stress on Fatigue Life," Symposium on X-Ray Studies of Material Strength, The Society of Materials Science, Tokyo, Japan, 1966, pp. 84-87.
47. K. Takao and T. Endo, "Effect of Mean Stress on the Fatigue Crack Initiation and Propagation of a Carbon Steel," Preprint for annual meeting of Japan Society of Mechanical Engineers, No. 203, April 1969, pp. 129-132.
48. R. H. Christensen, "Cracking and Fracture in Metals and Structures," Proc. of the Crack Propagation Symposium, Cranfield, England, 1961, Vol. II, pp. 326-374.
49. J. R. Rice, "Mechanics of Crack Tip Deformation and Extension by Fatigue," ASTM STP 415, 1967, pp. 415-457.

50. J. Schijve, "Significance of Fatigue Cracks in Micro-Range and Macro-Range," ASTM STP 415, 1967, pp. 415-457.
51. J. F. Martin, Private communication with the author concerning the data used in the preparation of Ref. 38, Oct. 1970.
52. J. Morrow, G. R. Halford, and J. F. Millan, "Optimum Hardness for Maximum Fatigue Strength of Steels," Proc. of the First International Conference on Fracture, The Japanese Society for Strength and Fracture of Materials, Sendai, Japan, Sept. 1965, Vol. 3, pp. 1611-1636.

TABLE 1 CYCLE COUNTING METHODS

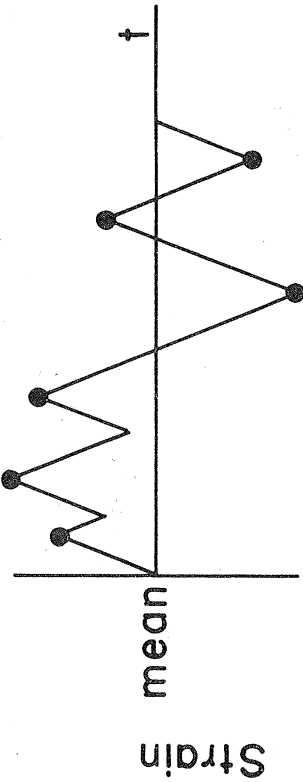
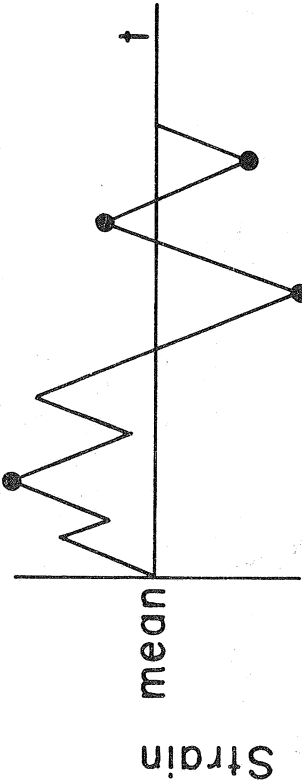
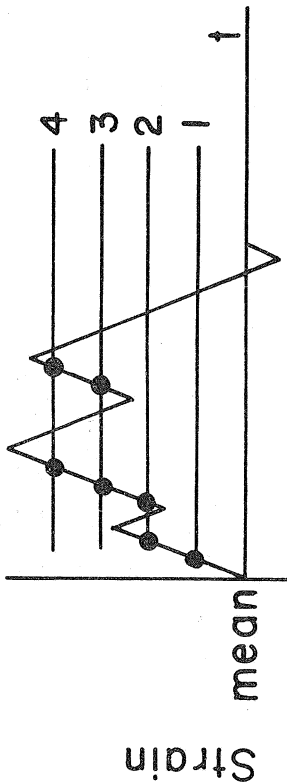
Name	Example	Description
Peak		All maximums above the mean and minimums below the mean are counted.
Mean crossing peak		Only the largest peak between successive crossings of the mean is counted.
Level crossing		All positive slope level crossings above the mean, and negative slope level crossings below the mean, are counted.

TABLE I CYCLE COUNTING METHODS (cont'd)

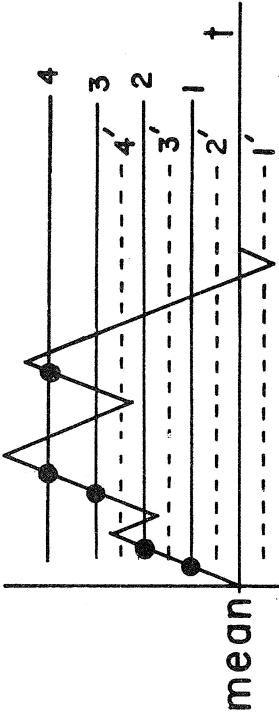
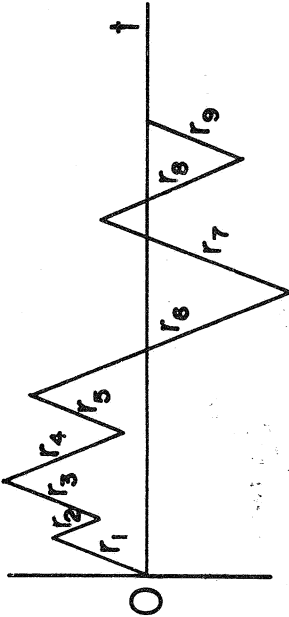
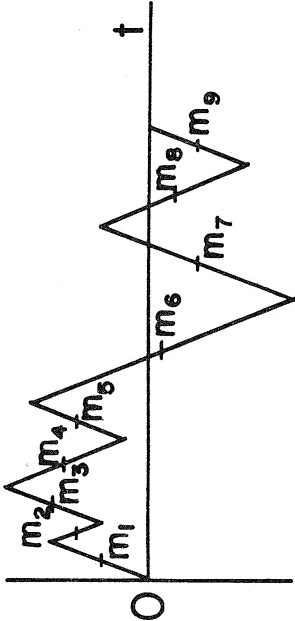
Name	Example	Description
Fatigue - meter	 <p>Strain</p>	<p>Similar to level crossing except that only one count is made between successive crossings of a lower level associated with each counting level.</p>
Range	 <p>Strain</p>	<p>Each range, i. e. the difference between successive peak values, is counted as 1/2 cycle, the amplitude of which is half the range.</p>
Range - mean	 <p>Strain</p>	<p>Ranges are counted as above and the mean value of each range is also considered.</p>

TABLE 2
EFFECT OF NUMBER OF CYCLES AND
AMPLITUDE OF PRESTRAIN

Prestrain Amplitude	Cycles of Prestrain	Cycles to Failure at ± 30 ksi
0.0050	1	1 224 500
0.0050	3	1 722 700
0.0050	10	629 900
0.0050	20	1 516 700
0.0070	10	390 400
0.0080	3	409 800
0.0100	1	668 900
0.0100	10*	462 900
0.0100	11	230 100
0.0100	20	340 200
0.0103	3	328 800
0.0200	1	274 200
0.0200	3	267 700
0.0200	10	281 300
0.0200	20	207 500

*Strain amplitude linearly decreased to zero during cycles 10 to 20.
See Fig. 14 (c).

Note: All specimens were prestrained in strain control, tested in stress control.

TABLE 3
FATIGUE LIVES AT ± 40 ksi AFTER
CYCLING IN COMPRESSION

Cycles in Compression	Cycles to Failure at ± 40 ksi	Summation of Cycle Ratios
n_1	n_2	$\Sigma (n/N_f)$
0	54 000	0.68
0	90 900	1.14
3 000	71 300	0.89
10 000	70 900	0.88
30 000	105 300	1.32
100 000	74 200	0.93
300 000	98 000	1.23
1 000 000	96 400	1.20
3 000 000	63 200	0.79

Notes:

1. The compressive cycling was between 0 and -50 ksi.
2. During the first 100 to 200 compressive cycles, the minimum stress was gradually decreased to -50 ksi as the specimen hardened. By this procedure the accumulated plastic strain during the compressive cycling was limited, the measured values all being between 0.0055 and 0.0075.

TABLE 4

EFFECT OF OVERLOAD CYCLES ON THE FATIGUE LIVES
AT DIFFERENT MEAN STRESSES

Mean Stress	Cycles Between Overloads	Type Overload	Cycles at $\Delta\sigma = 50$ ksi to Failure	Summation of Cycle Ratios
σ_o , ksi		ksi		$\Sigma (n/N_p)$
-10	200 000	± 60	>10 000 000	--
0	30 000	± 60	630 000	1.05
10	10 000	± 60	131 600	0.66
20	4 000	± 60	69 600	0.87
35	2 000	± 60	34 000	0.85
0	30 000	-60	900 000	1.50
10	10 000	-60	133 000	0.67
20	4 000	-60	65 900	0.82

Notes:

1. All specimens were prestrained 10 cycles at ± 0.012 similar to Fig. 14 (c), then tested in stress control at $\Delta\sigma = 50$ ksi.
2. Overload cycles were applied at intervals of 5% of the estimated fatigue lives.

TABLE 5
STRAIN CONTROL BLOCK SIZE EFFECT TESTS

Cycles at $\Delta\epsilon_2 = 0.0072$ Per Block	Cycles at $\Delta\epsilon_2 = 0.0072$ to Failure	Summation of Cycle Ratios
k		$\Sigma (n/N_p)$
2	3 160	1.21
6	8 580	1.29
20	14 750	1.00
40	17 800	0.89
100	19 200	0.75
300	25 800	0.89

Note: The mean strain was changed between +0.0039 and -0.0039 at intervals of $k/2$ cycles at $\Delta\epsilon_2$, giving a total strain range of $\Delta\epsilon_1 = 0.0150$.

TABLE 6
STRESS CONTROL BLOCK SIZE EFFECT TESTS

Cycles at $\Delta\sigma_2 = 31$ ksi Per Block	Cycles at $\Delta\sigma_2 = 31$ ksi to Failure	Summation of Cycle Ratios
k		$\Sigma (n/N_p)$
20	110 000	0.73
50	141 000	0.52
100	201 000	0.54
150	213 000	0.50
340	278 000	0.55
600	293 000	0.54

Notes:

1. The mean stress was varied in a triangular wave about +10 ksi at an amplitude of 30 ksi, giving a total stress range of $\Delta\sigma_1 = 91$ ksi.
2. The specimens for which $k = 100$ and 340 were prestrained 10 cycles at ± 0.012 similar to Fig. 14 (c). For all of the others, $\Delta\sigma_2$ was gradually increased to the test value as the specimen hardened during the first few blocks. This resulted in a mean strain of approximately 0.02 that did not increase measurably until the last 5% of the fatigue life.

TABLE 7
STRAIN CONTROL MEMORY EFFECT TESTS

Minor Strain Range	Sequence	Blocks to Failure	Summation of Cycle Ratios
$\Delta\epsilon_2$			$\Sigma (n/N_p)$
0.0040	a	721	1.20
0.0080	a	632	1.10
0.0120	a	590	1.34
0.0150	a	395	1.22
0.0170	a	304	1.15
0.0190	a	220	1.00
0.0040	b	639	1.06
0.0080	b	591	0.99
0.0120	b	507	0.86
0.0150	b	612	1.08
0.0170	b	553	1.04
0.0190	b	467	0.97

Notes:

1. Sequences (a) and (b) refer to Fig. 7 (a) and Fig. 7 (b), respectively.
2. For all tests $\Delta\epsilon_1 = 0.020$.

TABLE 8

TESTS WITH SINUSOIDAL VARIATION OF THE MEAN STRAIN

Total Strain Range	Blocks to Failure	Summation of Cycle Ratios
$\Delta\epsilon_1$		$\Sigma (n/N_p)$
0.0070	1 582	1.32
0.0120	414	0.56
0.0170	265	0.62
0.0220	131	0.46
0.0270	149	0.73
0.0320	109	0.73
0.0370	74	0.67

Note: For all tests $\Delta\epsilon_2 = 0.0070$ and $k = 50$

TABLE 9
STRAIN CONTROL RANDOM SEQUENCE TESTS

Maximum Strain Range	Blocks to Failure	Summation of Cycle Ratios
$\Delta\epsilon_{rs}$		$\Sigma (n/N_p)$
0.0170	111	0.88
0.0204	60	0.90
0.0238	34	0.83
0.0272	24	0.89
0.0306	15	0.78
0.0340	10	0.69

Note: The random sequence in Fig. 10 was attenuated by various amounts and used to control the strain.

TABLE 10
CONSTANT AVERAGE MEAN STRESS TESTS

Amplitude of Mean Change About +10 ksi	Total Stress Range	Cycles at $\Delta\sigma_2 = 50$ ksi to Failure	Summation of Cycle Ratios
$\Delta\sigma_o/2$, ksi	$\Delta\sigma_1$, ksi		$\Sigma (n/N_p)$
0	50	259 900	1.30
5	60	155 800	0.93
10	70	132 300	1.06
15	80	84 600	0.99
20	90	59 600	0.91
25	100	41 400	0.73

Notes:

1. The mean stress was changed between $10 + \Delta\sigma_o/2$ and $10 - \Delta\sigma_o/2$ at intervals of 20 cycles at $\Delta\sigma_2 = 50$ ksi.
2. All specimens were prestrained 10 cycles at ± 0.012 similar to Fig. 14 (c).

TABLE 11
TESTS WITH SINUSOIDAL VARIATION OF THE MEAN STRESS

Minor Stress Range $\Delta\sigma_2$, ksi	Blocks to Failure	Summation of Cycle Ratios $\Sigma (n/N_p)$
10	14 200	1.29
20	11 750	1.07
30	5 160	0.78
40	2 280	0.56
50	1 660	0.63
60	1 050	0.54
70	977	0.84
80	738	1.18
90	468	1.30

Notes:

1. For all tests $\Delta\sigma_1 = 100$ ksi and $k = 50$.
2. All specimens were prestrained 10 cycles at ± 0.012 similar to Fig. 14 (c).

TABLE 12

STRESS CONTROL RANDOM SEQUENCES AT TWO STATIC LEVELS

Maximum Stress Range During Random Sequence	Blocks to Failure	Summation of Cycle Ratios
$\Delta\sigma_{rs}$, ksi		$\Sigma (n/N_p)$
30	2 892	1.14
40	1 976	0.93
50	1 688	0.96
60	1 189	0.85
70	898	0.76
80	632	0.59
90	355	0.36
100	358	0.46
110	269	0.50
120	257	0.77

Notes:

1. The static stress level was changed between equal tensile and compressive values after each random sequence such that the total stress range was $\Delta\sigma_1 = 120$ ksi.
2. All specimens were prestrained 10 cycles at ± 0.012 similar to Fig. 14 (c).

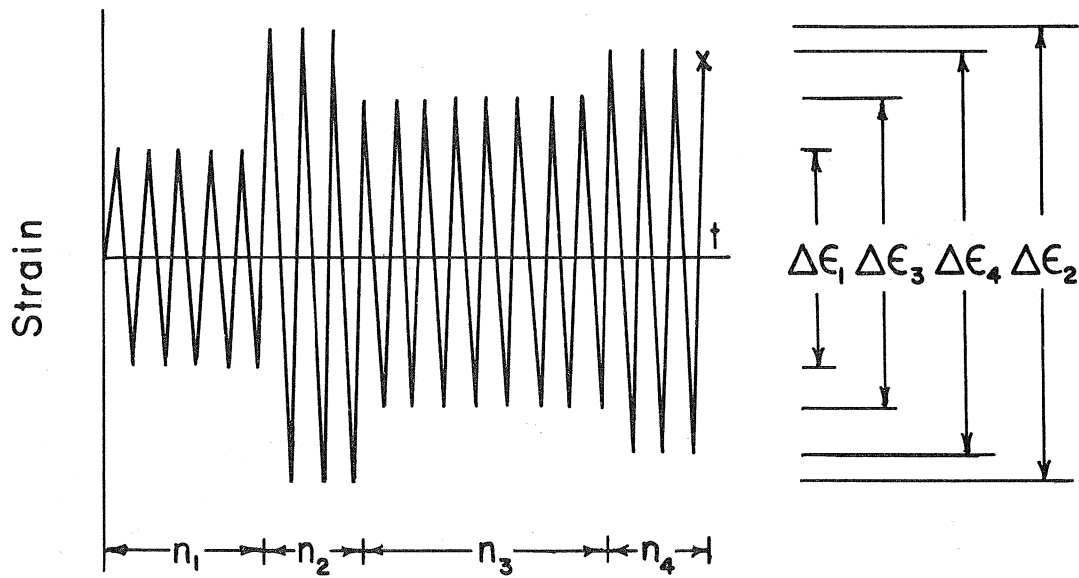
TABLE 13

STRESS CONTROL RANDOM SEQUENCES AT FIVE STATIC LEVELS

Repetitions of the Random Sequence Between Static Level Changes	Blocks to Failure	Summation of Cycle Ratios
j		$\Sigma (n/N_p)$
1	781	0.55
2	405	0.41
4	263	0.42
7	164	0.41
10	117	0.40

Notes:

1. For all tests $\Delta\sigma_{rs} = 50$ ksi and $\Delta\sigma_1 = 120$ ksi. The static stress level was changed according to the following: 0, +35, -15, +15, and -35 ksi.
2. All specimens prestrained 10 cycles at ± 0.012 similar to Fig. 14 (c).



n_i = number of cycles applied at $\Delta\epsilon_i$

N_{fi} = cycles to failure at a constant amplitude of $\frac{\Delta\epsilon_i}{2}$

Failure predicted when $\sum \frac{n_i}{N_{fi}} = 1$

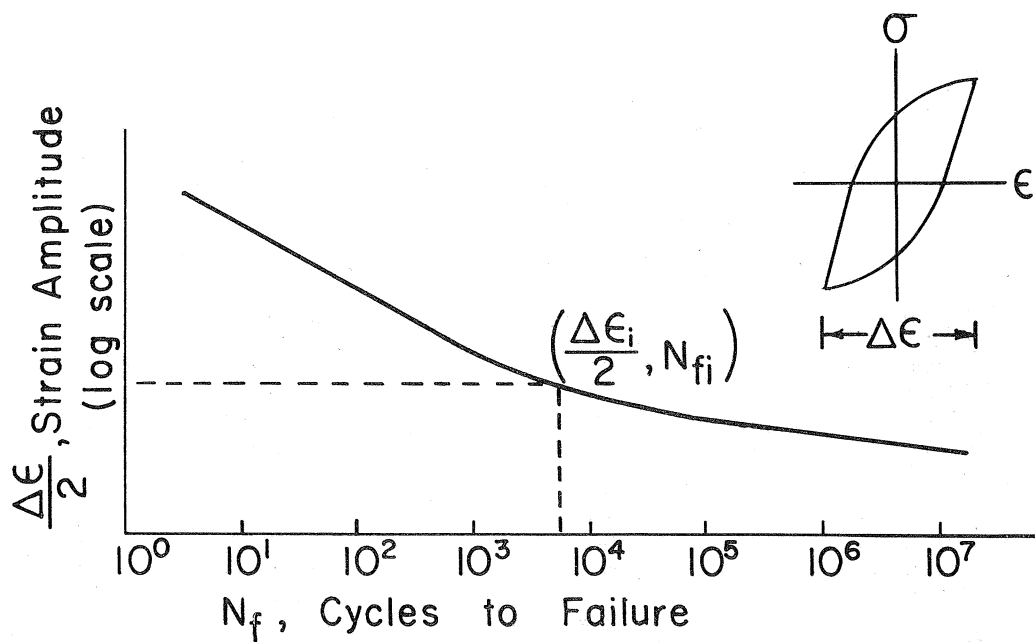


Fig. 1 Fatigue failure prediction by linear summation of cycle ratios based on strain amplitude

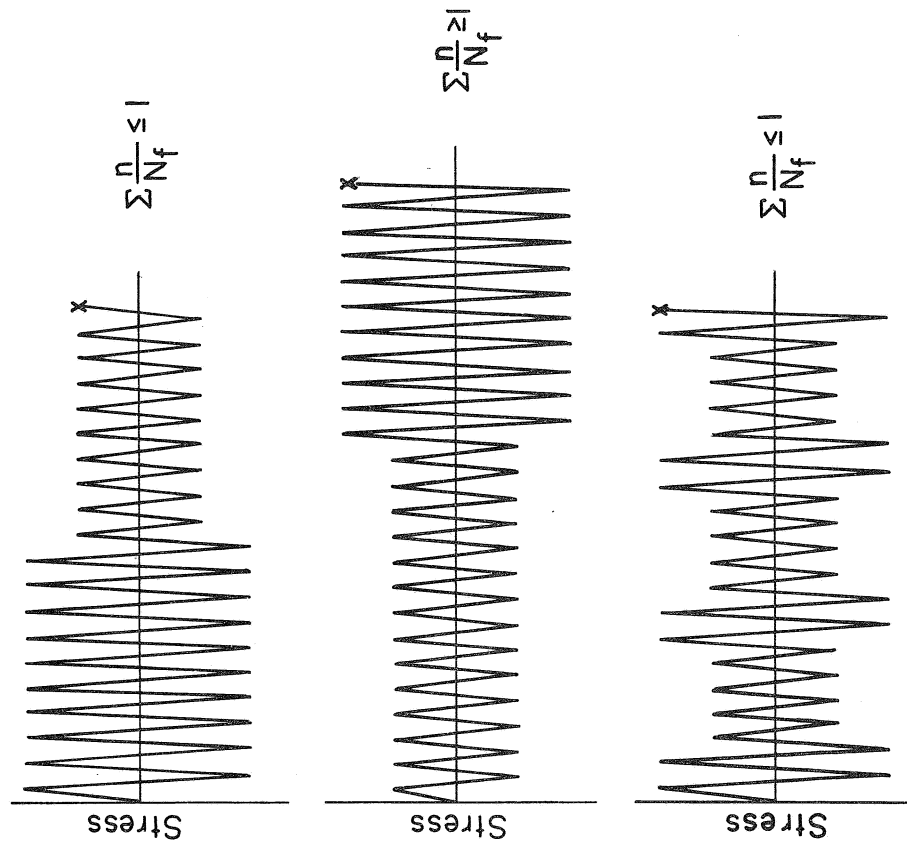
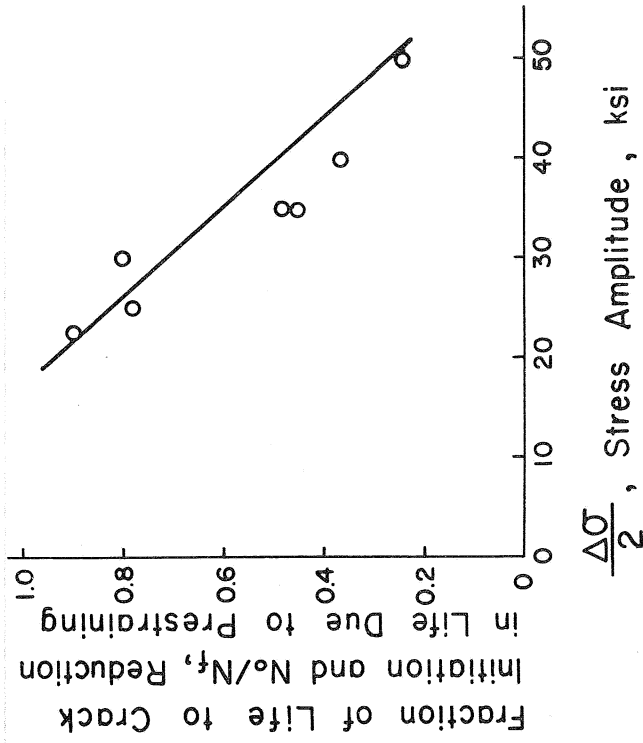


Fig. 2 Sequence effects due to crack initiation



- o Microscopy of 24S-T3 from Ref. 3
- Fatigue data on prestrained 2024-T4 from Ref. 12

Fig. 3 Comparison of crack initiation and effect of prestraining

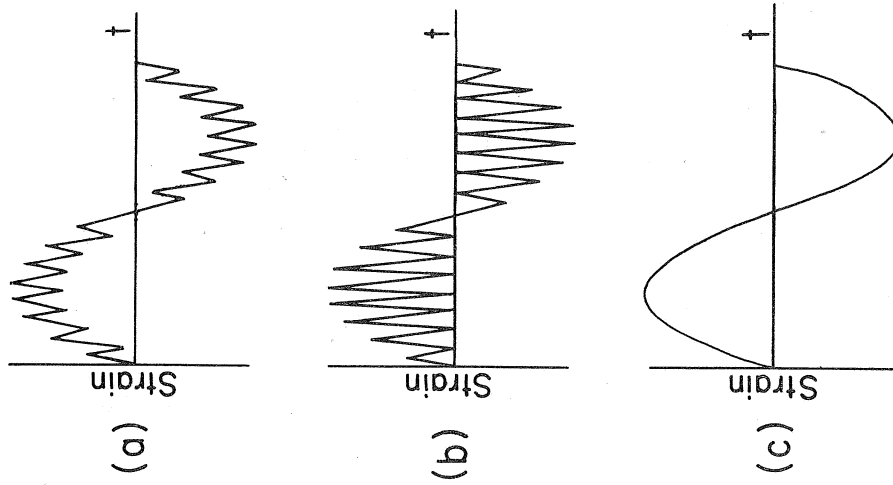


Fig. 4 Sequences which cause problems for several cycle counting methods

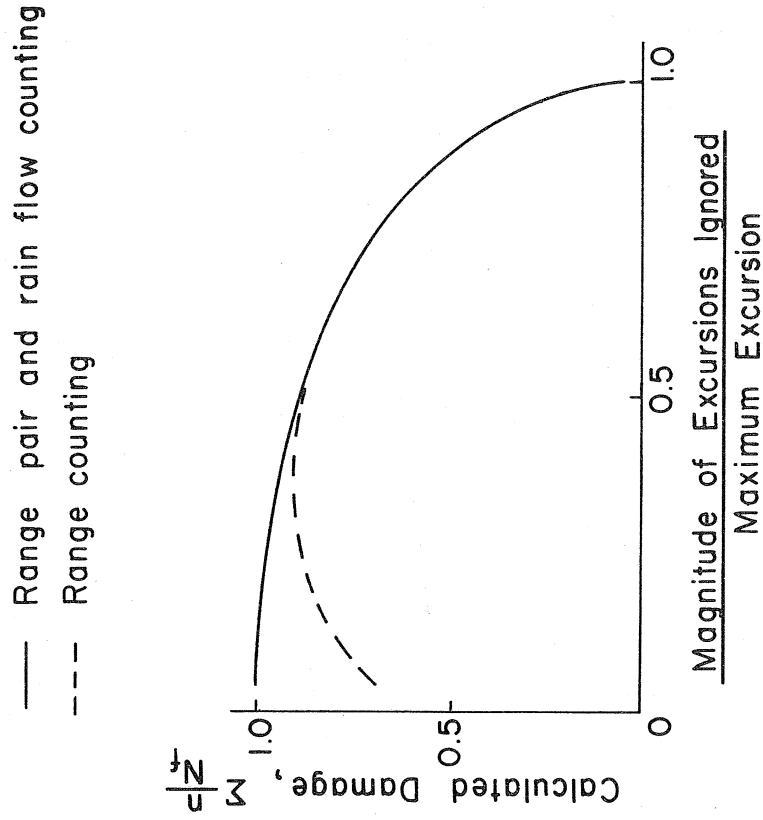


Fig. 5 The effect of ignoring all excursions smaller than a specified value

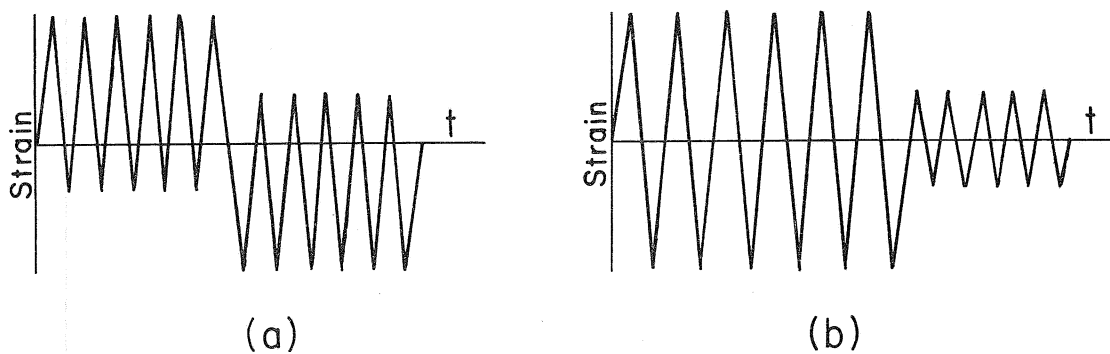


Fig. 6 Two sequences for which several counting methods give the same result

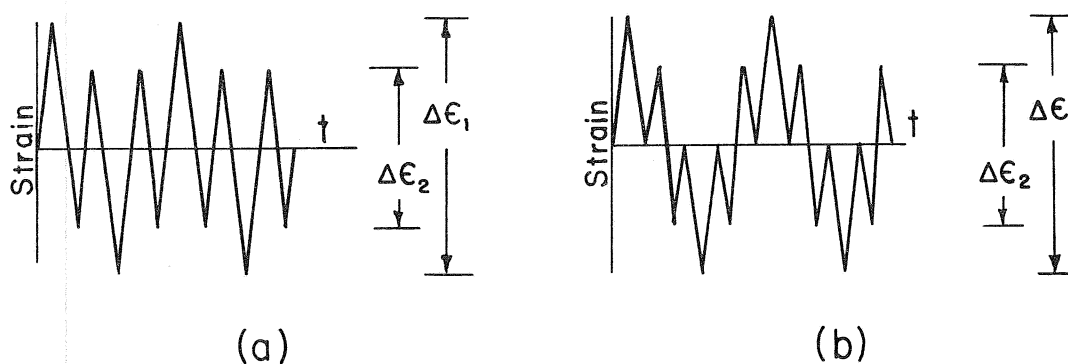


Fig. 7 A change in sequence that can affect the fatigue life

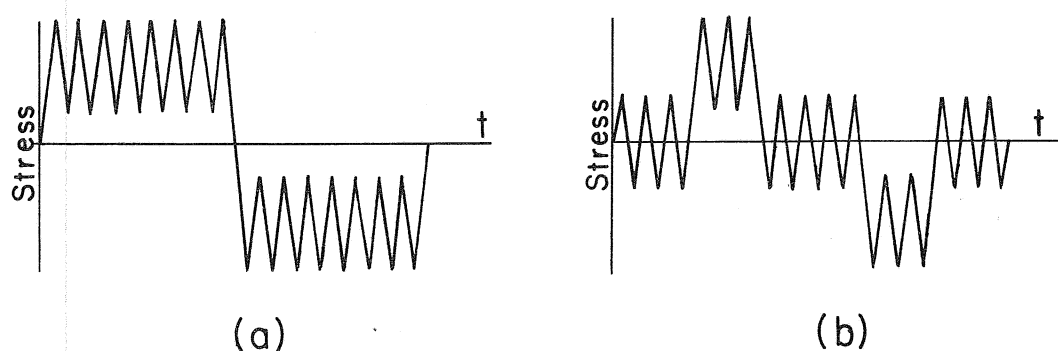
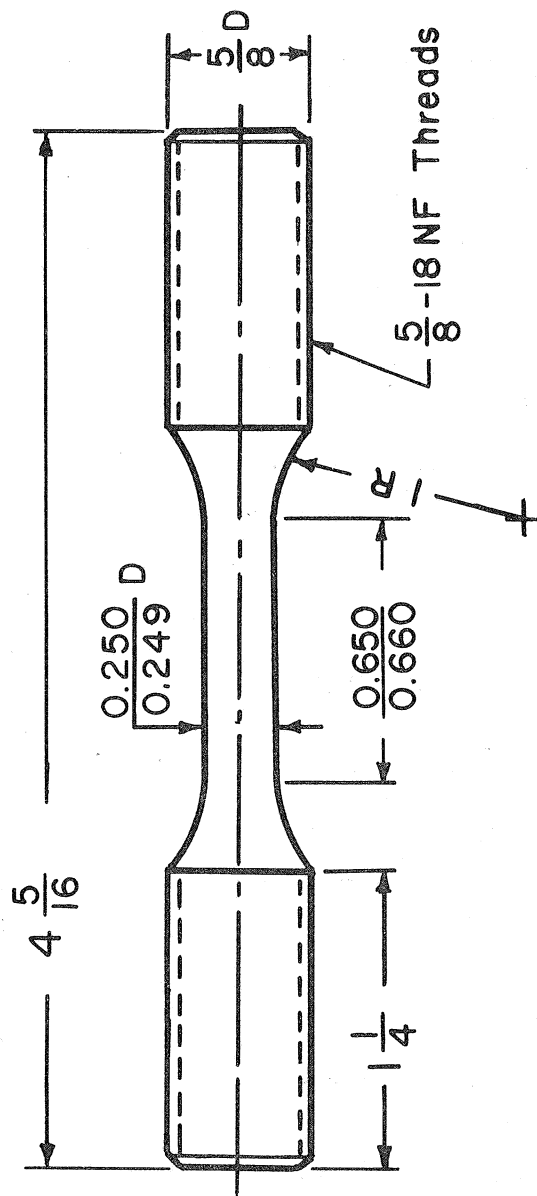


Fig. 8 Two sequences which have the same average mean stress



Notes:

1. All dimensions in inches
2. Final polish longitudinal with 3/0 emery

Fig. 9 Test Specimen

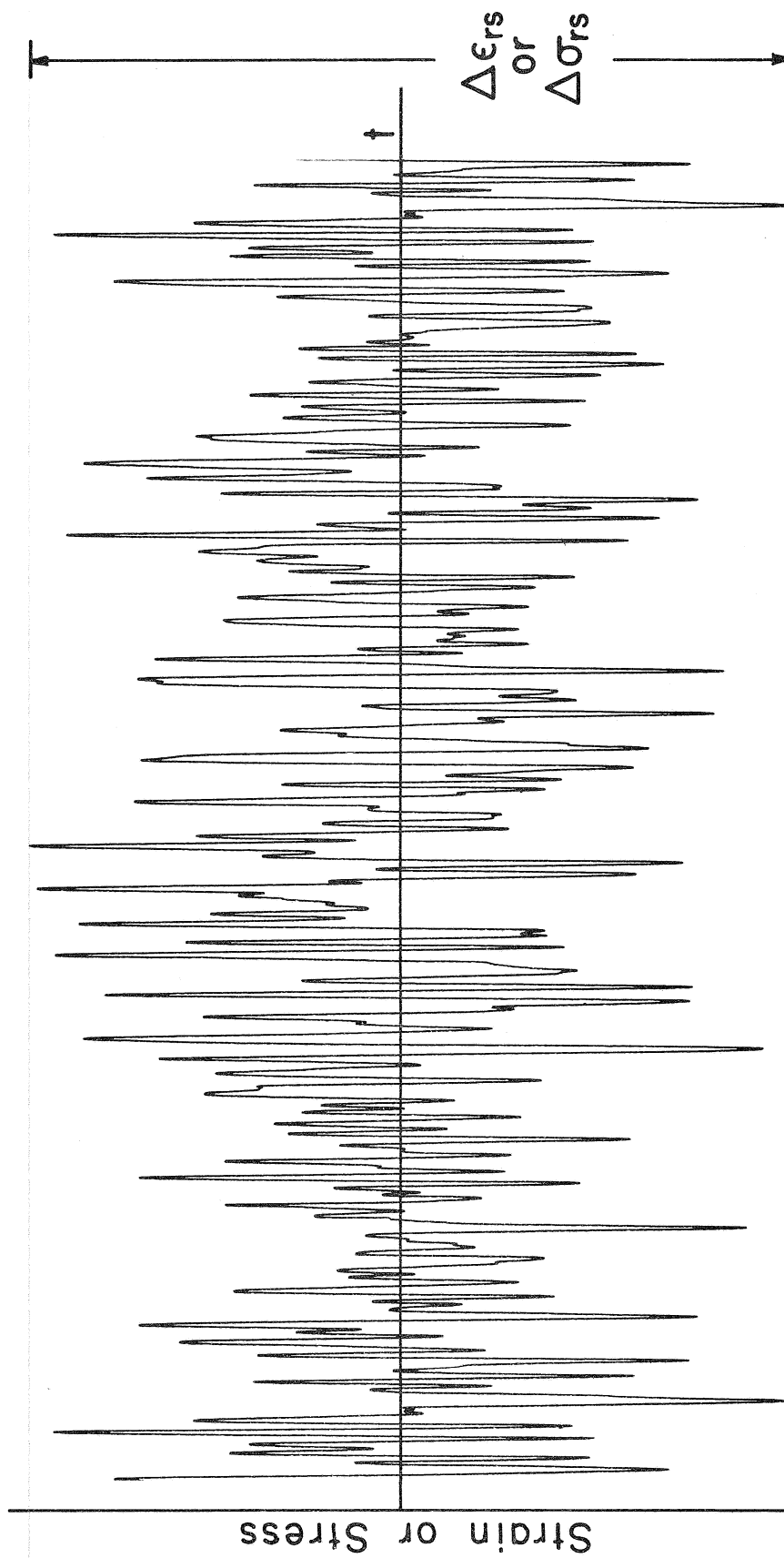


Fig. 10 The random sequence

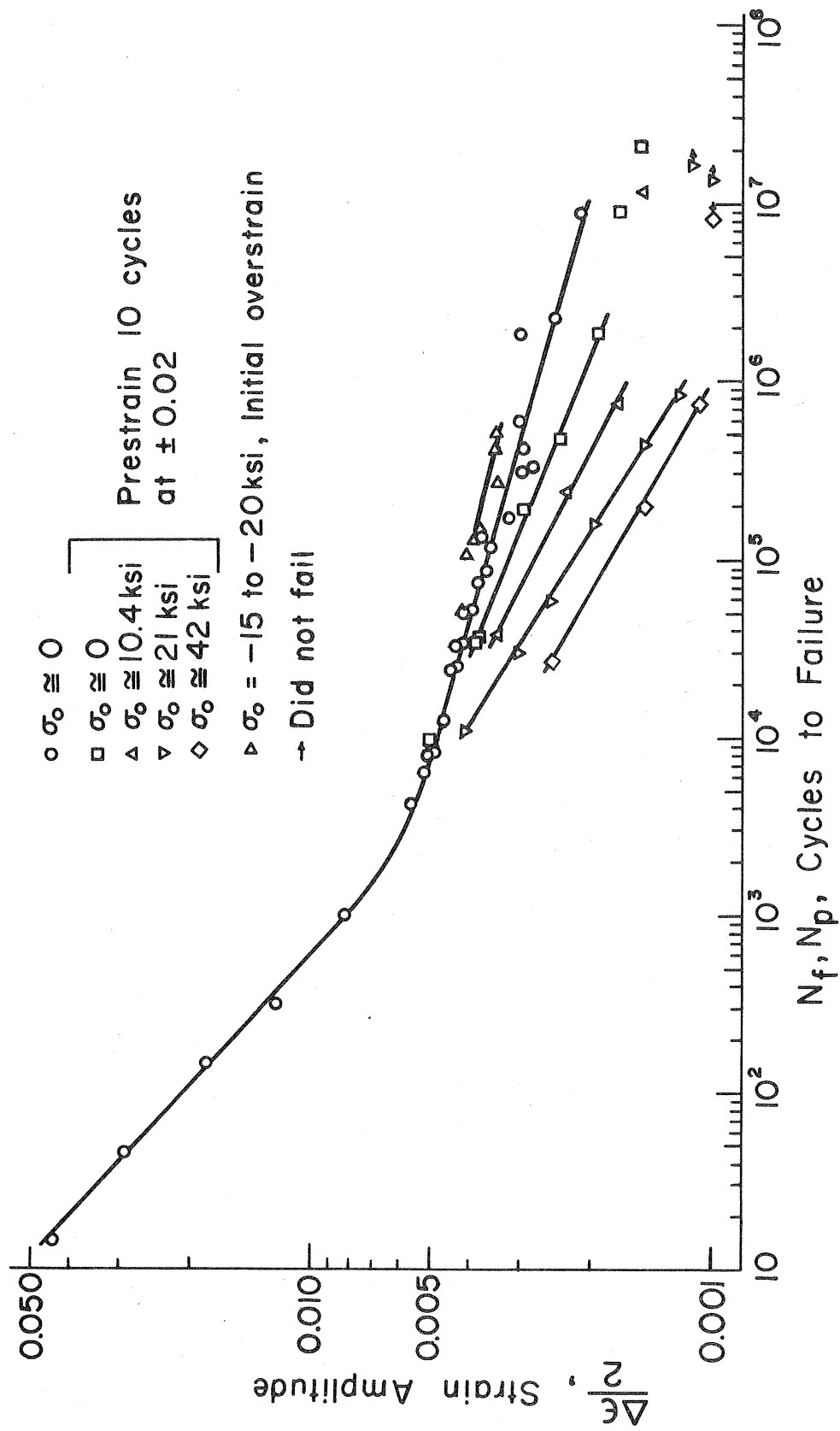
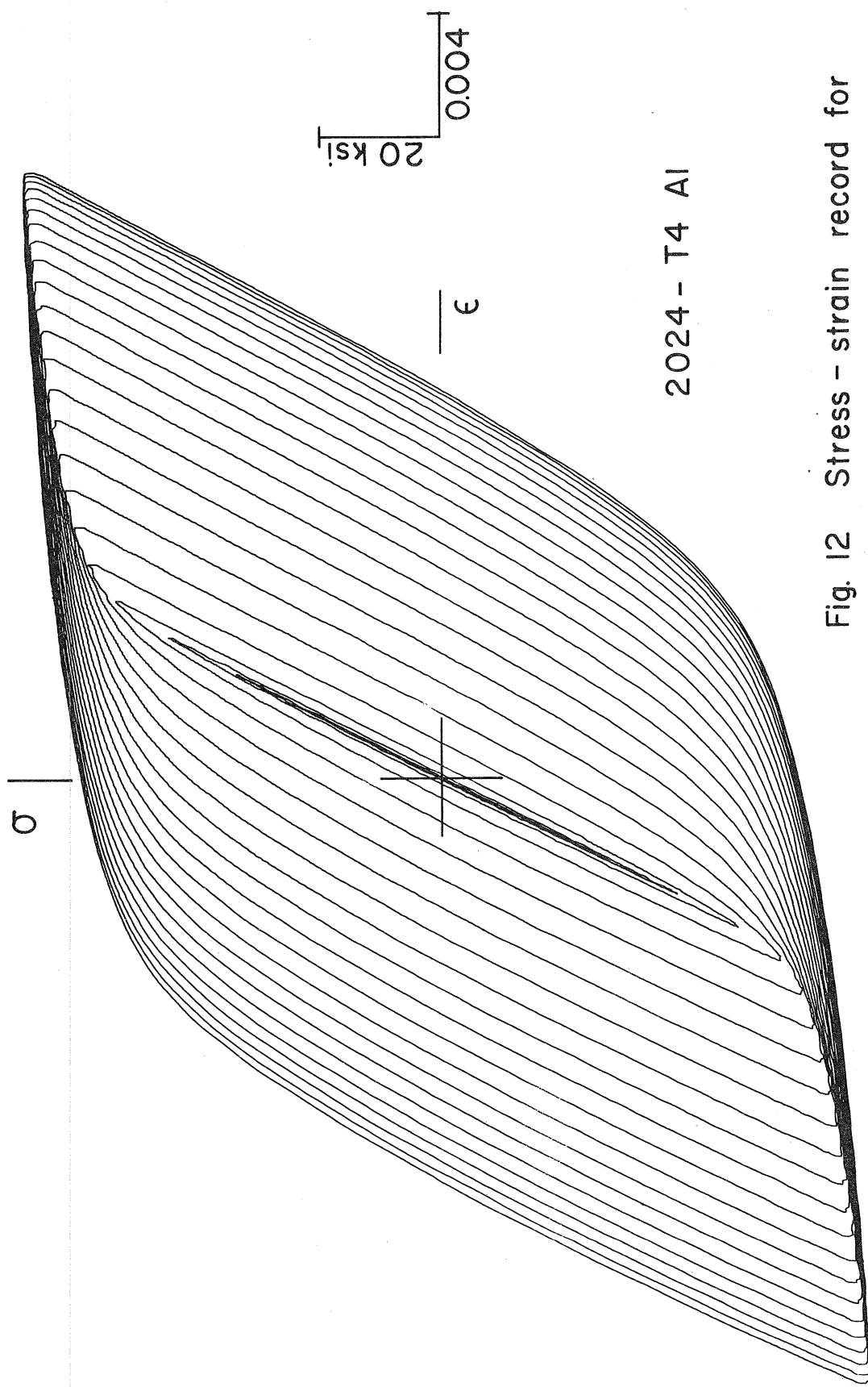
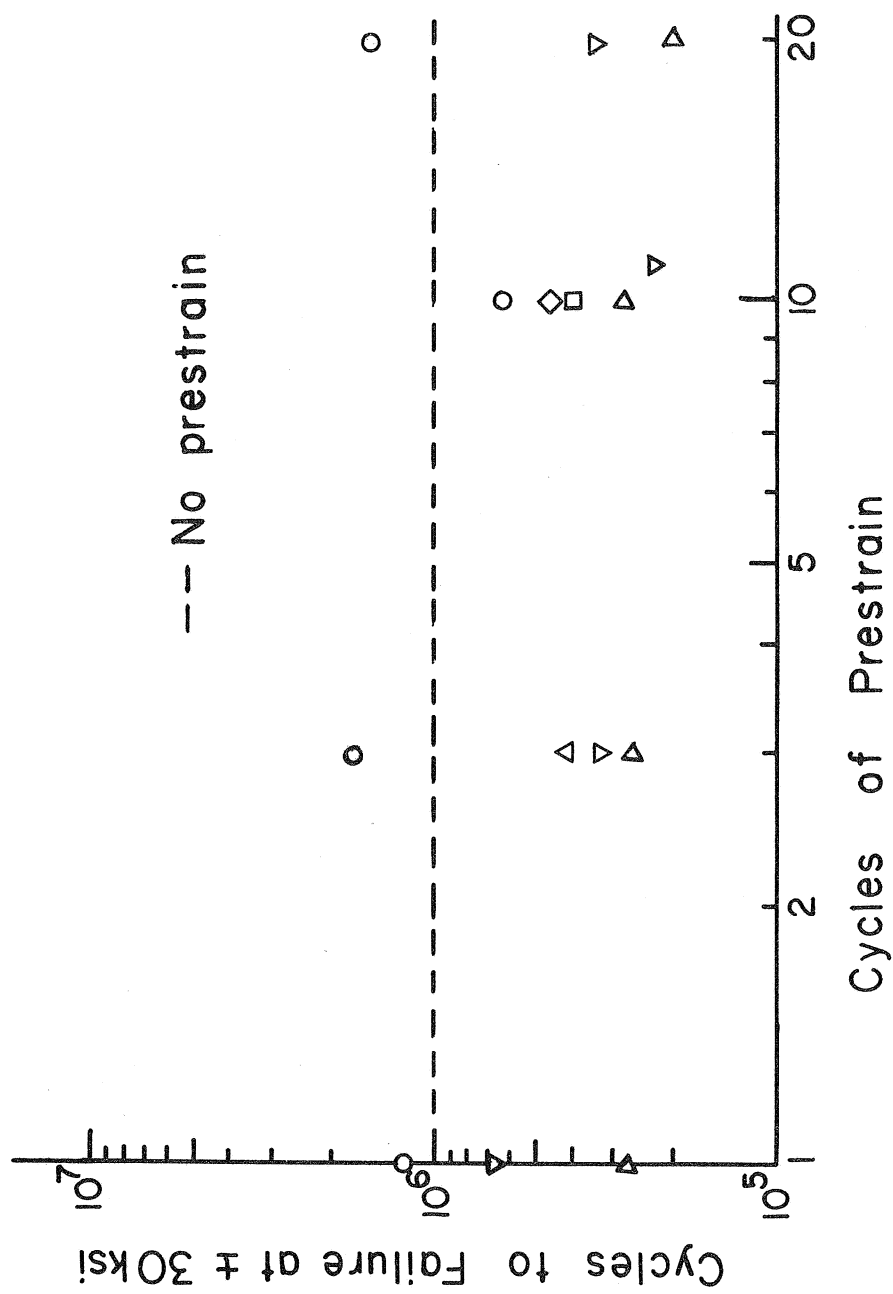


Fig. 11 Fatigue data from Refs. 12 and 45 for 2024-T4 Al



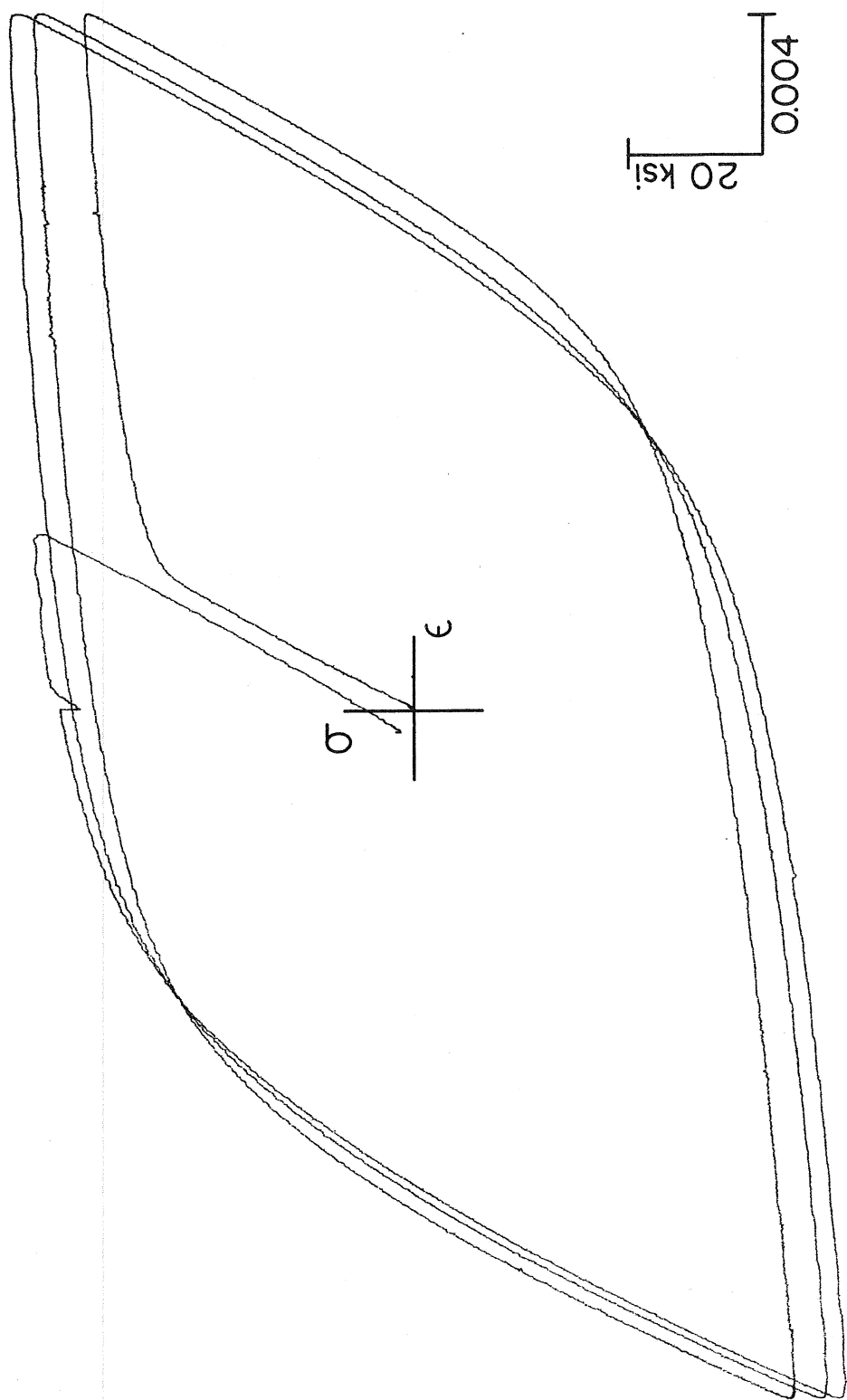
2024 - T4 Al

Fig. 12 Stress - strain record for incremental step test



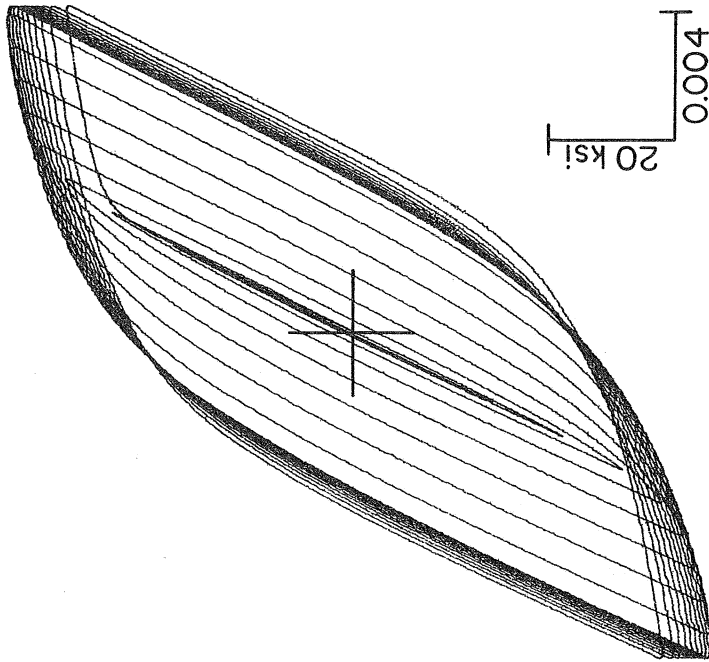
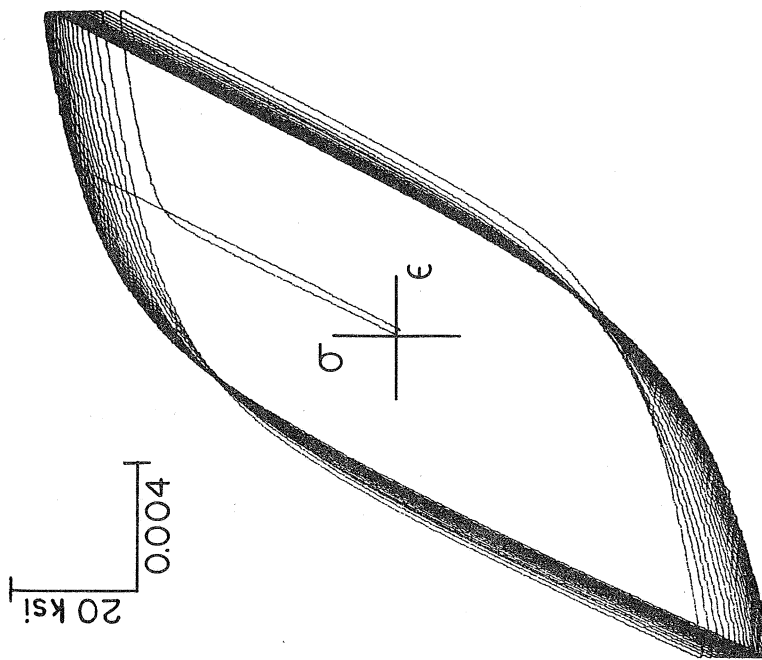
* See Table 2

Fig. 13 Effect of number of cycles and amplitude of prestrain



(a) Three cycles at ± 0.02

Fig. 14 Examples of stress - strain response during prestraining



(b) Twenty cycles at ± 0.01

(c) Ten cycles at ± 0.01 , then
linearly decrease $\Delta \epsilon$ to zero

Fig. 14 Examples of stress - strain response during prestraining
(cont'd)

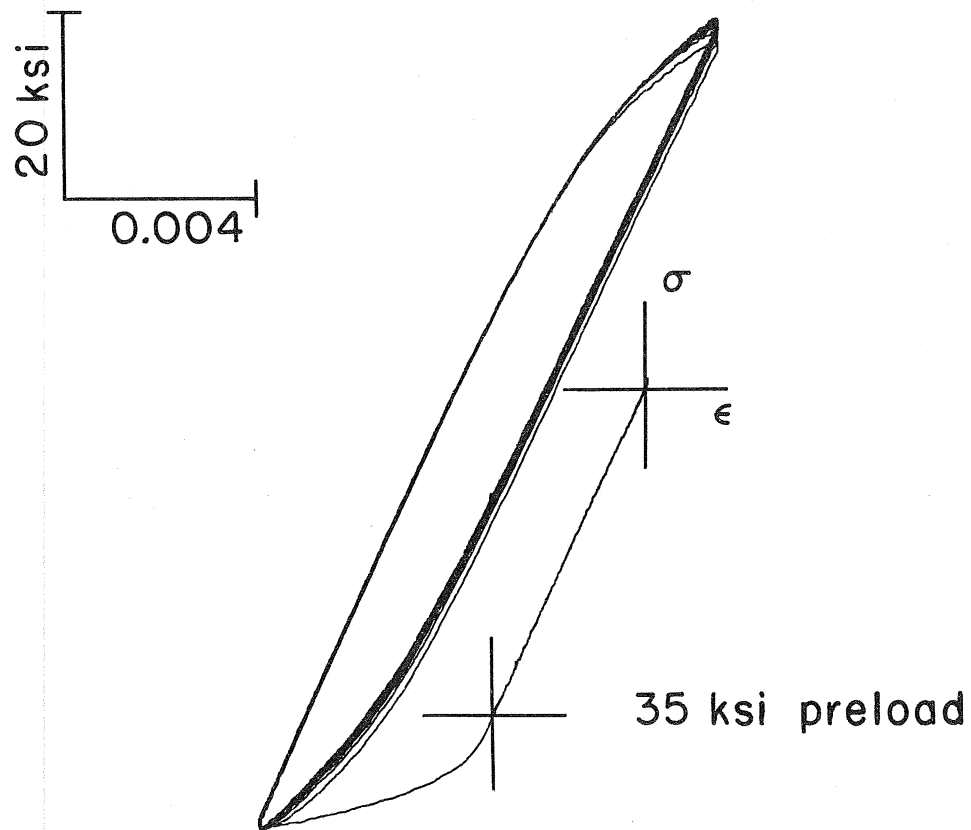


Fig. 15 Simulated removal of residual stress
by prestraining 10 cycles at ± 0.0048

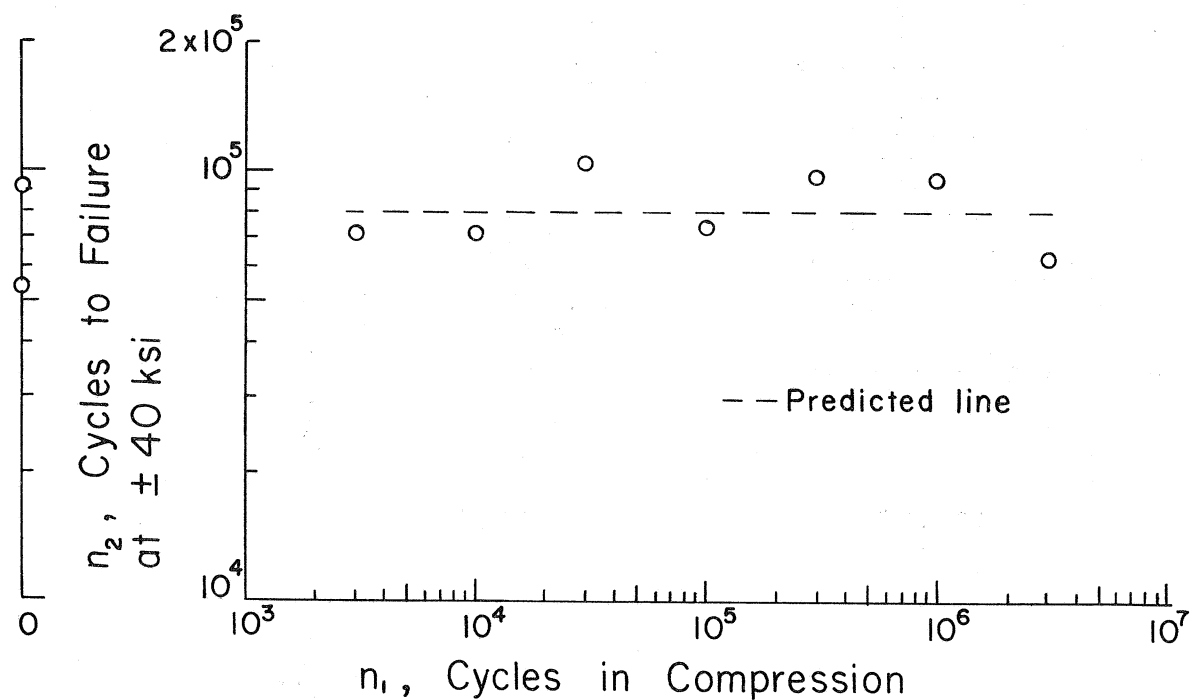


Fig. 16 Fatigue lives at ± 40 ksi after cycling in compression 0 to -50 ksi

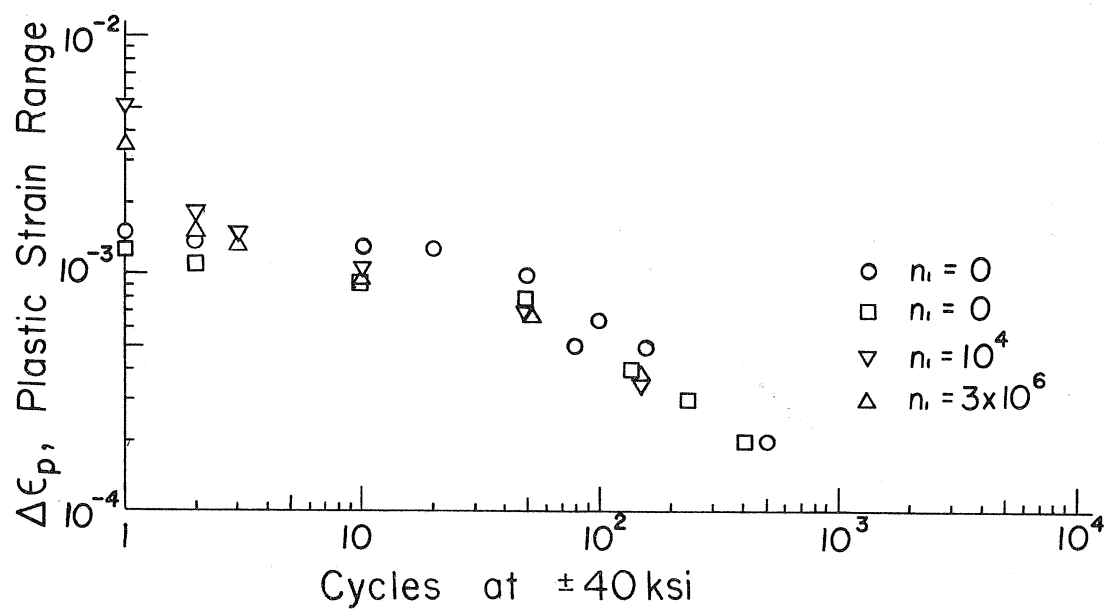
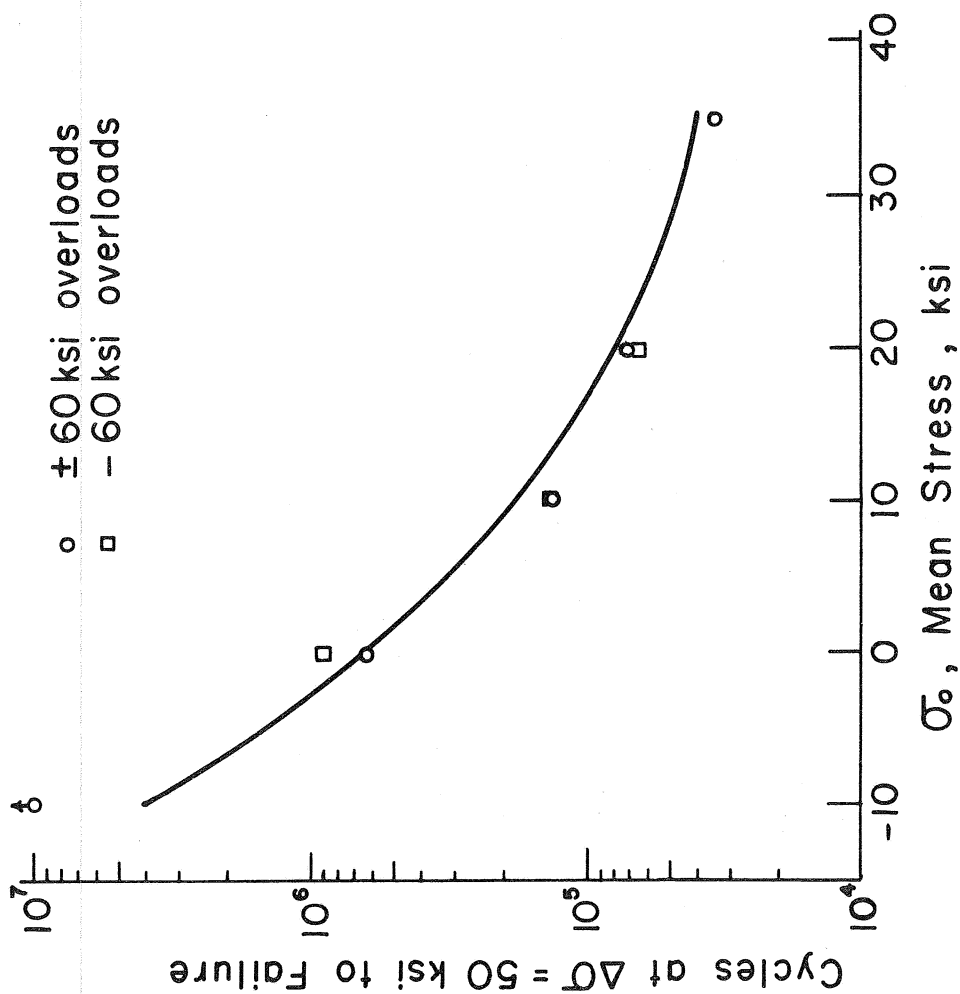
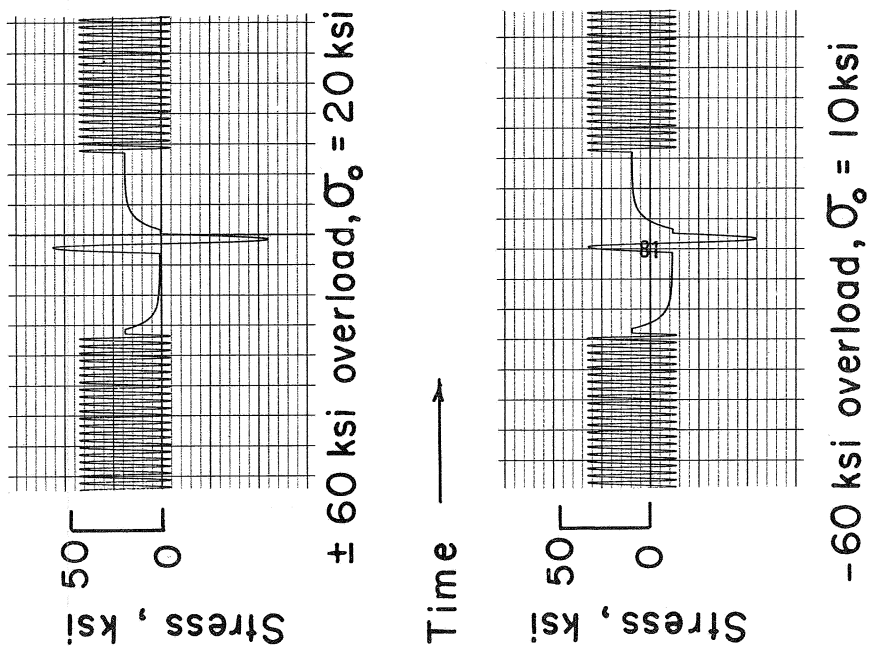


Fig. 17 Plastic strain range during cycling at ± 40 ksi after cycling in compression



(a) Test data and predicted line



(b) Typical overload cycles

Fig. 18 Effect of overload cycles on the fatigue lives at different mean stresses

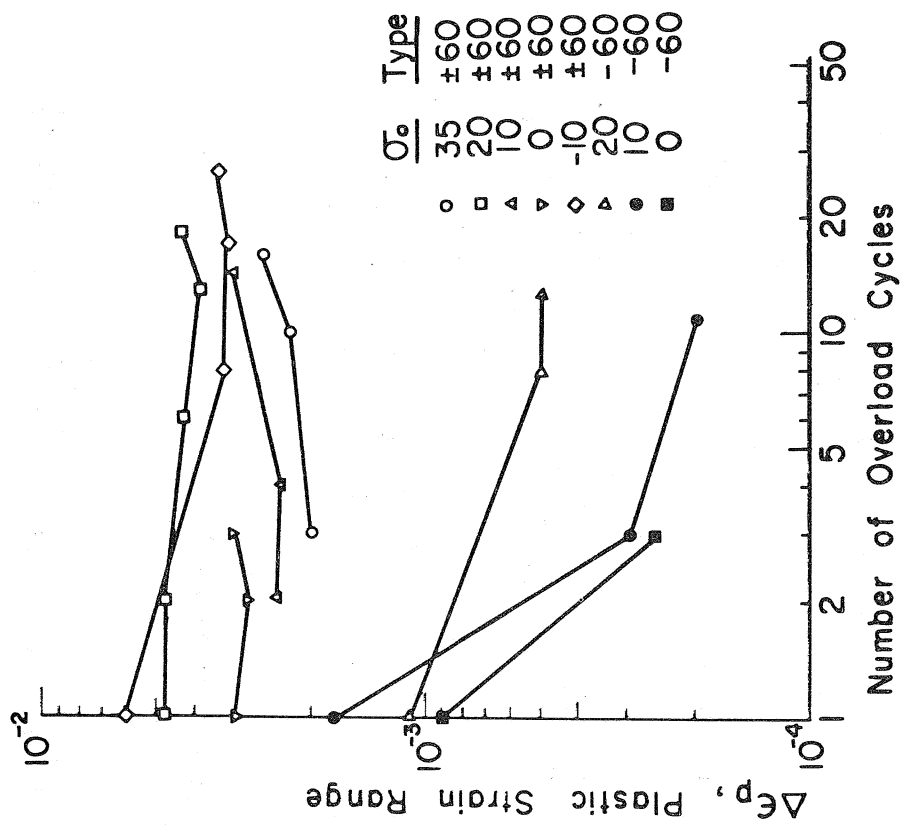


Fig. 19 Plastic strain range during overload cycles

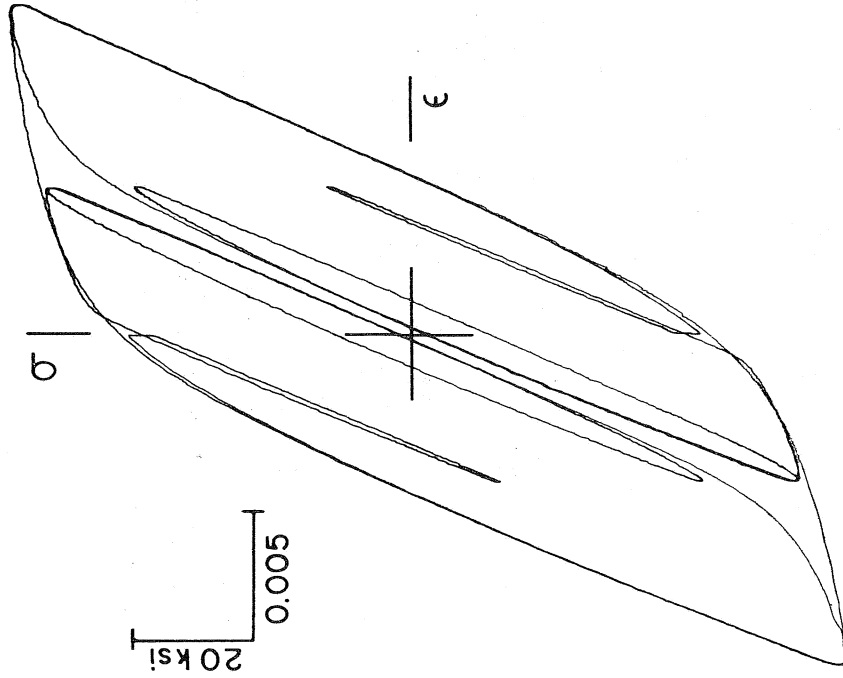
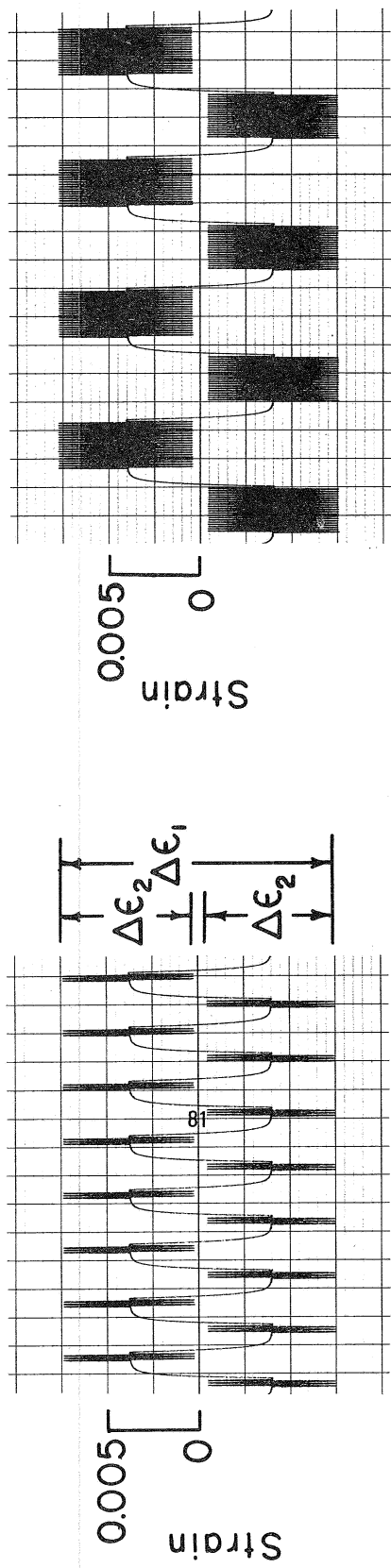
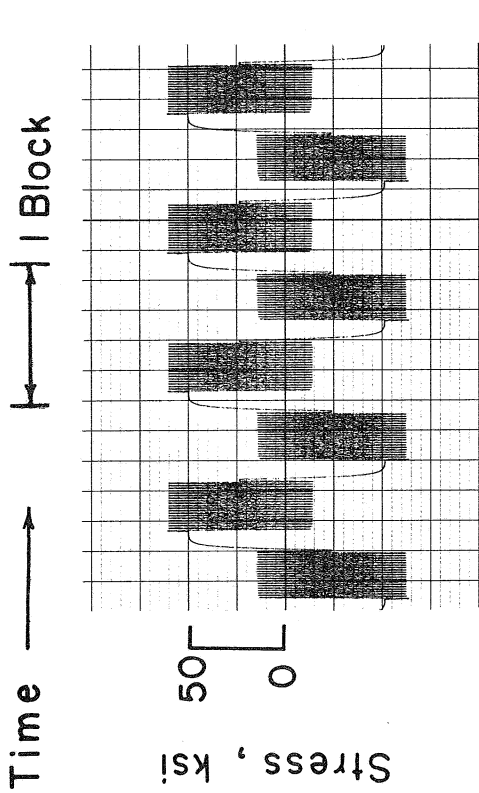


Fig. 20 Effect of mean stress on hysteresis loops

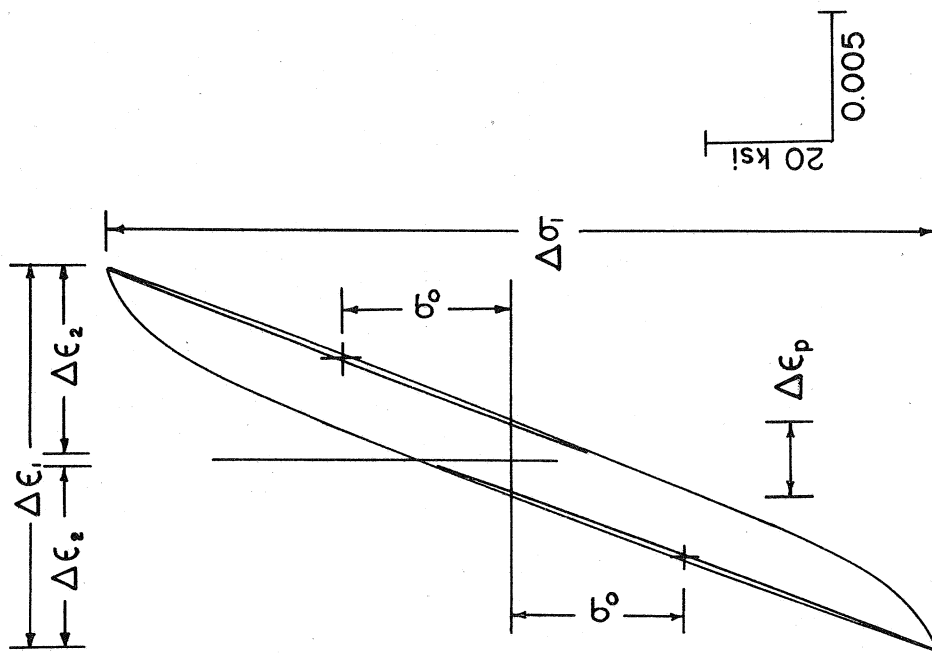


(a) Strain-time and stress-time recordings for $k=6$

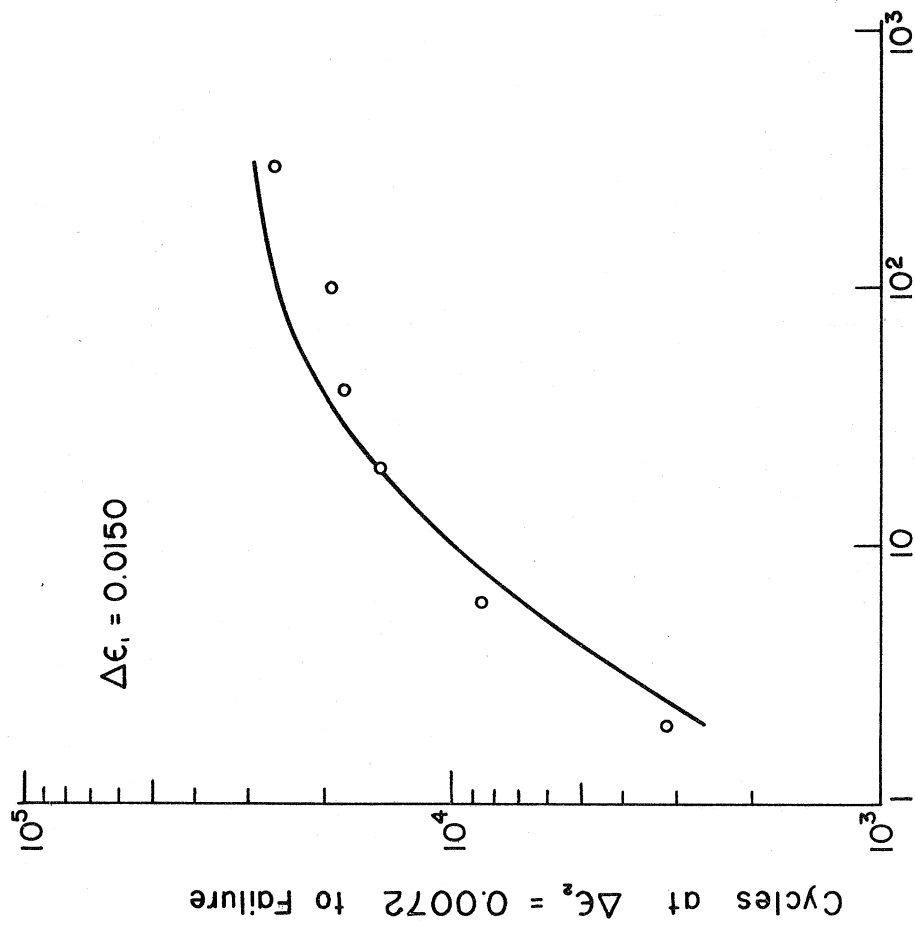


(b) Strain-time and stress-time recordings for $k=40$

Fig. 21 Strain control block size effect tests



(c) Typical stress-strain response



k, Cycles at $\Delta\epsilon_2 = 0.0072$ per Block

(d) Test data and predicted line

Fig. 21 Strain control block size effect tests (cont'd)

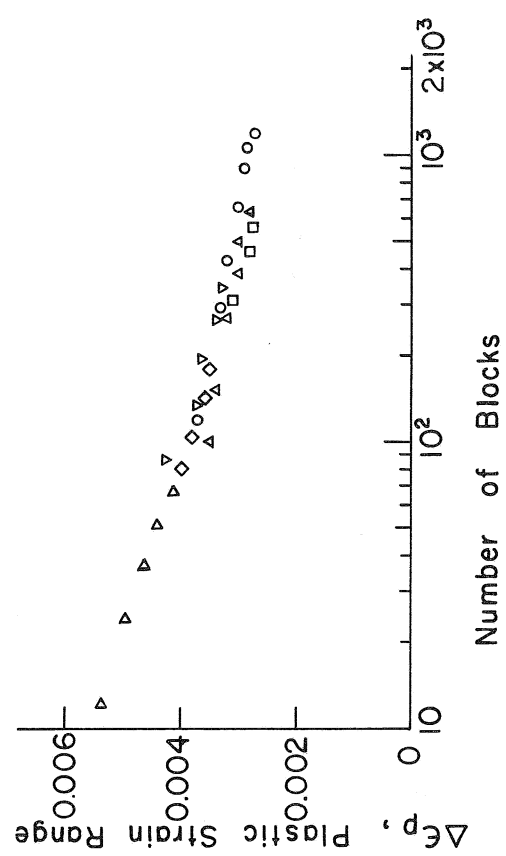
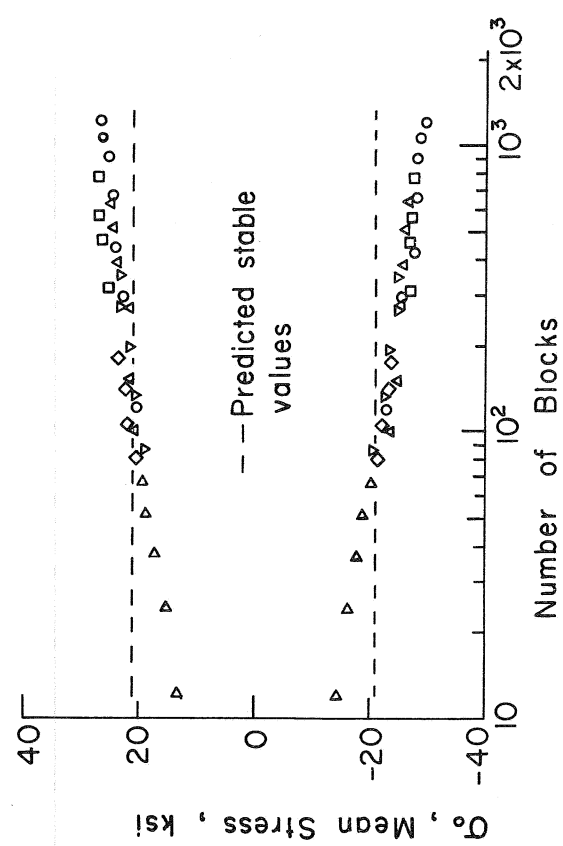
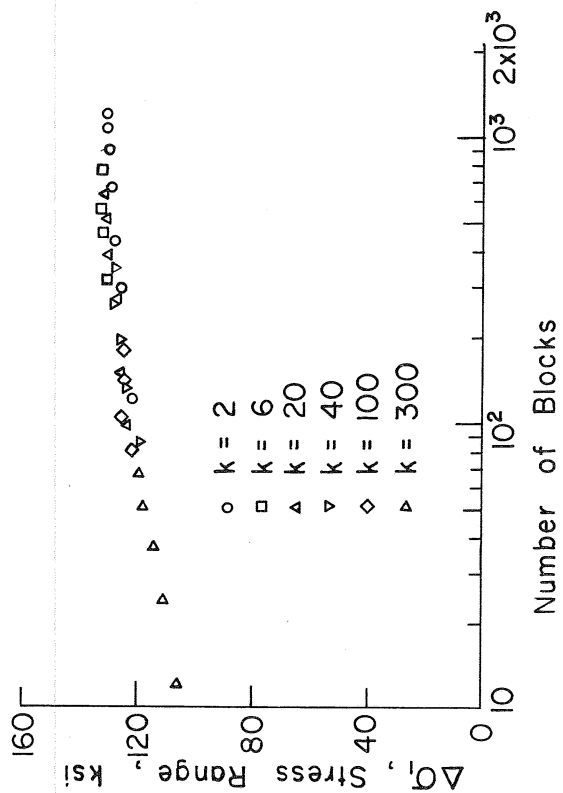
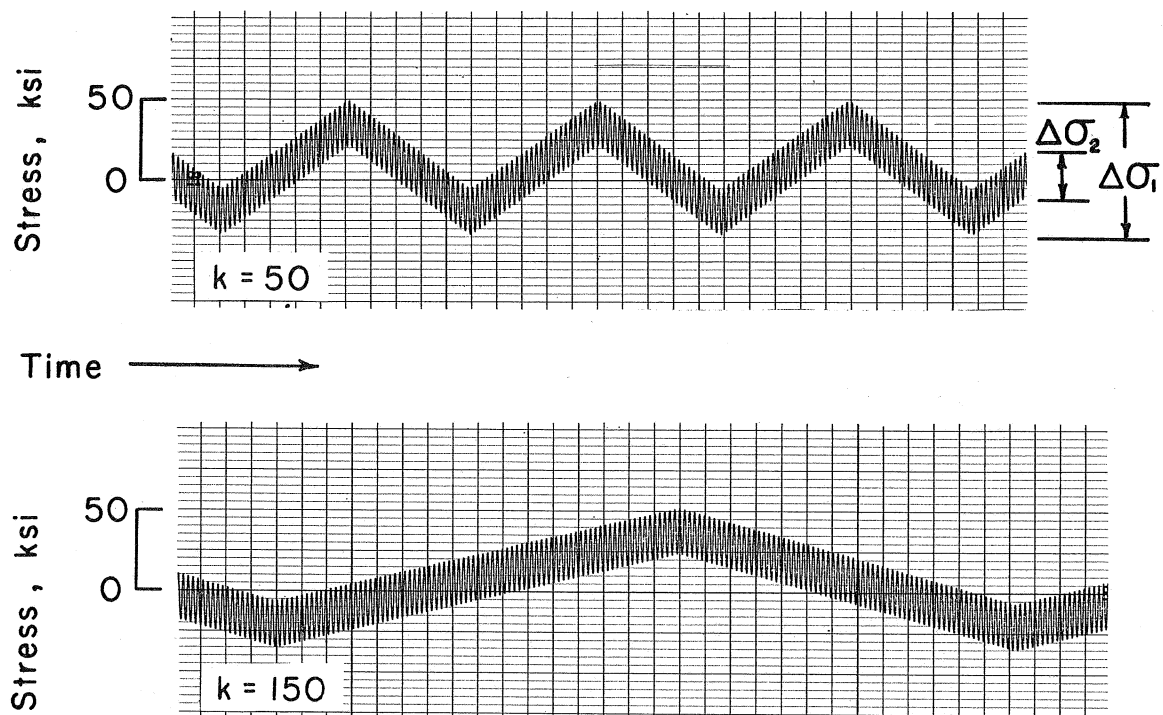
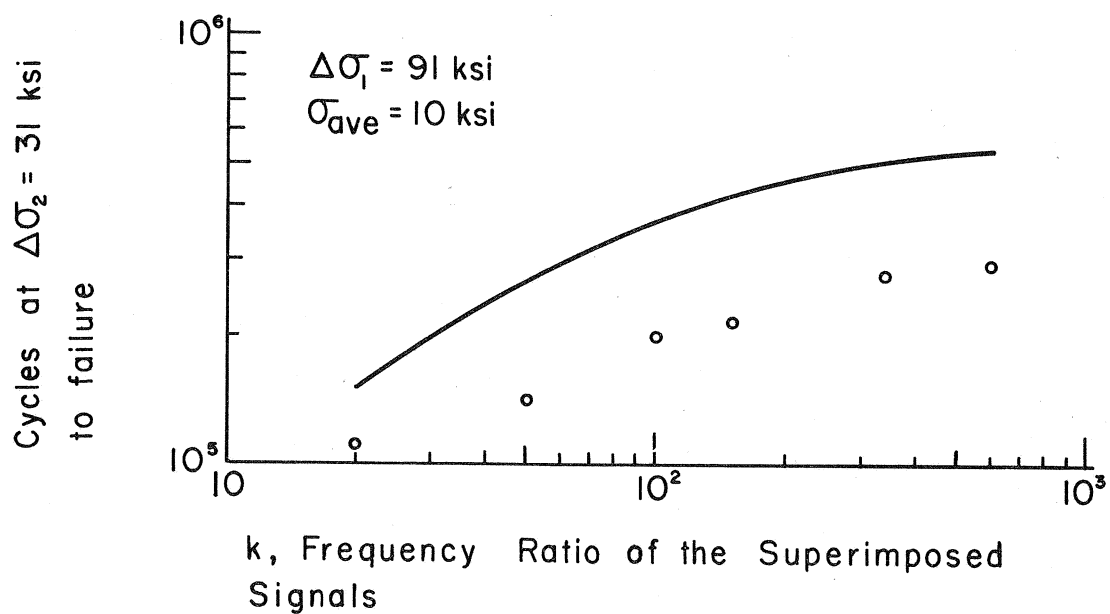


Fig. 22 Variations of total stress range, mean stress, and plastic strain range during strain control block size effect tests

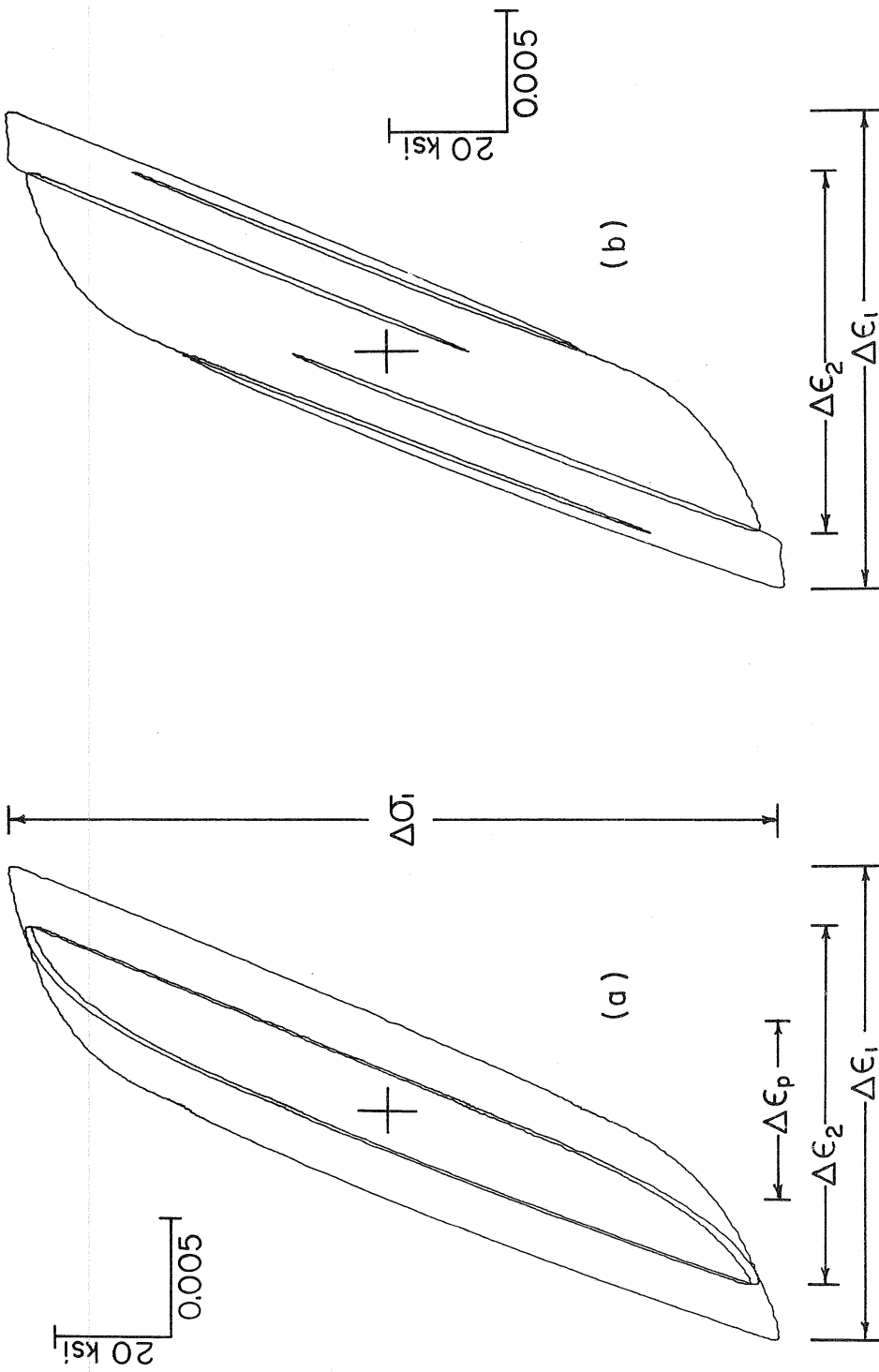


(a) Typical stress - time recordings

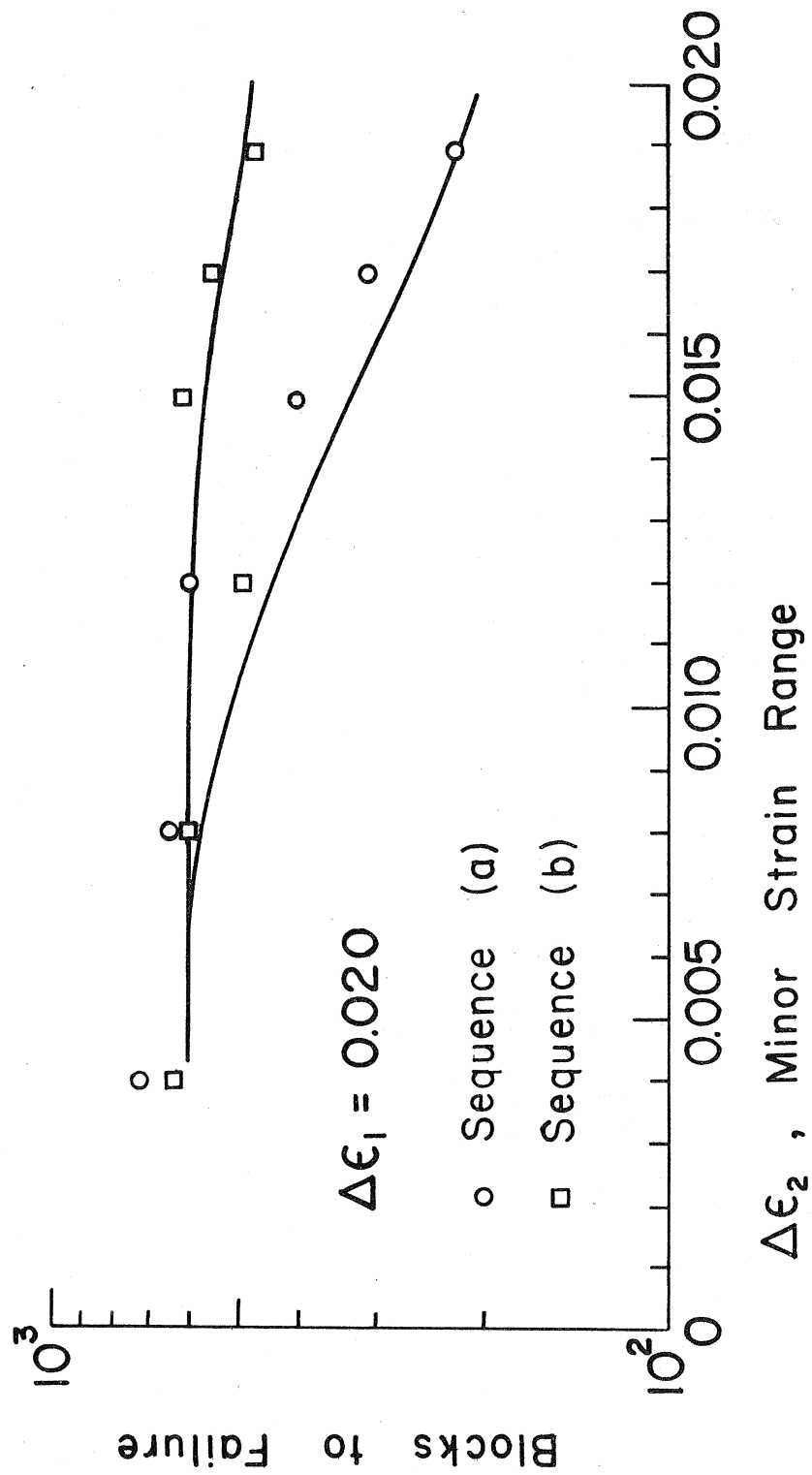


(b) Test data and predicted line

Fig. 23 Stress control block size effect tests



(a) and (b) Stress-strain response for sequences shown in Fig. 7(a) and (b)
 Fig. 24 Strain control memory effect tests



(c) Test data and predicted lines

Fig. 24 Strain control memory effect tests (cont'd)

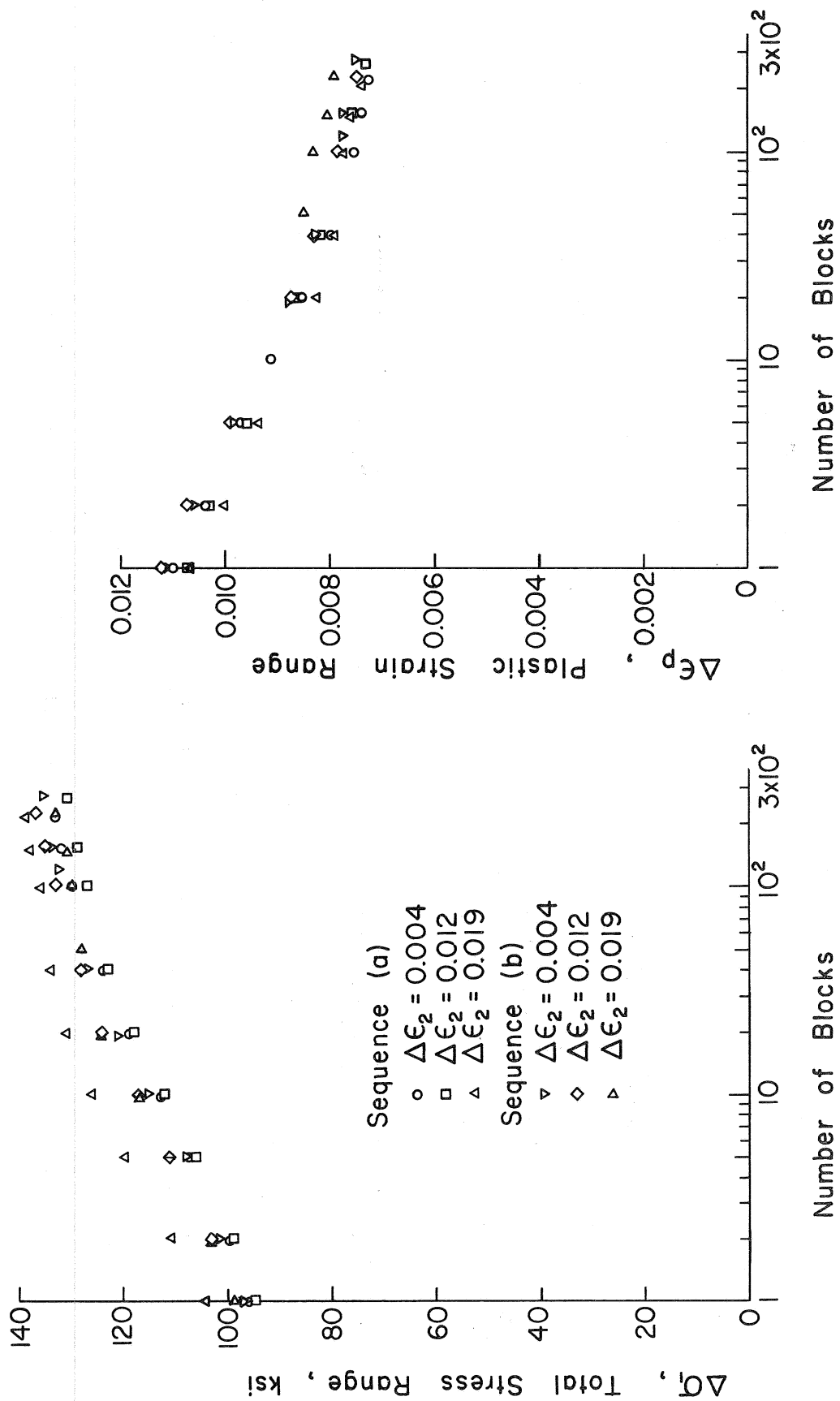
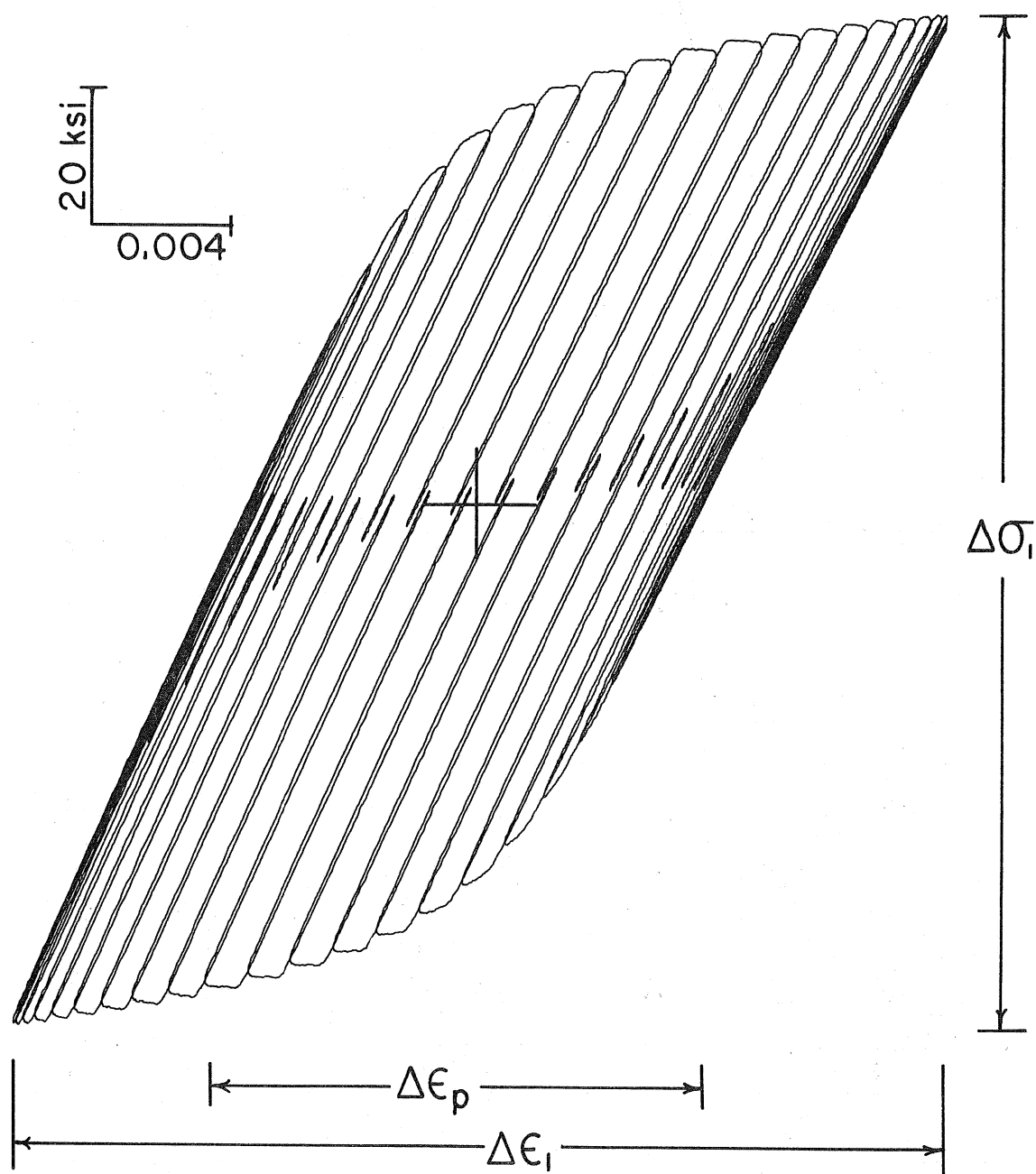
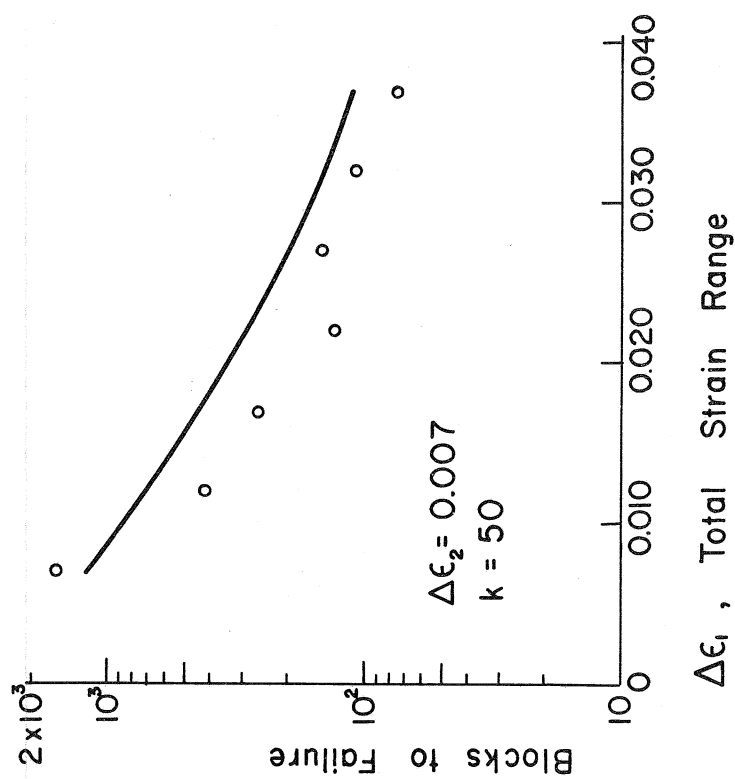
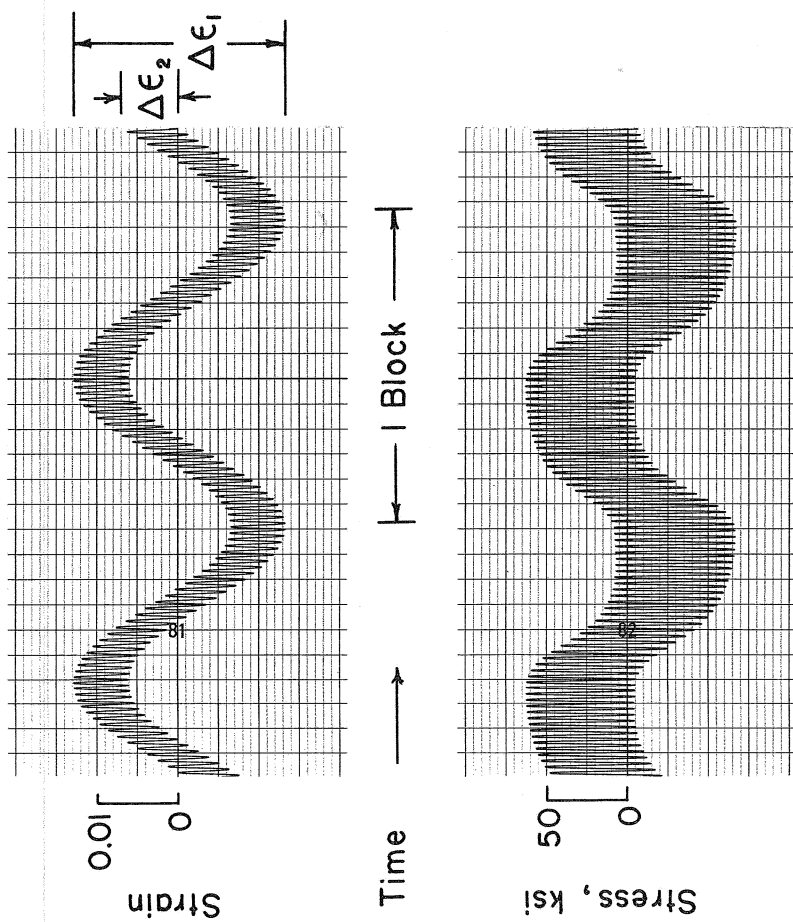


Fig. 25 Typical variations of total stress range and plastic strain range during memory tests



(a) Stable stress - strain response for $\Delta\epsilon_l = 0.027$

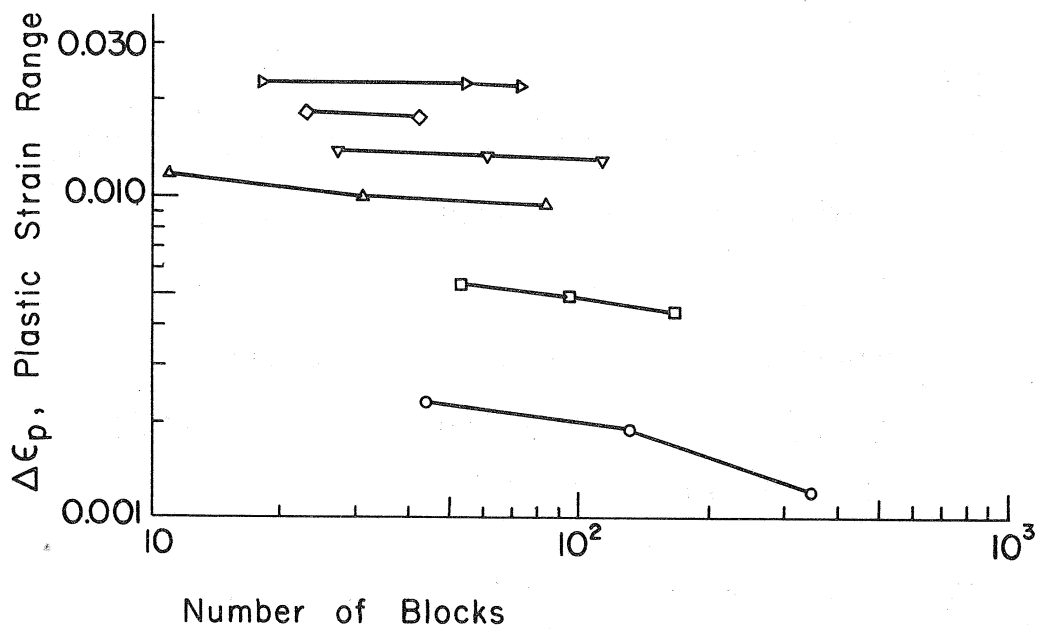
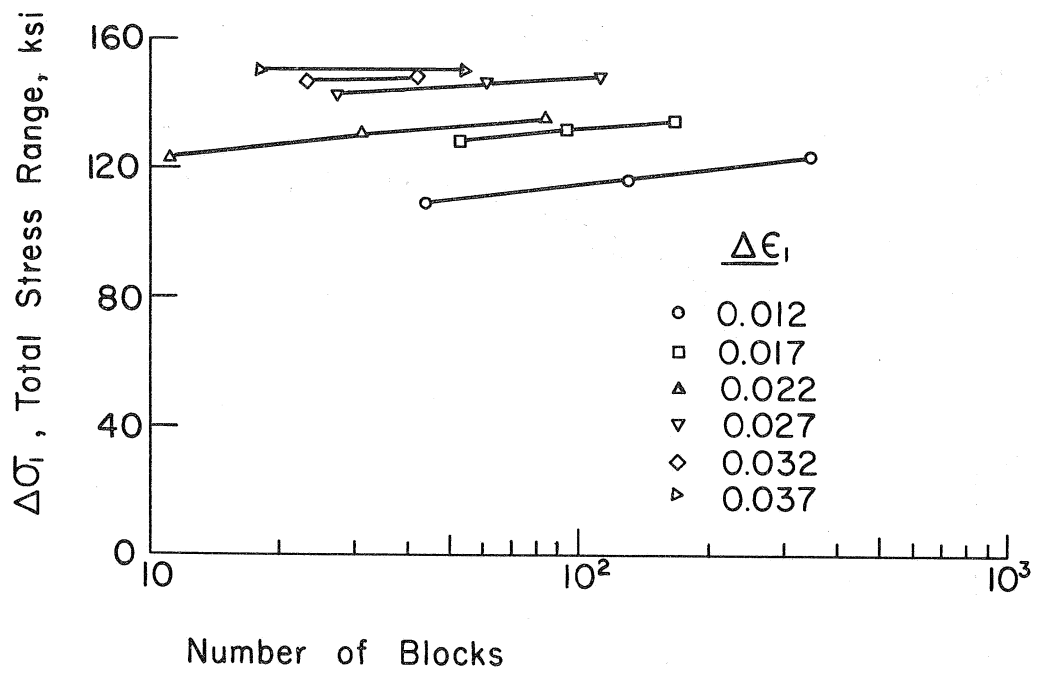
Fig. 26 Tests with sinusoidal variation of the mean strain



(b) Strain - time and stress - time recordings for $\Delta\epsilon_1 = 0.027$

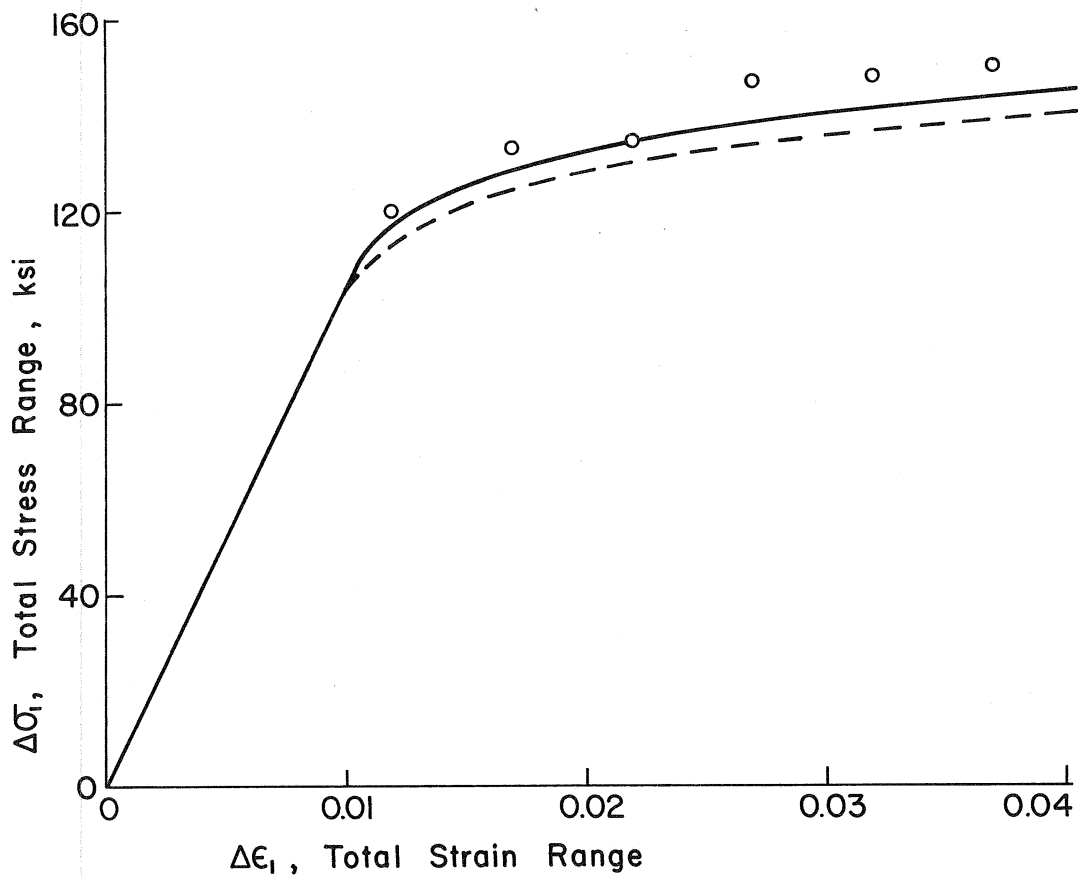
(c) Test data and predicted line

Fig. 26 Tests with sinusoidal variation of the mean strain (cont'd)



(a) Total stress range and plastic strain range

Fig. 27 Stress-strain behavior during sinusoidal variation of the mean strain



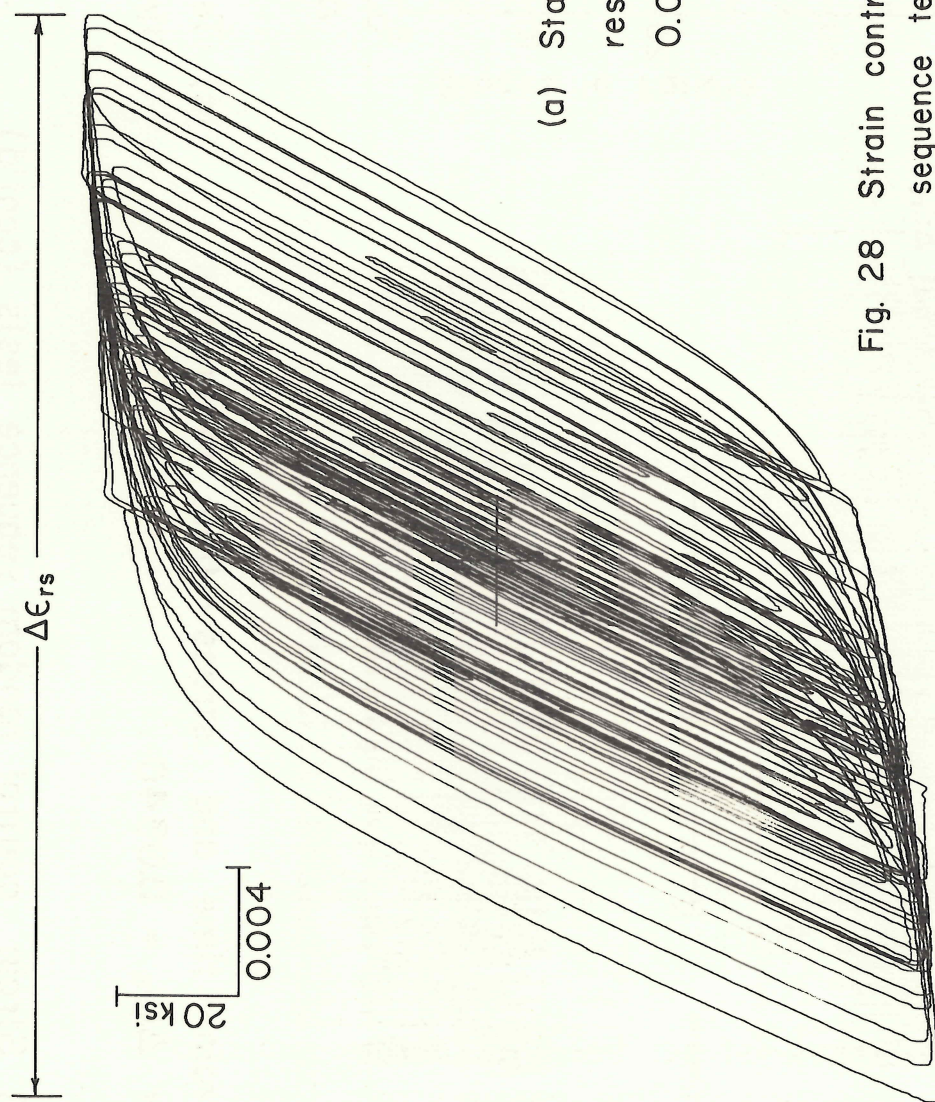
○ Sinusoidal variation of mean strain

— Cyclic σ - ϵ curve from Refs. 45 and 51

--- Incremental step test

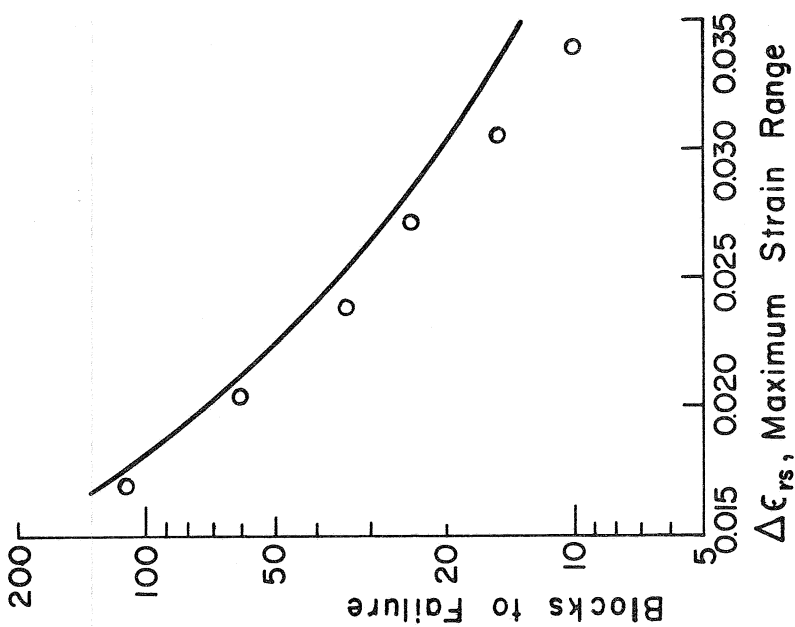
(b) Total strain range vs. total stress range after cyclic stabilization

Fig. 27 Stress-strain behavior during sinusoidal variation of the mean strain (cont'd)

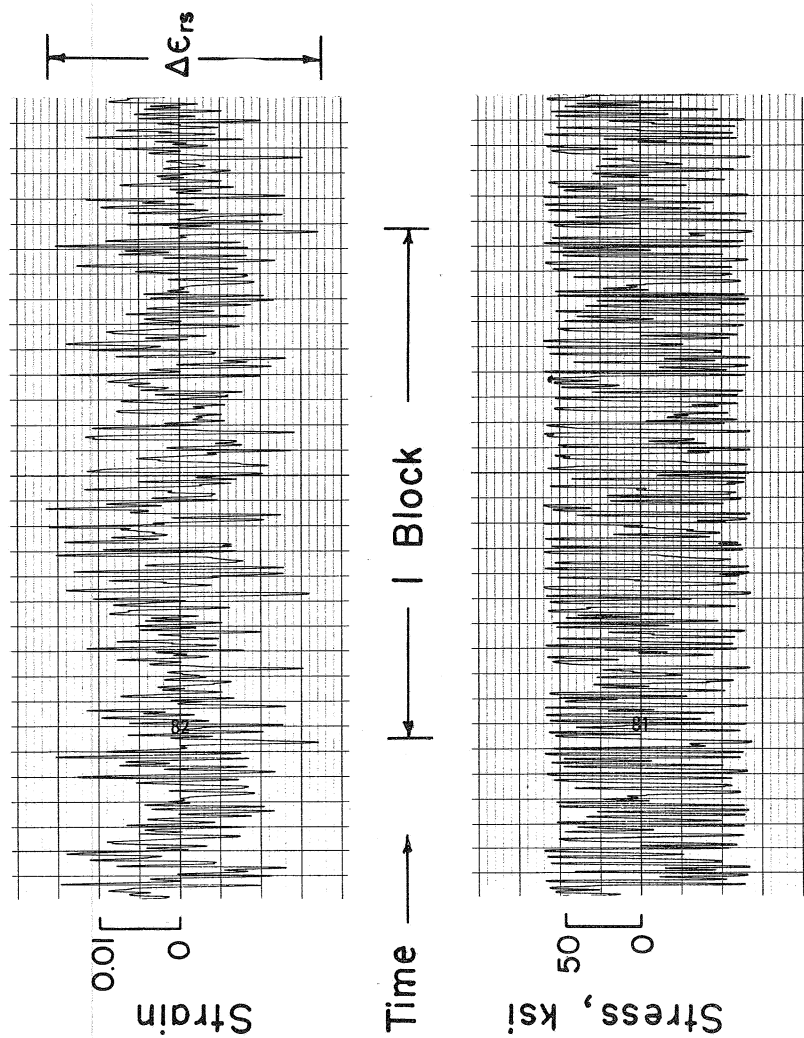


(a) Stable stress - strain
response for $\Delta\epsilon_{rs} =$
0.0340

Fig. 28 Strain control random
sequence tests



(c) Test data and predicted line



(b) Strain - time and stress - time recordings for $\Delta\epsilon_{rs} = 0.0340$

Fig. 28 Strain control random sequence tests (cont'd)

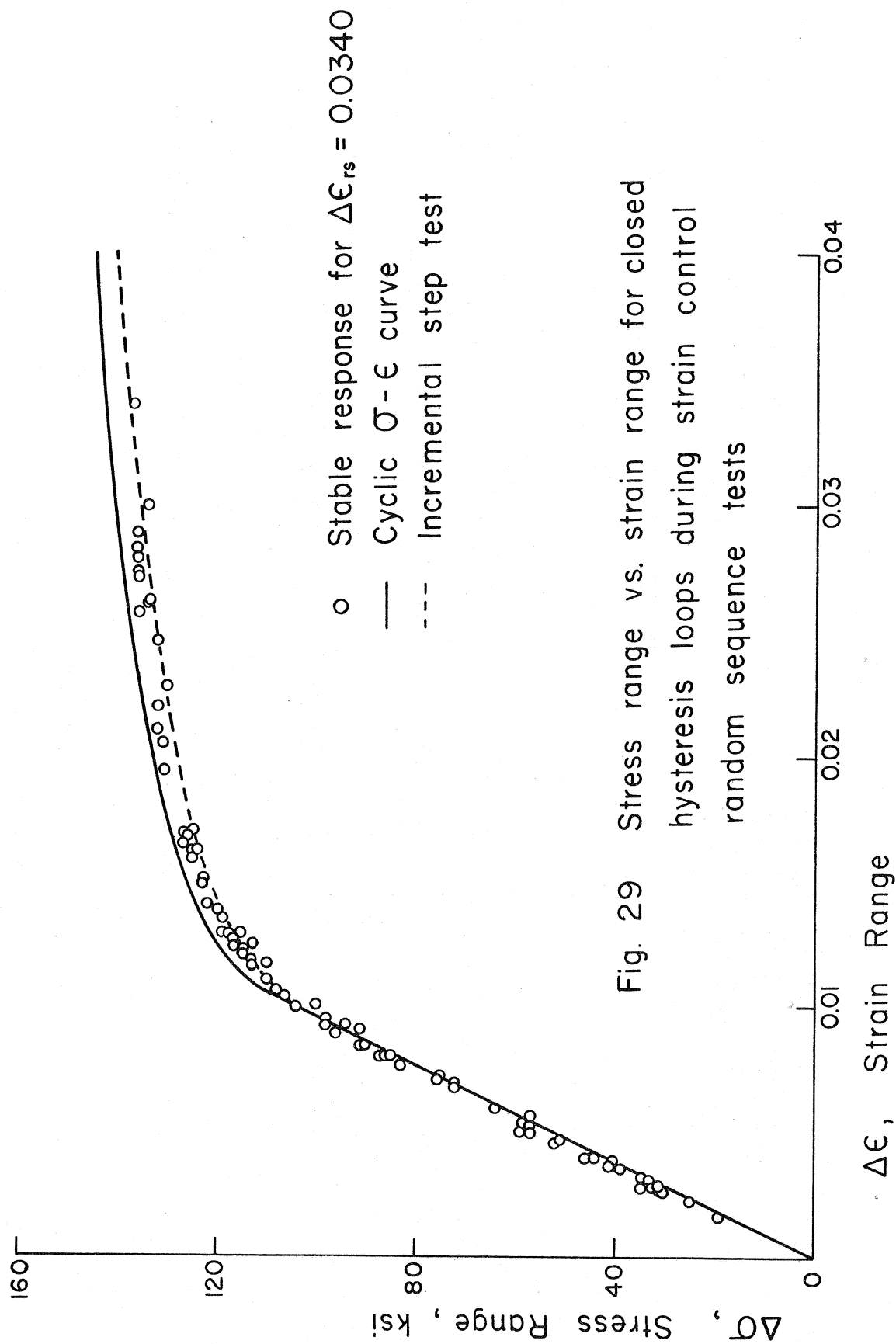
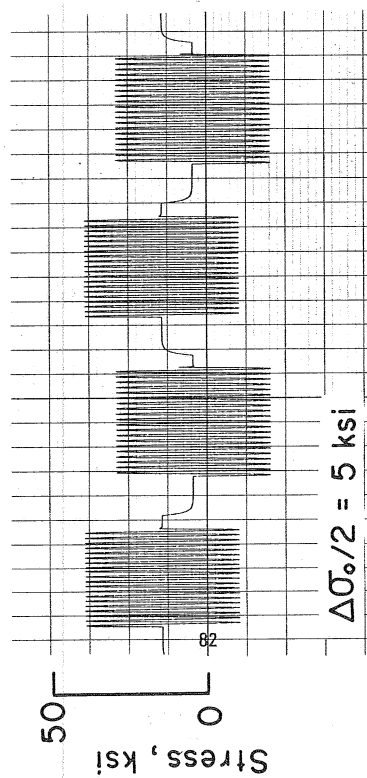
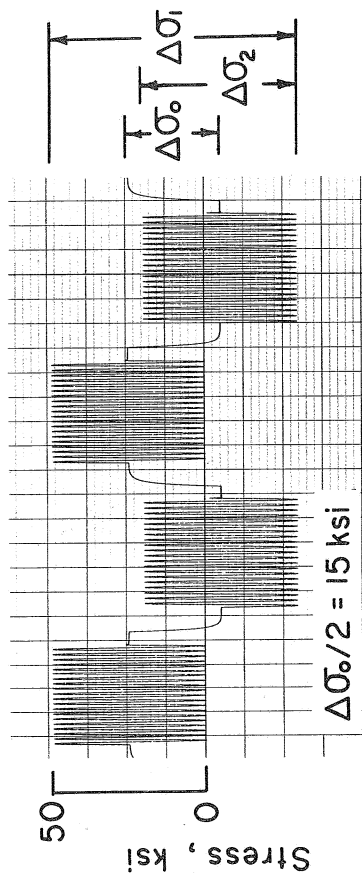


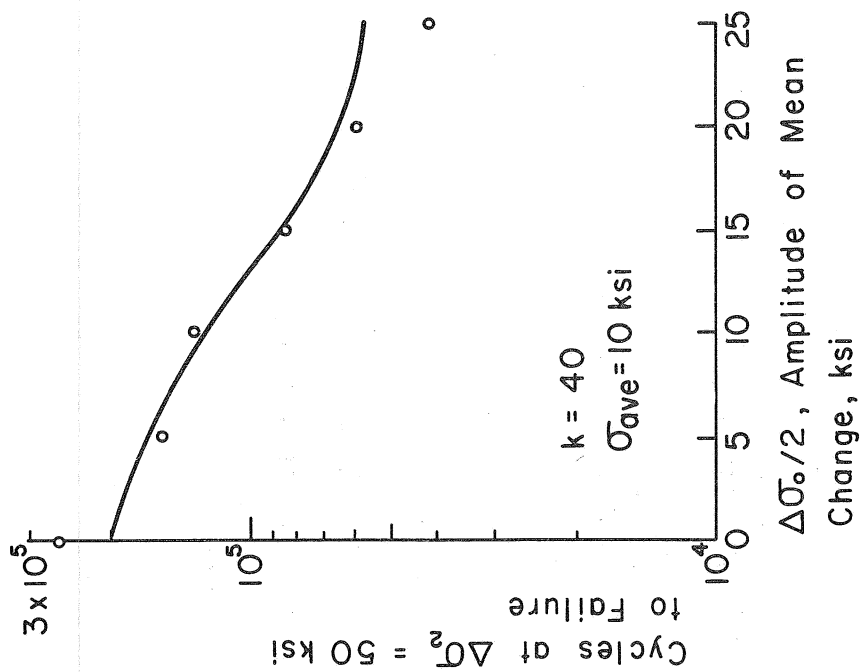
Fig. 29 Stress range vs. strain range for closed hysteresis loops during strain control random sequence tests



Time →

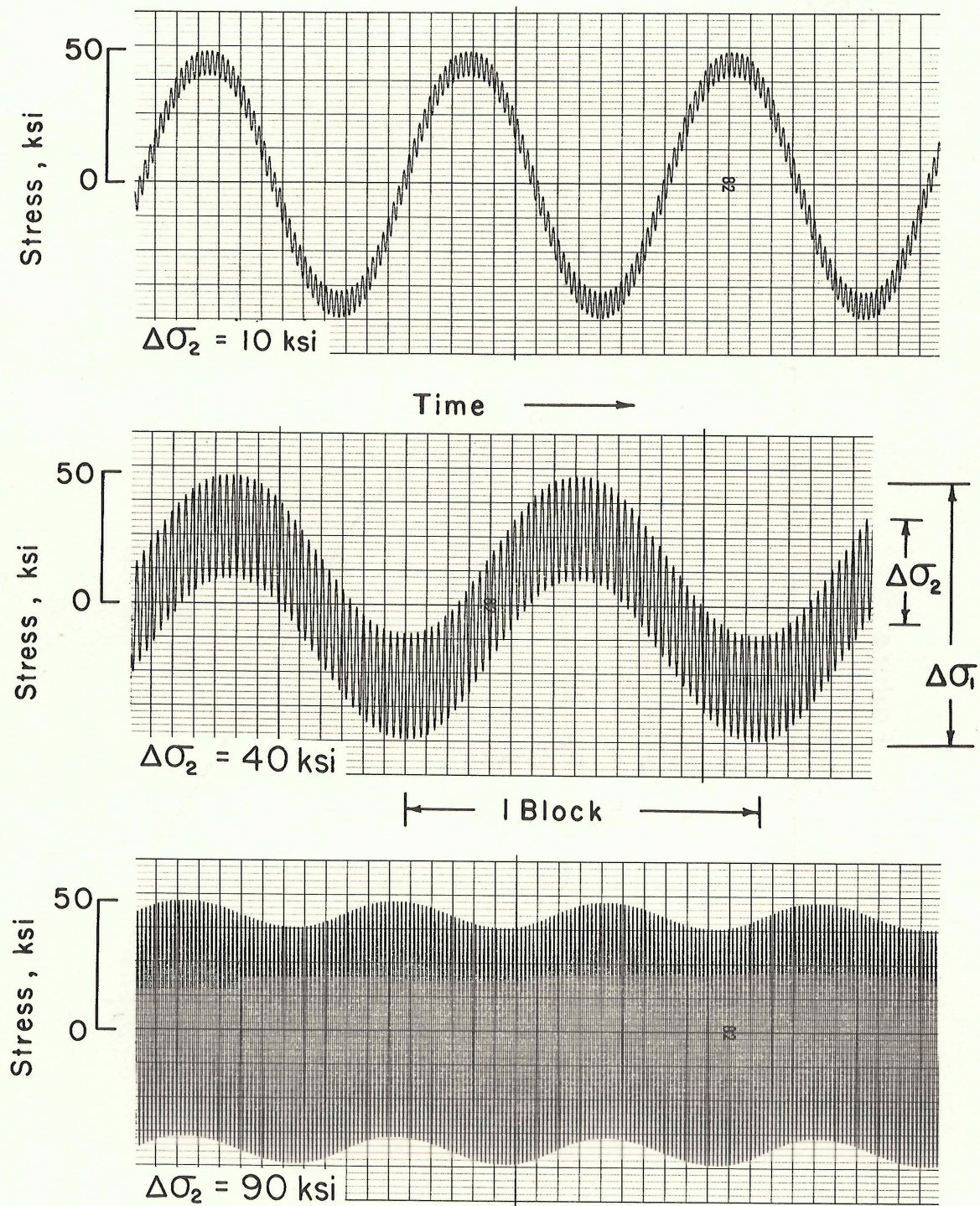


(a) Typical stress — time recordings



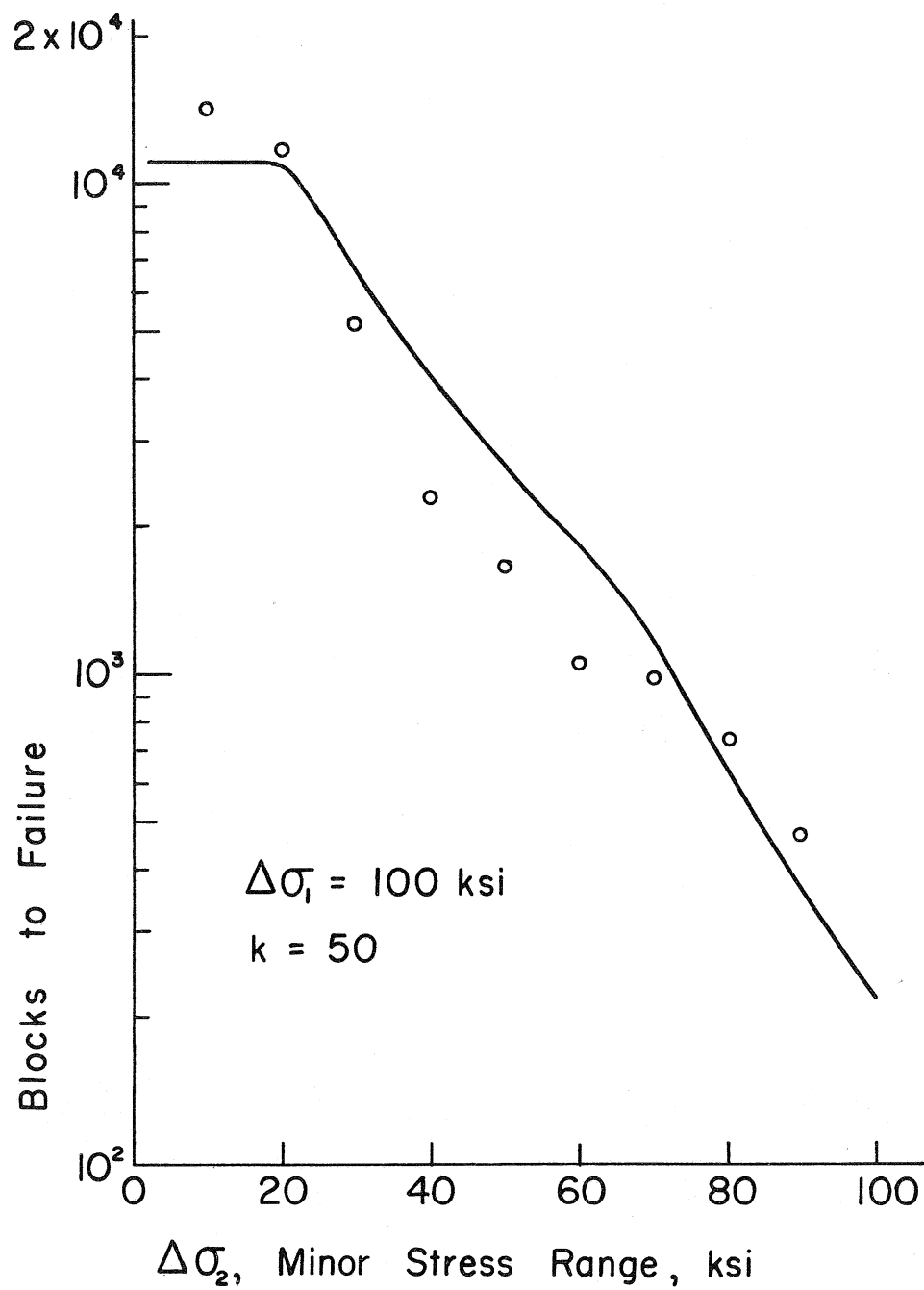
(b) Test data and predicted line

Fig. 30 Constant average mean stress tests



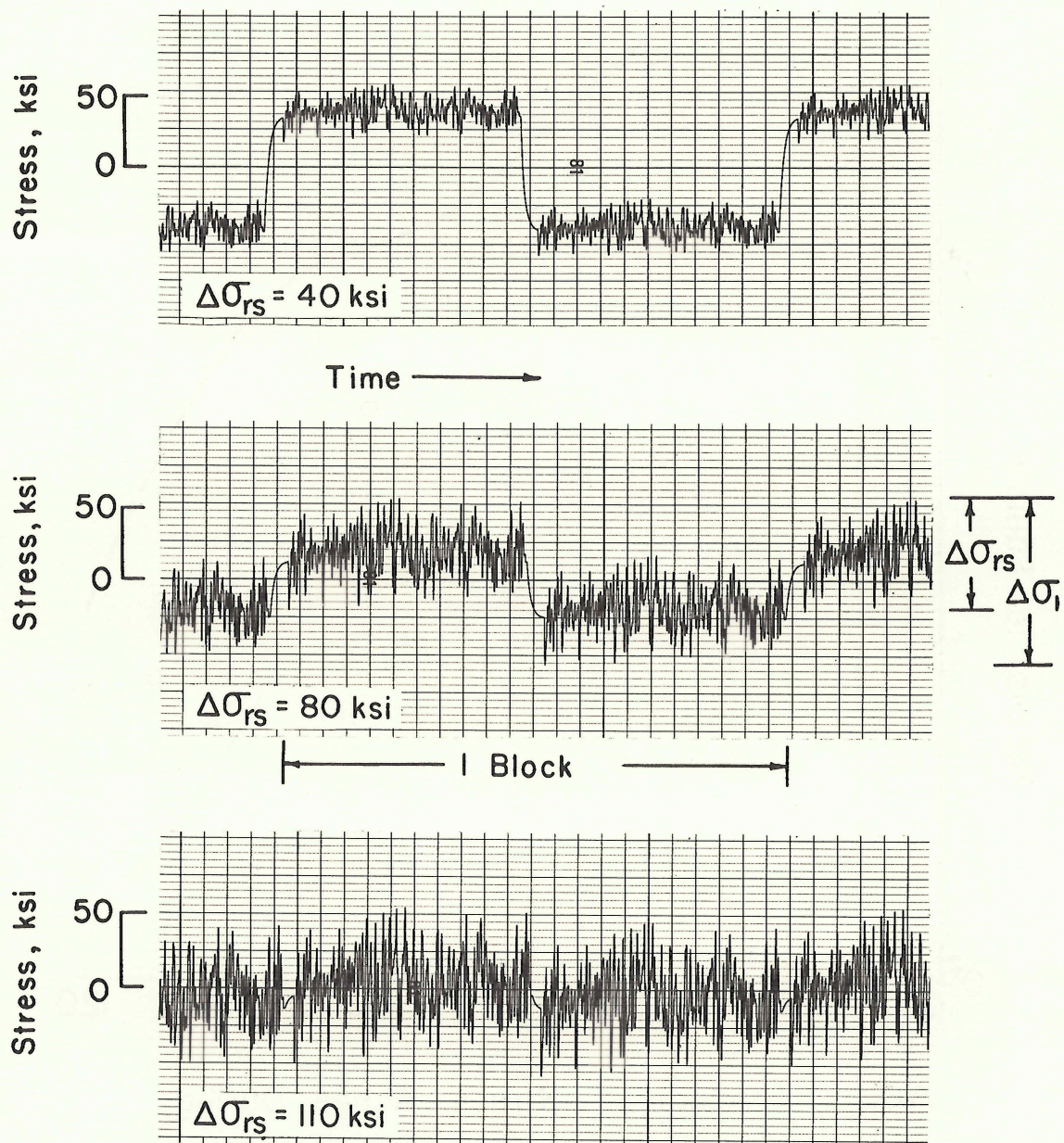
(a) Typical stress – time recordings

Fig. 31 Tests with sinusoidal variation of the mean stress



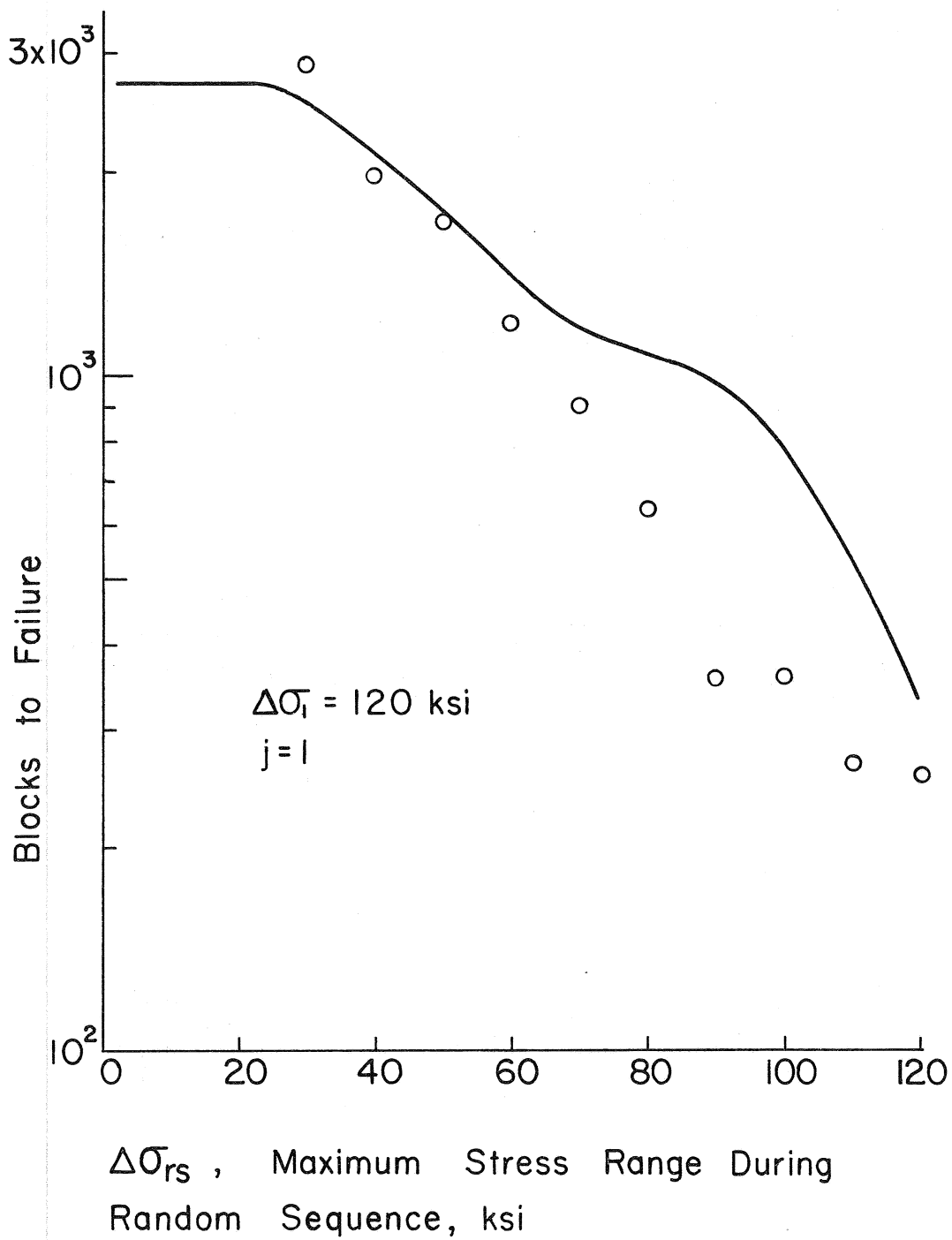
(b) Test data and predicted line

Fig. 31 Tests with sinusoidal variation of the mean stress (cont'd)



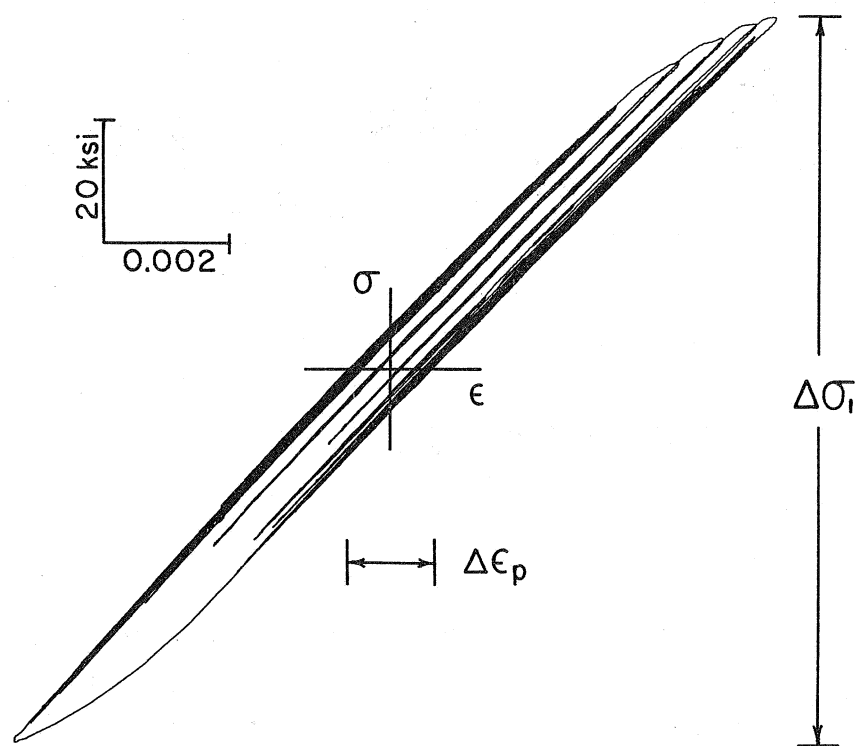
(a) Typical stress - time recordings

Fig. 32 Stress control random sequences at two static levels

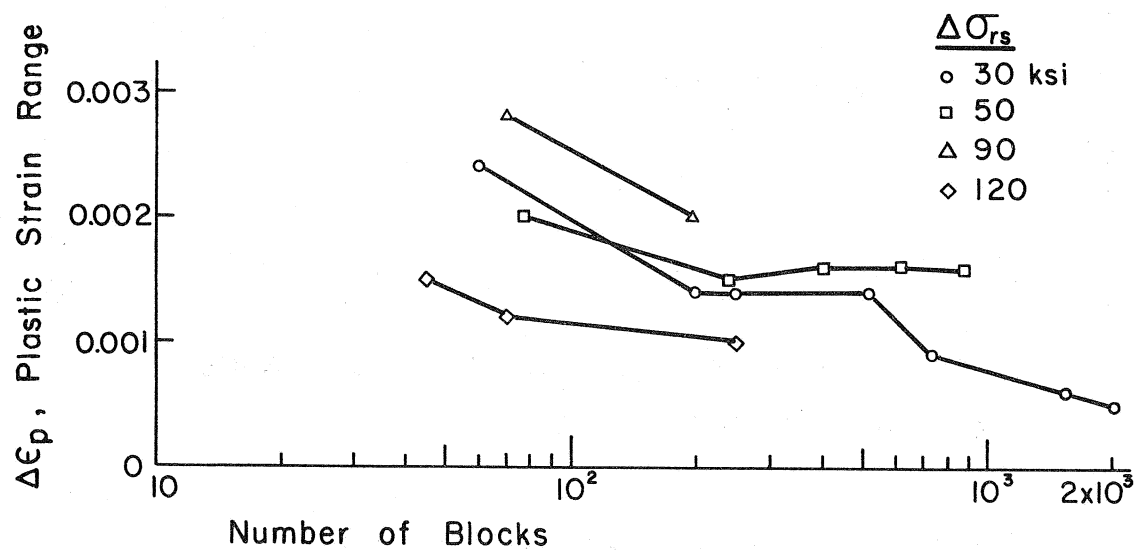


(b) Test data and predicted line

Fig. 32 Stress control random sequences at two static levels (cont'd)

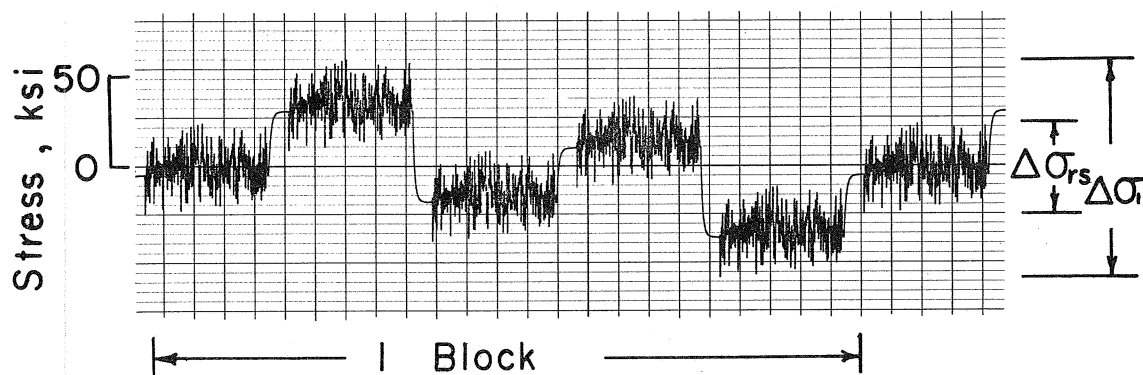


(a) Stable stress-strain response for $\Delta\sigma_{rs} = 100$

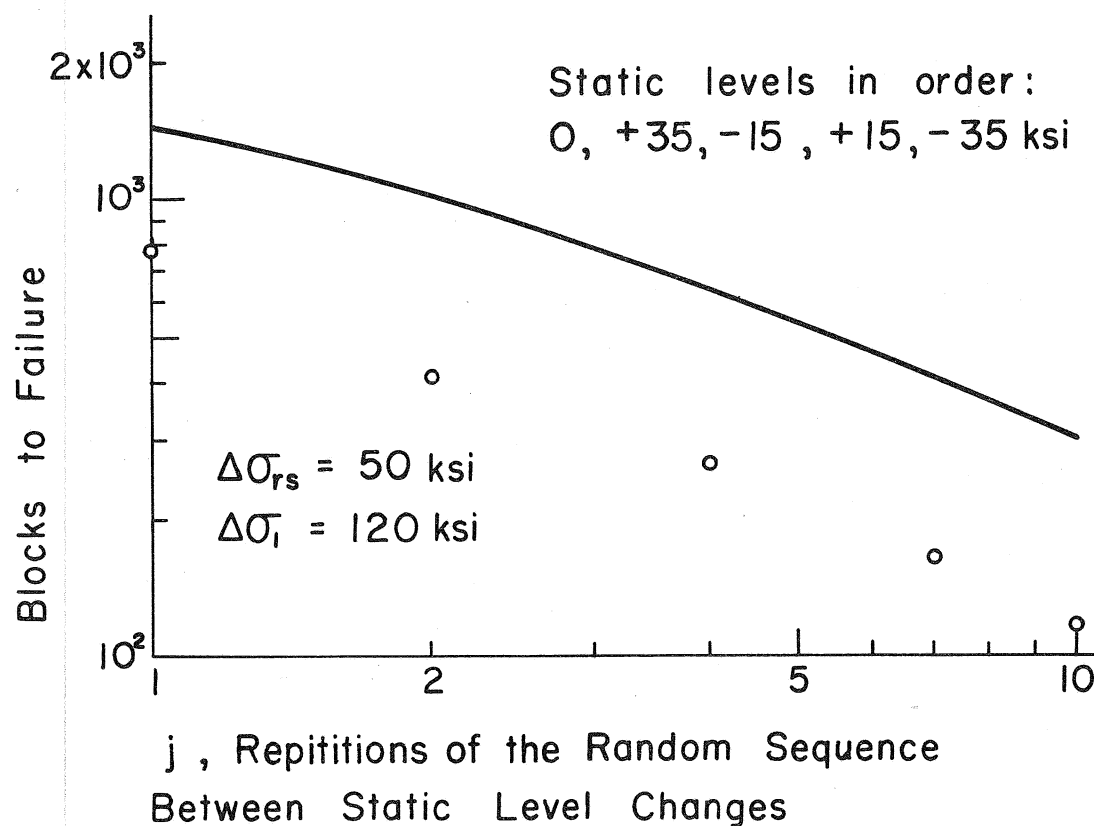


(b) Typical variations of plastic strain range

Fig. 33 Strain response during two level random tests



(a) Stress - time record for $j=1$



(b) Test data and predicted line

Fig. 34 Stress control random sequences at five static levels

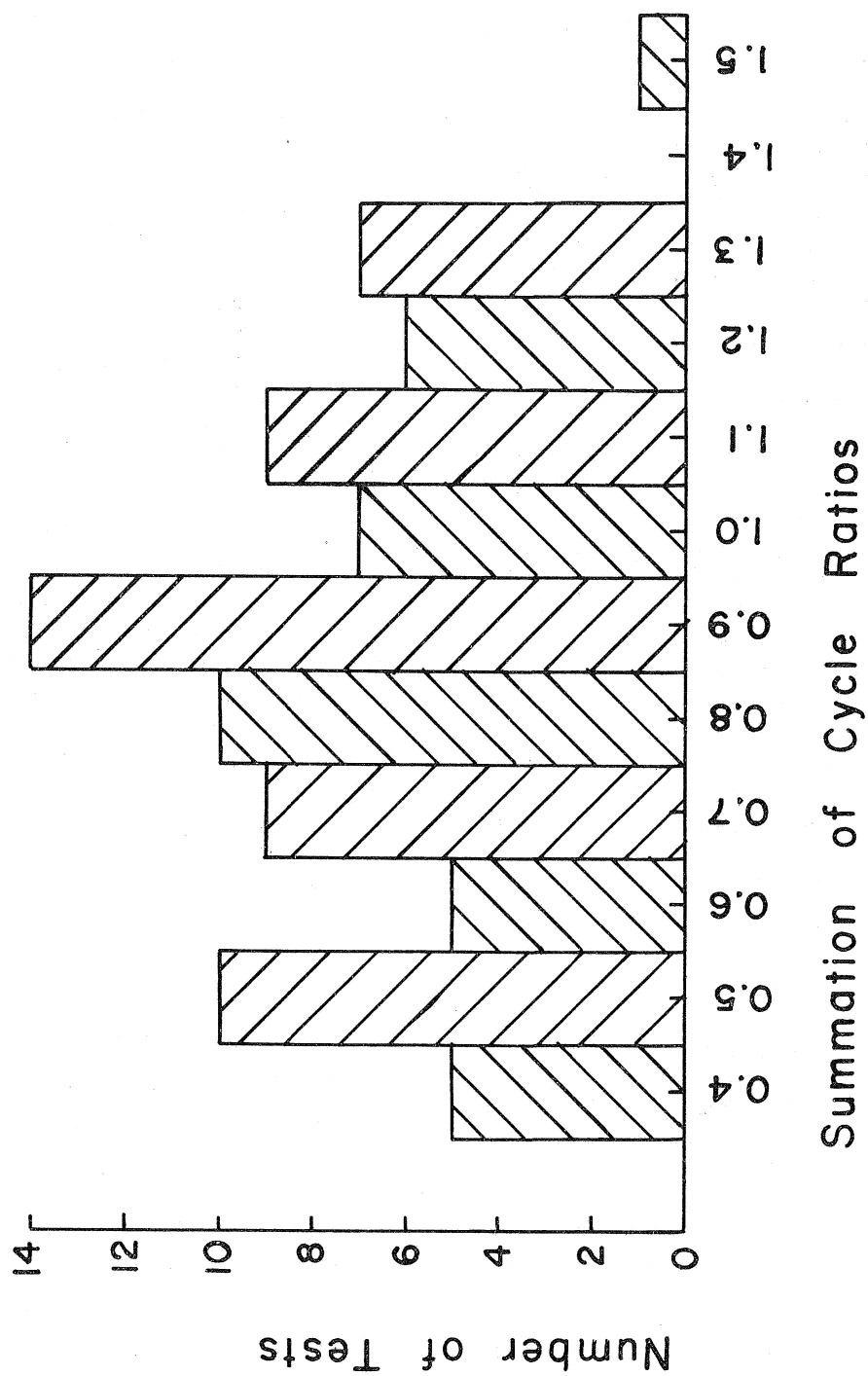


Fig. 35 Distribution of failure predictions

APPENDIX

RANGE PAIR AND RAIN FLOW CYCLE COUNTING METHODS

Range Pair Counting Method

The range pair counting method (21, 22) is illustrated in Fig. A1. A positive strain range is defined as a strain range during which the strain becomes more positive with time. A positive range is counted as a cycle if the strain becomes more negative than the initial peak of the range before the occurrence of a peak more positive than the terminal peak of the range. Negative ranges are similarly counted. In considering a range of a given size, interruptions consisting of smaller ranges are temporarily ignored. Note that each range counted as a cycle is associated or paired with part of another range of opposite sign, explaining why complete cycle rather than half cycle counts are made. A portion of a strain range that has been paired is therefore not further considered.

Rain Flow Counting Method

Examples of cycle counting by the rain flow method (23) are shown in Figures A2 and A3. The strain versus time record is plotted so that the time axis is vertically downward, and the lines connecting the strain peaks are imagined to be a series of pagoda roofs. Several rules are imposed on rain dripping down these roofs so that cycles and half cycles are defined. Rain flow begins at the beginning of the test and successively at the inside of each strain peak. The rain flow initiating at each peak is allowed to drip down and continue except that it stops when it comes opposite a maximum more positive (minimum more negative) than the maximum (minimum) from which it started. It must also stop if it meets the rain from a roof above. The beginning of the sequence being counted is considered a minimum if the initial straining is in tension, or a maximum if the initial straining is in compression. The horizontal length of each rain flow is counted as a half cycle at that strain range. Note that every part of the strain-time record is counted once and only once.

When this procedure is applied to a strain history, a half cycle is counted between the most positive maximum and the most negative minimum. Assume that of these two the most positive maximum occurs first. Half cycles are also counted between the most positive maximum and the most negative minimum that occurs before it in the history, between this minimum and the most positive maximum occurring previous to it, and so on to the beginning of the history. After the most negative minimum in the history, half cycles are counted which terminate at the most positive maximum occurring subsequently in the history, the most negative minimum occurring after this maximum, and so on to the end of the history. The strain ranges counted as half cycles therefore increase in magnitude to the maximum and then decrease.

All other strainings are counted as interruptions of these half cycles, or as interruptions of the interruptions, etc., and will always occur in pairs of equal magnitude to form full cycles. All strain ranges counted as cycles will form closed stress-strain hysteresis loops, and those counted as half cycles will not.

Comparison of the Range Pair and Rain Flow Cycle Counting Methods

All of the cycles counted by the rain flow method are counted as cycles by the range pair method, but the half cycles are either counted as full cycles or are not counted. This is a result of the fact that the rules used by the rain flow method reduce to the range pair method except when the half cycles are being counted. For example, the identical sequences in Fig. A1 and A2 are counted the same by the two methods except that the first half cycle counted by the rain flow method is counted as a full cycle by the range pair method, and the second and third half cycles are not counted. The range pair method therefore does not correspond to the stress-strain behavior as does the rain flow method. Slightly less damage will always be counted by the range pair method, but this difference is significant only in situations where the damage due to individual half cycles is important, namely where there are only a few reversals to failure or where there are insignificant minor reversals and most of the damage is done by a few major reversals.

It is therefore concluded that the rain flow and range pair cycle counting methods can be considered equivalent for most practical situations. In repeated block tests the rain flow method will count no half cycles except during the first and last blocks. The counting results of the two methods will therefore always be identical for repeated blocks.

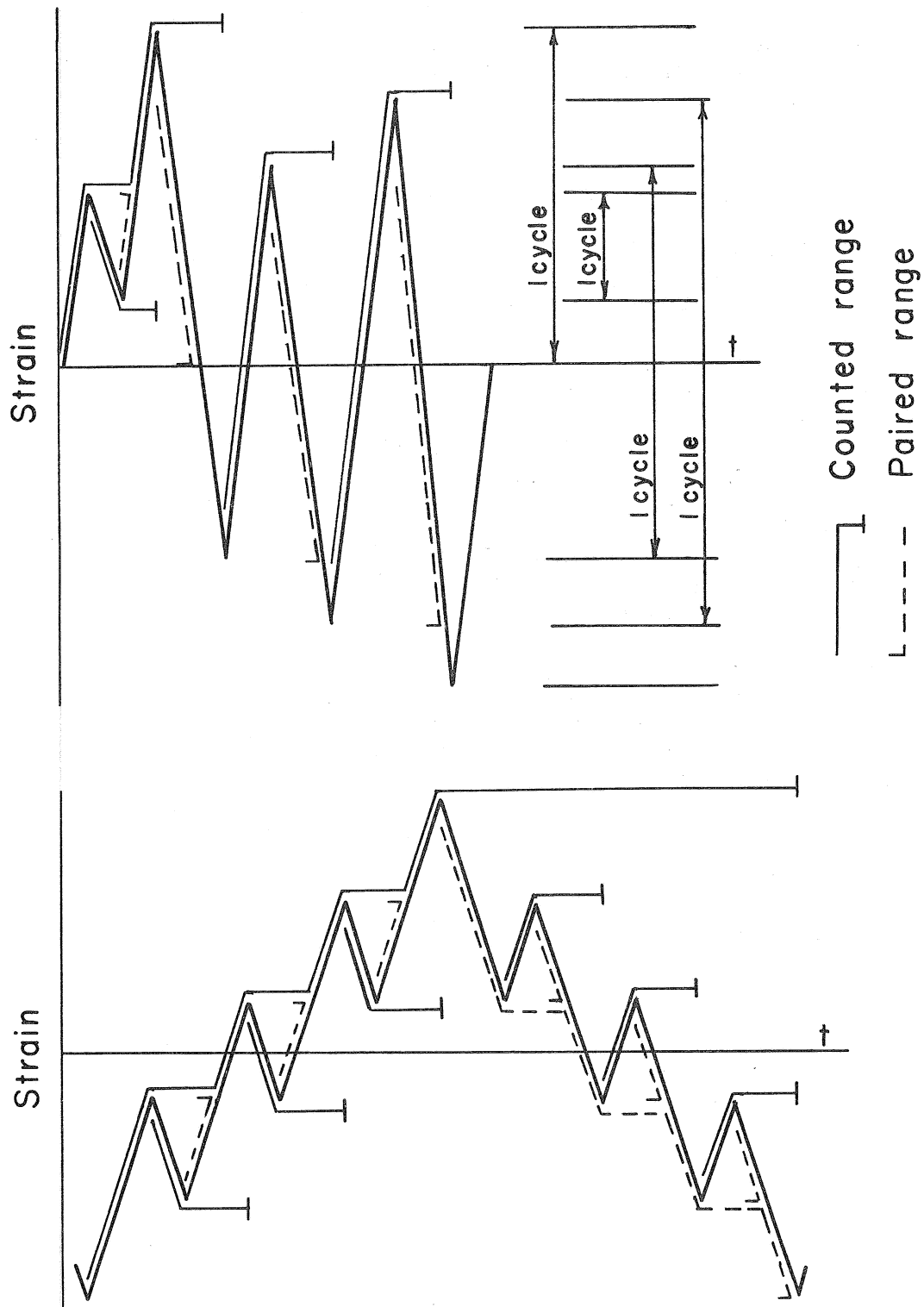


Fig. A1 Examples of range pair counting method

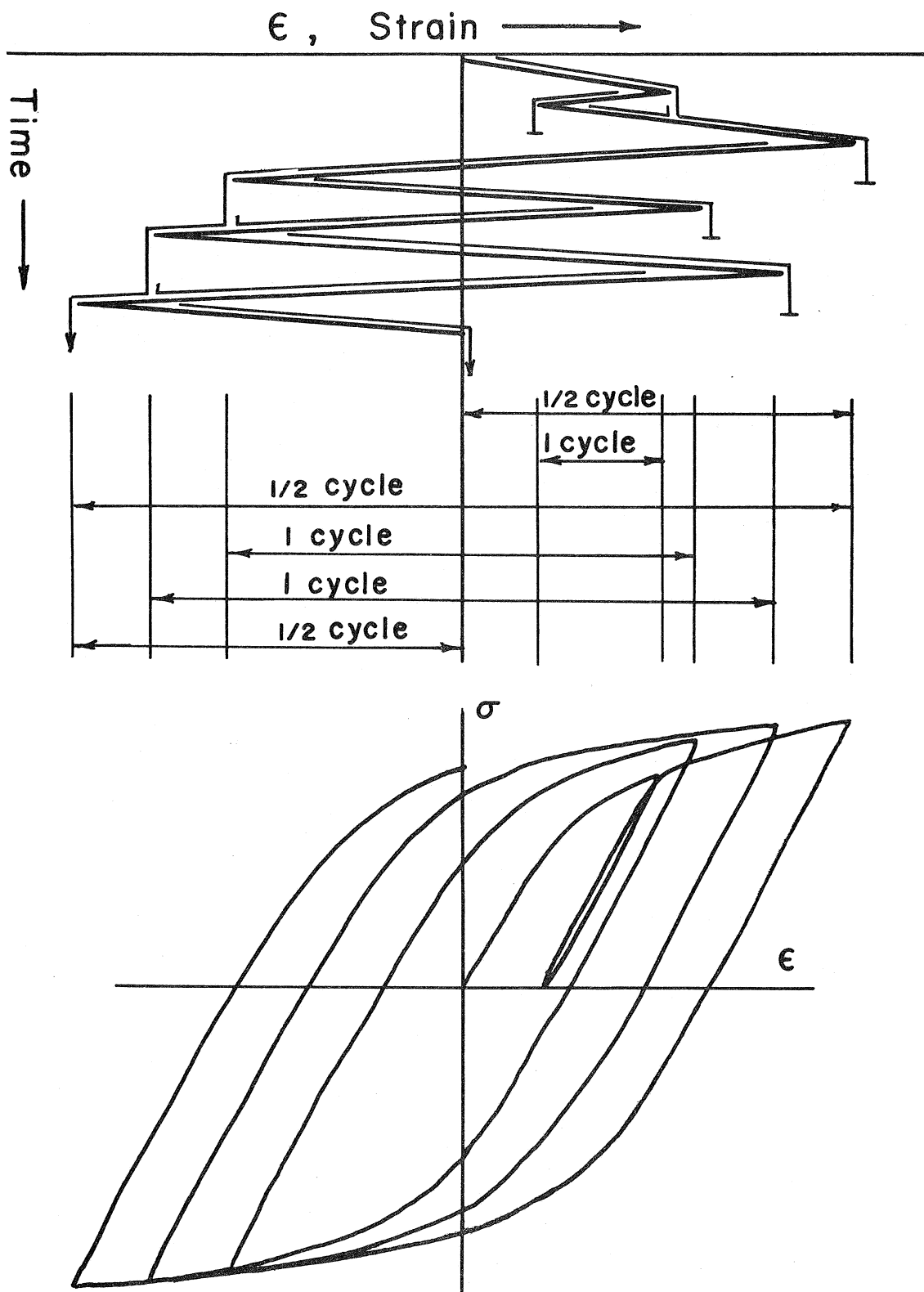


Fig. A2 Example of rain flow cycle counting method

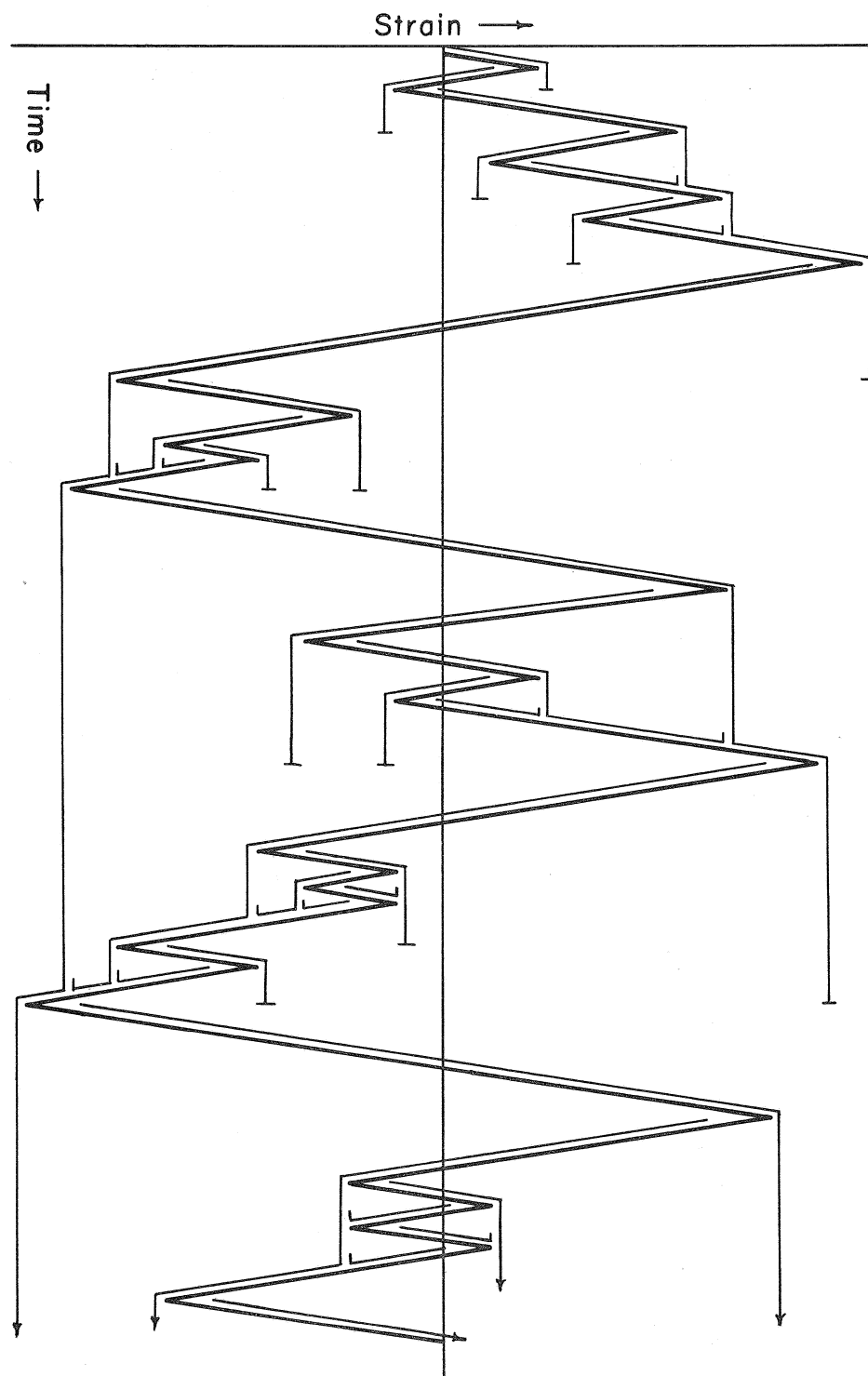


Fig. A3 Additional example of rain flow cycle counting method